Experimental nephrotic syndrome in mice with an inducible deletion of podocin and the role of plasminogen in sodium retention

Thesis submitted as requirement to fulfill the degree "Doctor of Philosophy" (Ph.D.)

at the
Faculty of Medicine
Eberhard Karls University
Tübingen

by

Mengyun, Xiao

from

Xining, China

2022

Dean:	Professor Dr. B. Pichler
First reviewer:	Professor Dr. F. Artunc
Second reviewer:	Professor Dr. R. Feil
Third reviewer:	Professor Dr. R. Lukowski
Date of oral examination:	11.01.2022

“The road ahead is long and has no ending; yet high and low I will search with my will unbending.”

(Qu Yuan)

Table of contents

List of figures and tables

List of abbreviations

Units	
%	percentage
bw	body weight
crea	creatinine
dl	deciliter
Ep	Eppendorf
g	gram
kDa	kilodalton
mg	milligram
min	minute
ml	milliliter
mM	millimolar
nm	nanometer
pg	petagram
µg	microgram
µl	microliter
µm	micrometer
µmol	micromolar
w/v	weight/volume
A	
A	aprotinin
ACEI	angiotensin-converting enzyme inhibitor
ANS	acquired nephrotic syndrome
ARB	angiotensin II receptor blocker
AUC	area under curve
B	
BGA	blood gas analysis
BW	bodyweight
C	
Ca	calcium
CAP1	channel-activating protease
cBSA	cationic bovine serum albumin
cHb	calculated hemoglobin concentration
CKD	Chronic kidney disease
CNS	congenital nephrotic syndrome
Cre-lox P	Cre enzyme and the original Lox site

D	
ddH2O	distilled water
DF	dilution factor
DIN	doxorubicin induced nephrotic
DNA	deoxyribonucleic acid
E	
ELISA	enzyme-linked immunosorbent assay
ENaC	epithelial sodium channel
ENS	experimental Nephrotic syndrome
F	
FSGS	focal-segmental glomerulosclerosis
G	
GFB	glomerular filtration barrier
GFR	glomerular filtration rate
H	
Hct	hematocrit
HCO_3^-	bicarbonate ion
het	heterozygote
HNO3	Nitric acid
I	
i.p.	intraperitoneal injection
IF	immunofluorescence
K	
K^+	potassium
ko	knockout
L	
L	low salt diet
LPS	lipopolysaccharides
M	
M	metabolic cage
MCD	minimal change disease
Max.	maximum
Min.	minimum
N	
N	nephrotic
Na^+	sodium
$nphs2^{\Delta ipod}$	doxycycline sensitive inducible nphs2 knock out with podocyte specific

NS	nephrotic syndrome
O	
OCT compound	optimal cutting temperature compound
OD	optical density
P	
P	plasma/placebo
p	probability value
PAN	puromycin-aminonucleoside
PAs	plasminogen activators
PAS	Periodic acid–Schiff staining
PBS	phosphate-Buffered Saline
PCR	polymerase chain reaction
PFA	paraformaldehyde
PH	power of hydrogen
plg	plasminogen
P_O	open probability
R	
RAAS	renin-angiotensin-aldosterone system
RBC	red blood cells
RT	room temperature
rtTA	reverse tetracycline transactivator
S	
SD	slit diaphragm
SDS-PAGE	sodium dodecyl sulfate–polyacrylamide gel electrophoresis
Sec	second
SEM	standard error of the mean
SGK1	serum-and-glucocorticoid-kinase 1
std	standard
T	
TAE Buffer	Tris-Acetate-EDTA buffer
tPA	Tissues-type plasminogen activator
Tris buffer	tris(hydroxymethyl)-aminomethane buffer
U	
U	uninduced/urine
uPA	urokinase-plasminogen activator
V	

V	vehicle
vs.	versus
vol	volume
W	
wt	wild type
WB	Western blot
WBCs	white blood cells

1. Introduction

1.1 Definition and causes of the nephrotic syndrome

Nephrotic syndrome (NS) is a characteristic collection of symptoms, including large proteinuria, hypoalbuminemia, edema, and hyperlipidemia. Among those symptoms, massive proteinuria is considered as the essential condition to induce NS. A nephrotic-range proteinuria is defined as a concentration of urinary protein > 3.5 g/24h, or urinary protein/creatinine ratio > 3.5 g/g creatinine from a spot urine sample. In accordance with the age of onset, NS can be categorized as congenital nephrotic syndrome (CNS) and acquired nephrotic syndrome (ANS). It can also be classified as primary nephrotic syndrome with a disease-specific to the kidneys or secondary nephrotic syndrome due to systemic diseases for example diabetes and systemic lupus erythematosus[1]. Primary NS is the most prevalently presented kidney disease in childhood, with a reported incidence of 2-7/100,000 children[2]. The causes of primary NS are highly variable due to age, region, and race. Pathologically, minimal change disease (MCD) is the common type of primary NS in children[3], while in white Caucasian adults, the leading cause is membranous glomerulonephritis[4]. The focal segmental glomerulosclerosis (FSGS) is the main reason of NS in African natives, and the incidence of FSGS has been tending to increase worldwide recently[5-10].

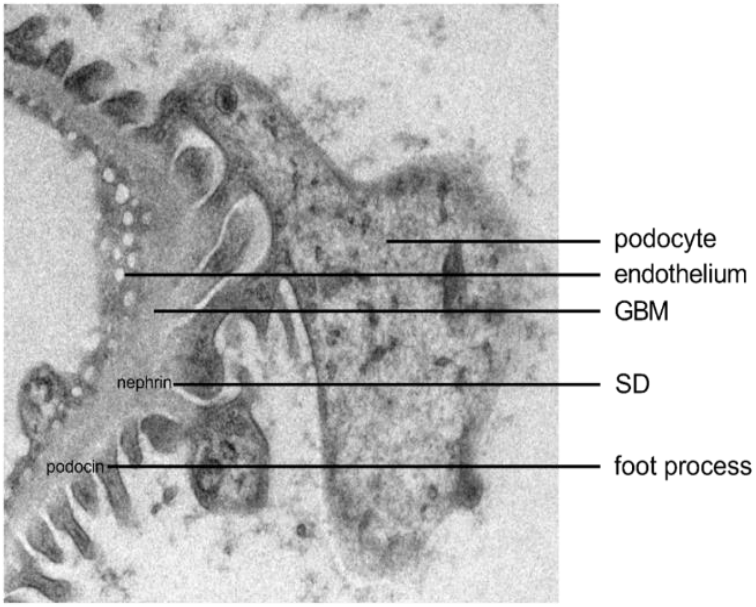

Figure 1 Ultrastructure of glomerular filtration barrier observed by electron microscope

Image provided by III. Department of Medicine, University Medical Center Hamburg-Eppendorf, Hamburg, Germany.

In a healthy kidney, large molecule-compounds such as protein and platelets are not able to transit the glomerular filtration barrier (GFB). GFB consists of three layers – fenestrated endothelial cell, glomerular basement membrane (GBM), visceral epithelial cells (podocyte) with the foot processes slit diaphragms (SD)[11] (Figure 1).

The selective filtration of GFB is mainly based on the size of molecules[12]. Molecules with a radius smaller than 2 nm are freely filtered. Proteins cannot pass the GFB with a radius of more than 4.2 nm or a molecular weight >69 kDa, while those molecules between 2 – 4.2 nm are poorly percolated and can be re-uptaken by the proximal tubule. Thus, protein is barely detectable in urine samples with normal renal function (Figure 2). On the contrary, massive proteinuria will be present when the GFB is damaged (Figure 2). To the current knowledge, the functional or structural damage of podocytes (Figure 2) is the leading cause of a damaged GFB and proteinuria[2,13-15]. Podocyte dysfunction typically leads to NS which is the most extreme manifestation of a proteinuric renal disease[2,10,11,16,17].

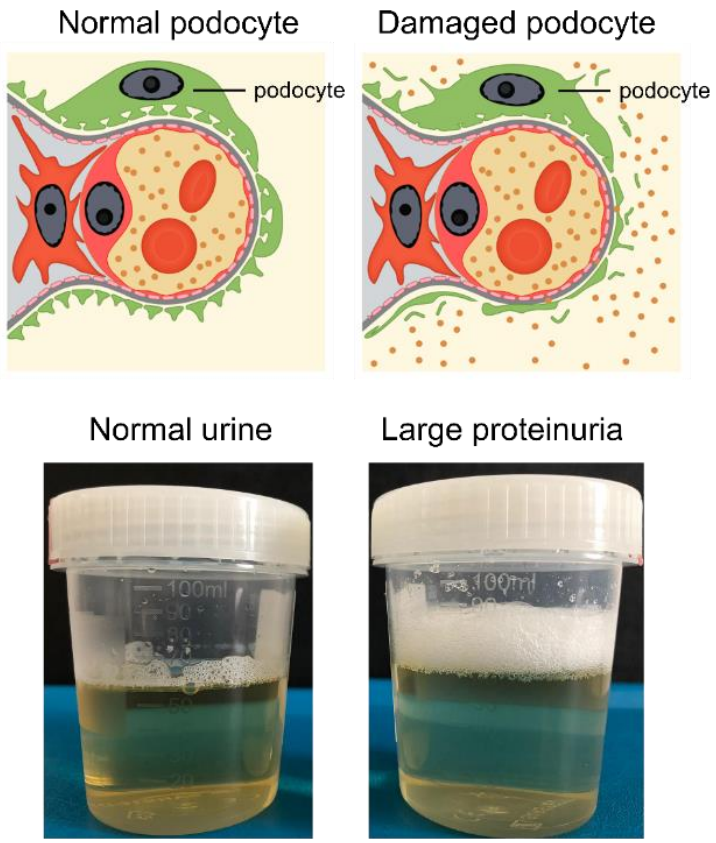

Figure 2 Illustration of podocyte damage and proteinuria

Damage of podocyte leads to large proteinuria (photos of urine samples are provided by Dr. Bohnert).

Podocytes are highly differentiated and non-regenerable cells expressing unique proteins which are critical for an intact GFB[18]. *Nphs1,* which encodes nephrin, was the first gene identified and localized in podocytes[19]. Further studies conducted using *nphs1* knockout animal models[19] showed that mice with *nphs1* deficiency developed massive proteinuria and nephrotic syndrome. Histologically, enlarged Bowman's spaces, dilated tubuli, effaced foot processes and absent slit diaphragm were visible which recapitulated all features of Finnish type of congenital nephrotic syndrome (CNS) in humans[20]. Podocin is encoded by the *nphs2* gene and expresses on the foot process of podocytes[16] (Figure 1). Genetic defects in *nphs2* similarly lead to CNS[11,16,21,22]. Podocin and nephrin as well as other molecules interact with each other and maintain the normal structure of podocyte and the slit diaphragm[23]. CNS due to nephrin and podocin deficiency manifest as nephrotic syndrome in early infancy and lead to progressive renal failure necessitating renal replacement therapy.

1.2 Mouse models of experimental nephrotic syndrome

Animal models are essential tools to simulate NS in vivo and to study the mechanisms as well as potential therapeutic approaches to NS. Mouse, rat, and zebrafish are used for modeling NS; among those models, mice or rats with experimental NS are most commonly used due to its genetic similarity to human, short reproduction cycle, and ease of handling.

Experimental models of NS can be basically classified into genetic, toxic, and other models. Genetic models are based on mice with modified genes that are typically members of the slit diaphragm and expressed by the podocytes. The genes encoding the molecules of the podocytes have been recognized and localized by studies in the past years, such as *nphs1*, *nphs2*, *lamb2*, *actn4*, *wt1*, and *cd2ap*[11,20,21,23-25]. Among all those genes, *nphs1* and *nphs2* are the most frequently targeted genes to establish genetic NS models. Constitutive deletion of those genes usually causes CNS manifesting immediately after birth and leading to severe or even lethal disease within a short time. Therefore, CNS models with constitutive deletion of these proteins have only a limited value to study NS[21,26].

Thanks to the development of genetic engineering, it has become possible to remove genes specifically from a particular tissue and conditionally in adult-animals[27-29].

Conditional gene manipulation methods are mainly based on the tetracycline-controlled transcriptional activation systems, Tet-on, and Tet-off systems. Tet-on and Tet-off systems are depended on the resistance to tetracycline or its analogues in Gram-negative bacteria[30]. The Tet-on system functions when the reverse tetracycline transactivator (rtTA) protein is activated by binding to tetracycline or one of its derivatives, doxycycline. This induces expression of Cre recombinase that cleaves floxed alleles of the target gene. A model based on the conditional deletion of *nphs2* (encoding for podocin) using the Tet-on system was reported in 2009 imitating NS effectively with massive proteinuria, hypoalbuminemia and hypercholesterolemia of the mice[31]. Yet the disadvantage of that conditional nephrotic model is the requirement of three mutated alleles which necessitates time-consuming breeding of the mice.

On the other hand, experimental NS can be induced in mice using the anthracycline adriamycin or doxorubicin[32-36]. This model has been adapted to mice[32] and resembles the puromycin-aminonucleoside (PAN) model in rats[37-39]. Doxorubicin-induced nephrotic mice and PAN-induced nephrotic rats were reported to develop typical features of NS. However, these toxic drugs could cause tubule damage to animals, and the response rate to toxic substances is highly related to species[34,40-42] and dose[33,43,44].

Other methods, such as induction by repeated injection of cationic bovine serum albumin (cBSA) in ICR (outbred) or BALB/c mice[45,46], lipopolysaccharides (LPS) injection to BALB/c, C57BL/6 and 129 mice, and injection of sheep anti-rabbit glomeruli antibody to mice[47-50] are also reported to establish adult-nephrotic models. However, the proteinuria reported in these models does not reach the magnitude of nephrotic range proteinuria.

1.3 The activation of epithelial sodium channel (ENaC) by proteasuria causes sodium retention in nephrotic syndrome

Sodium retention and oedema are the traits of NS and the leading symptom of patients with acute NS. The mechanisms of sodium retention and oedema in NS are generally explained by two theories, the overfill, and the underfill theory (Figure 3). The underfill theory was proposed about 100 years ago[51], claimed that low plasma protein, as a consequence of massive proteinuria, leads to intravascular volume depletion[52] and buildup of fluid in the interstitial space. This activates the renin-angiotensin-aldosterone

system (RAAS), causing increased Na^+ up-taken by the kidneys. However, underfill theory is not able to explain the mechanism of edema for all nephrotic cases as there has been evidence indicating that RAAS activation is absent in many cases of NS from patients or animal models[52,53].

Thus, overfill theory was formulated[54], stating that edema formation could be a result of an intrarenal mechanism that stimulates tubular sodium reabsorption (Figure 3). The ENaC, which has three subunits (α, β, and γ)[55], and is expressed in distal nephron (Figure 4), is considered as the site of the Na^+ retention and volume expansion in NS[56-58].

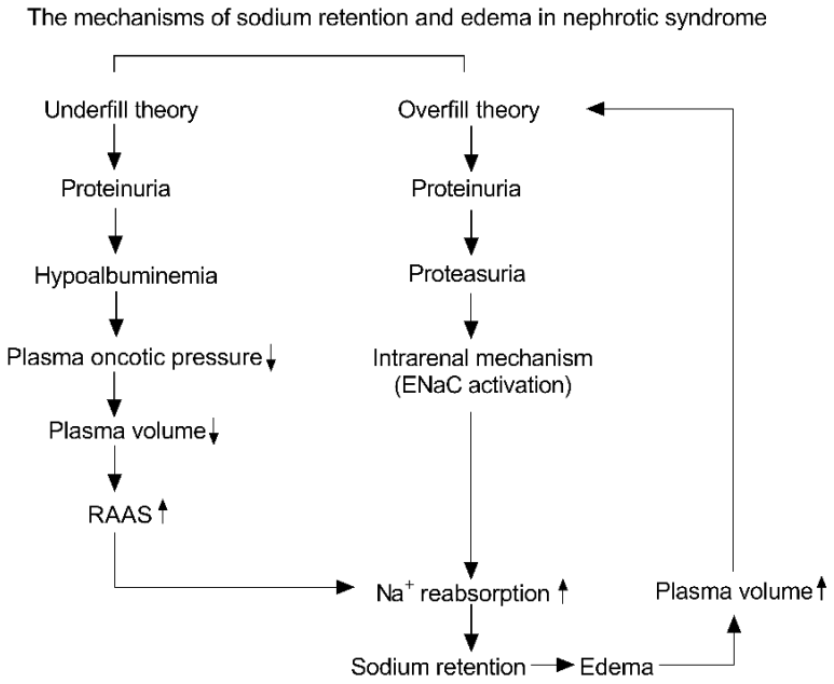

Figure 3 The underfill theory and overfill theory of sodium retention in nephrotic syndrome. ↑ indicates increase; ↓ indicates decrease

Increased ENaC activity in NS has been demonstrated by micropuncture studies in experimental NS[57,58]. One study reported that treatment with the blocker of ENaC, amiloride, protected nephrotic mice from ENaC activation and sodium retention[35]. This study suggested an essential role of ENaC activation as the cause of edema formation in NS.

Aldosterone is the primary mineralocorticoid hormone, which is synthetized by the adrenal cortex[59]. The increased reabsorption of sodium at the collecting duct in experimental NS was thought to be associated with the increased ENaC expression, which is regulated by aldosterone (Figure 4). This finding was reported in PAN treated nephrotic

rats, which presented high plasma-aldosterone, increased number of ENaC, more specifically α-ENaC[60]. In addition, elevated plasma aldosterone redistributed ENaC towards to the apical region of the principal cells of collecting duct, which was called 'apical targeting'[61]. In nephrotic rats with adrenalectomy, the abundance of ENaC expression was upregulated, however, the apical targeting was abolished. Rats experienced sodium retention despite the absence of aldosterone[61]. However, the apical targeting was not observed[61]. In another study, blocking the mineralocorticoid receptor by canrenoate did not prevent Na^+ retention and edema in experimental NS as well[35]. Similar to that, the mice with serum-and-glucocorticoid-kinase 1 (SGK1) deficiency which represents aldosterone-resistance developed sodium retention after induction of NS[32]. Besides the evidence from experimental models, nephrotic patients do not always display an increased level of plasma aldosterone[53]. All these findings point to some other mechanism of ENaC regulation in NS than hyperaldosteronism.

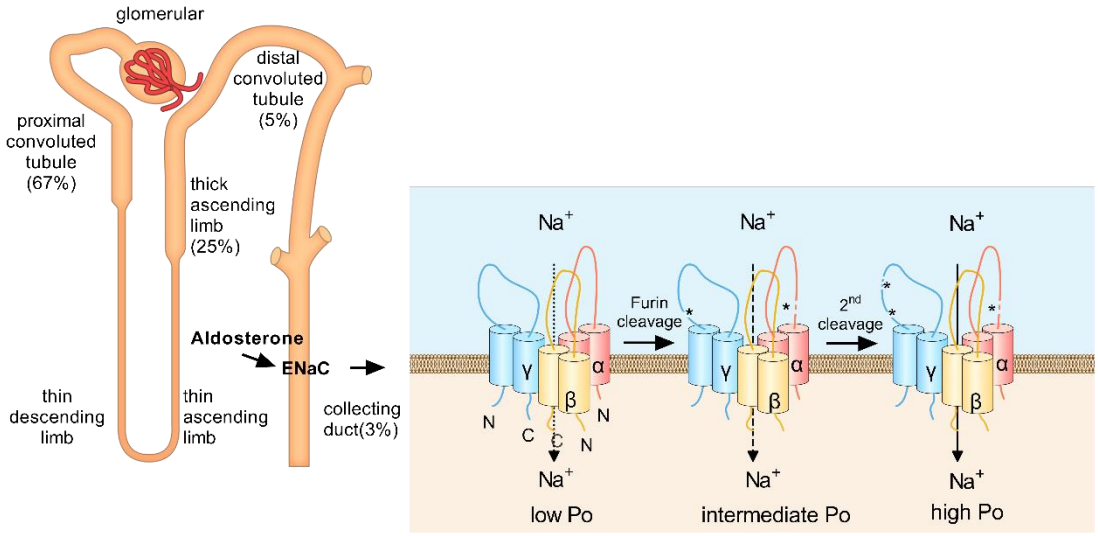

Figure 4 Location, molecular structure and regulation of ENaC by urinary serine proteases

ENaC is sensitive to aldosterone and regulates 3-5% reabsorption of filtered sodium and excess fluid. The serine protease furin cleaves the α subunit twice, whereas the extracellular serine proteases cleave the γ subunit once. The open probability (P_O) of ENaC is increased to the intermediate level accordingly. A secondary cleavage-events of γ-ENaC by some other proteases increases the P_O of ENaC into a very high level (this figure was drawn by Mr. Hao Tian).
* indicates the cleavage sites.

Accumulative studies have proved that aberrantly filtered urinary serine proteases (proteasuria) due to defective filtration barrier in NS, activate ENaC by proteolysis and lead to sodium retention and edema[35,62-64]. Nephrotic mice receiving the treatment with

serine proteases inhibitor avoided Na^+ retention as effective as treatment with amiloride[35], indicating the special regulation of ENaC by serine proteases. It was found in one study that ENaC was activated in a *Xenopus* kidney epithelial cell line (A6) by co-expression with one of the serine proteases, which was named as channel-activating protease (CAP1)[65]. In this study, the authors also observed that by adding aprotinin, a nonspecific serine protease inhibitor, to the A6 cells, ENaC activity was reduced. The sodium transport could be recovered by adding extracellular trypsin afterward, which is also a serine protease. Later on, a study discovered that ENaC activity correlates with cleavage of the channel by the intracellular serine protease furin, by using furin-deficient cells or furin-specific inhibitors in vitro study[66]. Subsequently, the two cleavage sites of furin at the α subunit, and a single cleavage site at γ subunit were identified[67] (Figure 4). The furin-mediated cleavage was proven to be responsible for the basal current (I_{Na})[68,69](Figure 4). In 2007, a cleavage event was located at the γ subunit[70], situated away from the Furin-cleavage site, and was related to the high open possibility (Po) of the channel. The same group observed that a second cleavage at the γ subunit between the Furin-cleavage site and a polybasic tract stimulated the full activation of ENaC[71] (Figure 4).

1.4 Role of plasminogen in activation of ENaC

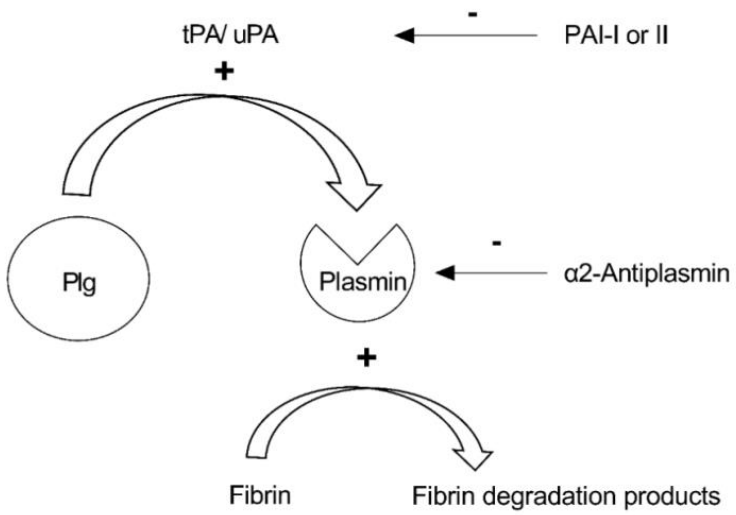

Figure 5 The role of plasminogen in fibrinolysis and the regulations of its activation.

+ indicates activation; - indicates inhibition

Plasmin is a serine protease released as a zymogen (plasminogen) from the liver into the circulation and degrades fibrin clots. The plasminogen activators (PAs) present in tissues (tPA) and in soluble form (urokinase-type or uPA) activate plasminogen[36,62,72]. Activity of plasmin and its activators can be regulated by several inhibitors (Figure 5).

In 2009, a study identified plasminogen-plasmin as the primary urinary serine protease in nephrotic patients and rats[62]. In this study, the γ-ENaC existing on mouse collecting duct cells (M-1) and in *Xenopus laevis* oocytes *in vitro* can be cleaved by nephrotic urine. To confirm if uPA converts plasminogen to plasmin, researchers applied the combination of uPA and plasminogen to M-1 cells and *Xenopus laevis* oocytes. Results revealed the whole-cell currents sensitive to amiloride were stimulated[62]. Since then, plasmin was proposed as the essential serine protease in activating ENaC in NS (Figure 6). However, these conclusions were only drawn by the *in vitro* study. During the last decade, the *in vivo* proof of plasmin in ENaC regulation in NS was still missing.

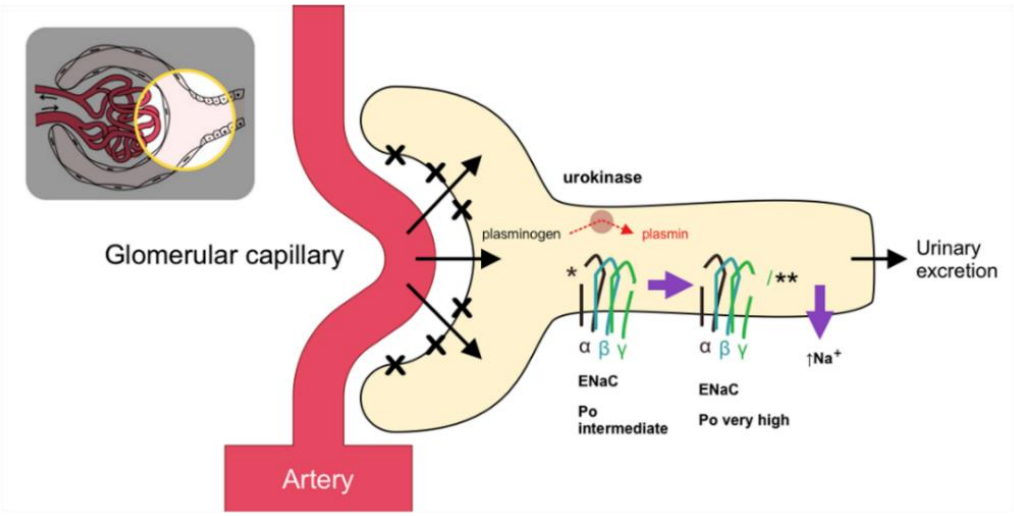

Figure 6 The theory of plasmin in ENaC regulation in NS

The current hypothesis about plasmin in ENaC activation is based on the increased filtration of plasminogen along with the leakage of massive proteinuria in NS. Aberrantly filtered urinary plasminogen is activated by uPA into plasmin which is supposed to activate ENaC at the distal tubule and to increase the sodium reabsorption (this figure was drawn by Mr. Hao Tian).

Ten years after the uPA-plasminogen-plasmin axis was brought up, two studies were published simultaneously which investigated the role of uPA in activating ENaC, by using two different experimental NS mouse-models[36,73]. In Hinrichs' study[72], researchers applied either amiloride or an uPA-antibody in tamoxifen-induced podocin-deficient nephrotic mice. Results revealed that amiloride treatment abolished the transformation of

plasminogen to plasmin and Na^+ retention. Mice with anti-uPA treatment reduced the cumulative sodium and avoided the cleavage of γ-ENaC[73]. However, the inhibition of sodium retention and edema was not complete by the application of the uPA antibody. In another study performed by our group, uPA deficient mice underwent doxorubicin-induced nephrotic syndrome [36]. Results showed that in nephrotic *uPA-ko* mice, the decrease in urinary Na^+ excretion and an increased body weight, as well as the response effects to amiloride treatment were not significantly different from *uPA-wt* mice. The finding indicated that uPA deficiency did not prevent mice from developing sodium retention and edema. Yet, trace amounts of plasmin in nephrotic *uPA-ko* mice could not be ruled out.

In humans, a study including two hundred and three NS patients was performed to investigate the hypothesis of plasminogen-plasmin in ENaC activation[63]. Patients were assigned into different groups according to the progression of edema. This study found that urinary plasminogen-plasmin/creatinine ratio was closely associated with edema and was an independent risk factor for more severe edema[63].

All those findings mentioned above did not reveal an essential causal role of plasminogen-plasmin in ENaC activation. Thus, an experimental nephrotic mouse model with plasminogen deficiency is necessarily required.

1.5 Aims of the study

This study aimed to investigate the role of plasminogen in ENaC activation and sodium retention *in vivo* by applying an experimental NS mouse model with absolute plasminogen deficiency. Therefore, a new mouse model using a tetO-Cre-lox-P system with conditional *nphs2* gene deletion ($nphs2^{\Delta ipod}$) had to be introduced and evaluated for the features of experimental NS. These $nphs2^{\Delta ipod}$ mice had then to be mated with plasminogen deficiency mice to generate a double knock-out ($nphs2^{\Delta ipod}$*$plg^{-/-}$) mouse model that allowed to induce experimental NS with plasminogen deficiency. Due to the detrimental effects of plasminogen deficiency and fibrin deposition in mice, uninduced $nphs2^{\Delta ipod}$*$plg^{-/-}$ mice needed to be studied for underlying renal disease. Another aim of the study was to testify the treatment effect on edema with aprotinin in nephrotic $nphs2^{\Delta ipod}$*$plg^{-/-}$ mice. Finally, the long-term effect on kidney function of plasminogen deficiency in nephrotic mice had to be studied.

2. Methods

2.1 Study design

2.1.1 Section I: Characterization of an experimental NS mouse model based on inducible nphs2 deficiency

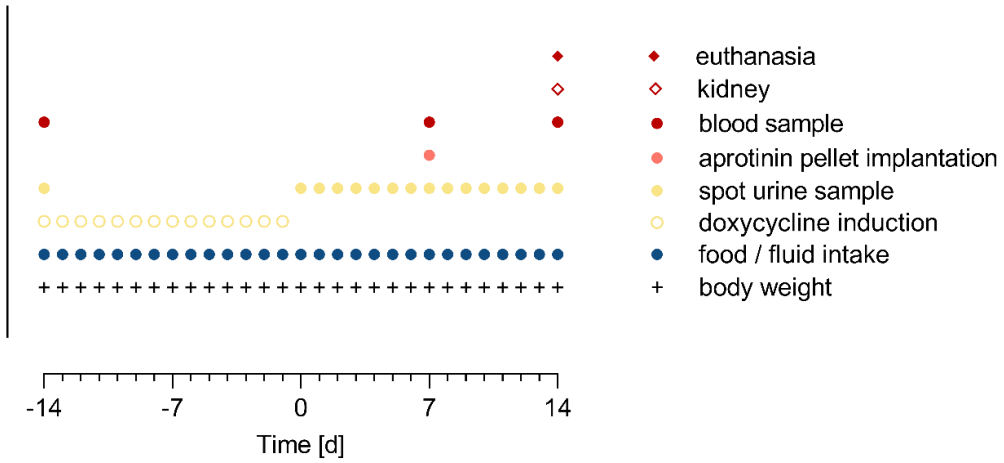

Figure 7 Timeline for the study of section I

To generate an inducible experimental NS in this study, a genetic mouse model by using tetO-Cre-lox P system was applied. This mouse model was established by mating mice which has a pair of floxed *nphs2* alleles (Bl6-Nphs2$^{tm3.1Antc}$), with mice carrying both a tetracycline-controlled transcriptional activator of a Cre recombinase (Tg (tetO-cre)^{1Jaw}), and a nephrin-targeted driven promoter (Tg (Nphs1-rtTA*3G)^{8Jhm})[74]. The genotype of these mice were Bl6-Nphs2$^{tm3.1Antc}$*Tg (Nphs1-rtTA*3G)^{8Jhm}*Tg (tetO-cre)^{1Jaw} and were referred to as *nphs2$^{\Delta ipod}$* mice[74]. Mice have two podocin alleles modified with flox but absent of either the Tg (tetO-cre)^{1Jaw} or Tg (Nphs1-rtTA*3G)^{8Jhm}, were served as control[74]. These mice were a kind gift from Dr. Florian Grahammer (University of Hamburg). Originally, he received Bl6-Nphs2$^{tm3.1Antc}$ mice from Géraldine Mollet and Corinne Antignac (Imagine Institute of Genetic Diseases, Paris, France, first published in 2009[31]) and Tg (Nphs1-rtTA*3G)^{8Jhm} mice from Jeffrey H. Miner (Washington University, St. Louis, USA[75]).

To characterize the model (Figure 7), *nphs2$^{\Delta ipod}$* mice (n=19) and control mice (n=10) received oral doxycycline administration for 2 weeks, and were observed for 2 weeks after induction. The first day started with doxycycline induction was defined as day -14.

The end of oral doxycycline administration was designated as day 0. Blood samples were collected before induction. Body weight, food, and fluid intake were daily monitored, and spot urine samples were daily collected until day 14.

To characterize the ENaC activation by proteasuria in this genetic model, a pellet containing extended release aprotinin were implanted to 4 nephrotic *nphs2*$^{\Delta ipod}$ mice on day 7 (Figure 7). *Nphs2*$^{\Delta ipod}$ mice were divided into two groups on day 7; 4 mice received aprotinin treatment at a dose of 1 mg per day. The rest of the mice did not receive any treatment. On day 14, blood samples were taken, and both kidneys were removed from both *nphs2*$^{\Delta ipod}$ mice and control mice. One kidney was harvested for Western Blot (WB), and the other one was used for immunofluorescence (IF).

2.1.2 Section II: Effect of plasminogen deficiency on sodium handling before and after induction of NS

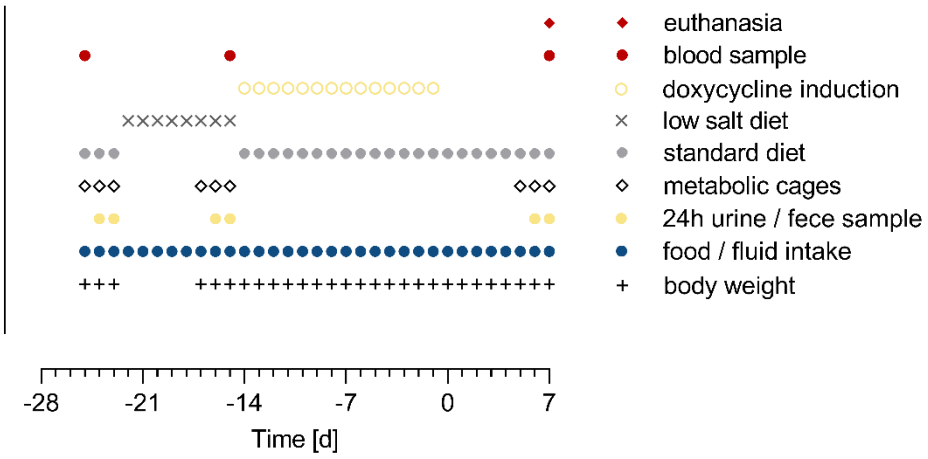

Figure 8 Timeline for Section II

To generate an experimental NS model with plasminogen deficiency, the *nphs2*$^{\Delta ipod}$ mice were intercrossed with plasminogen deficient mice (Bl6-Plg^{tm1Jld} or *plg*$^{-/-}$, hereinafter referred to as *nphs2*$^{\Delta ipod}$**plg*$^{+/+}$ mice and *nphs2*$^{\Delta ipod}$**plg*$^{-/-}$ mice respectively)[74]. *Plg*$^{-/-}$ mice were a kind gift from Edward Plow (Lerner Institute, Cleveland, USA[76]). All mice were on C57Bl/6 background, and the offspring was born at the expected Mendelian frequency [74].

To study the influence of plasminogen deficiency on ENaC dealing with sodium, uninduced *nphs2*$^{\Delta ipod}$ **plg*$^{+/+}$ mice (n=10) and *nphs2*$^{\Delta ipod}$**plg*$^{-/-}$ mice (n=11) were observed starting on day -25 (16 days before doxycycline treatment, Figure 8). Mice were housed

in metabolic cages individually for two days with a standard sodium-replete diet. Urine and feces were collected, food and fluid intake were monitored for calculating sodium balance. Results of sodium balance were averaged by data from two consecutive days. Mice were then put back into standard cages, and a low salt diet was given from day -22 until day -15. After a 5-day low salt diet, the observation in metabolic cages was repeated for the same mice on day -17 to day -15. The same procedure in the same mice in metabolic cages was repeated after induction of NS from day 5 to day 7, to investigate the effect of plasminogen deficiency on sodium balance in nephrotic animals. The finding of a significantly decreased urinary Na^+ excretion in 24h urine/ a positive sodium balance with a standard diet condition would be clear evidence of sodium retention in nephrotic mice. Food, fluid intake, and BW were monitored daily. Blood samples were taken on day -25 as a baseline, on day -15 after receiving low-salt diet, and on day 7 after induction, respectively. In a subset of mice from each genotype, kidneys were removed for histology study as the uninduced control. Mice were euthanized at the end of observation.

2.1.3 Section III : The effect of plasminogen deficiency on the course of experimental NS

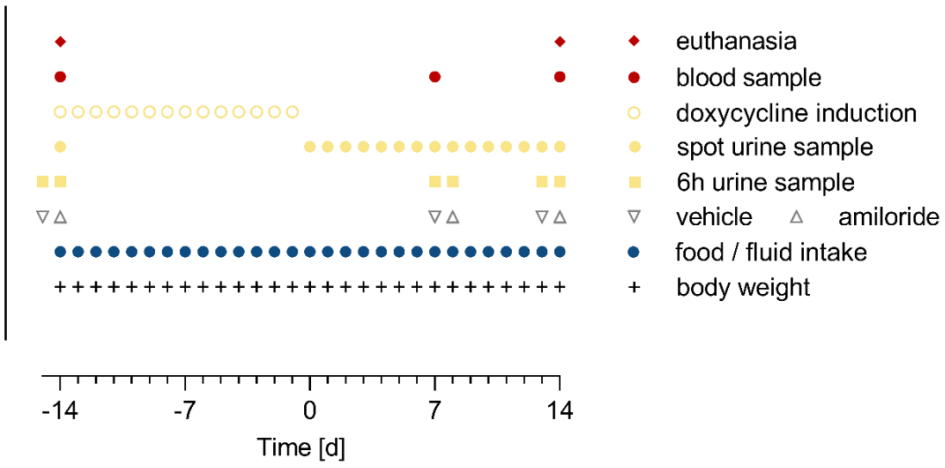

Figure 9 Timeline for section III

For the investigation of ENaC activity in experimental NS with plasminogen deficiency, an observation for amiloride-natriuresis during 7 days after induction of NS was performed in both genotypes (Figure 9). *Nphs2*$^{\Delta ipod}$**plg*$^{+/+}$ (n=10) mice and *nphs2*$^{\Delta ipod}$ **plg*$^{-/-}$ (n=11) mice received an intraperitoneal injection of injectable water or amiloride, respectively, on day -15 and day -14, as the baseline value. Mice started the oral

doxycycline treatment on day -14 after the amiloride injection. Vehicle and amiloride intraperitoneal administration was repeated on day 7, and day 8, successively. Mice were euthanized on day 8 after amiloride injection. ENaC activity was evaluated as a significantly decreased Na^+ concentration in 6h-urine after a vehicle injection, and an increased amiloride-sensitive urinary sodium excretion 6h after amiloride injection.

Because of the unexpectedly remission of sodium retention presenting body weight loss and increased urinary sodium excretion starting from day 11, amiloride-natriuresis study was performed in a subset of nephrotic *nphs2*$^{\Delta ipod}$ **plg*$^{+/+}$ mice (n=5) and nephrotic *nphs2*$^{\Delta ipod}$ **plg*$^{-/-}$ mice (n=6) on day 13 and day 14, respectively (Figure 9). The aim was to prove the ENaC activity during the "wash-out" phase was downregulated and was not blocked by amiloride any more. Mice were induced of NS by doxycycline treatment, and underwent blood sampling (75µl) on day 7. At the end of this cohort, One *nphs2*$^{\Delta ipod}$ **plg*$^{+/+}$ mouse and two *nphs2*$^{\Delta ipod}$**plg*$^{-/-}$ mice were ruled out because of the illness. Eventually, four mice of each genotype received vehicle and amiloride injection, and were euthanized after amiloride injection. An additional cohort was performed for short-term observation of the effect of plasminogen deficiency on sodium retention, and full characters of experimental NS in *nphs2*$^{\Delta ipod}$**plg*$^{-/-}$ mice (n=12) (Figure 9). *Nphs2*$^{\Delta ipod}$**plg*$^{+/+}$ mice (n=16) were used as control. Body weight, food and fluid intake were daily recorded. Spot urine samples were daily collected for laboratory measurements. Blood samples and kidneys were taken on day 14. Sodium retention was evaluated by increase of body weight, decrease of urinary Na^+ excretion in daily spot-urine samples.

2.1.4 Section IV: Effect of aprotinin treatment in nephrotic mice with plasminogen deficiency

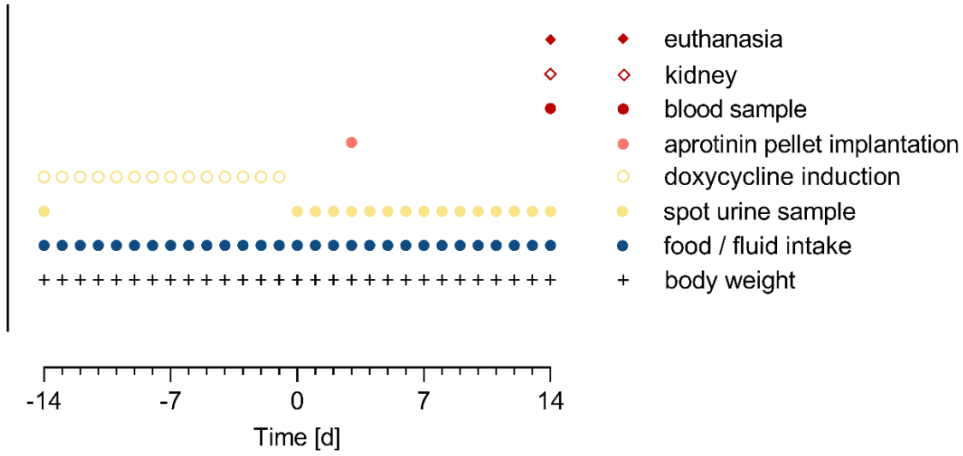

Figure 10 Timeline for section IV

To find out the effectiveness of aprotinin on nephrotic mice lacking plasminogen, pellets containing extended release aprotinin were implanted to each mice with plasminogen deficiency and the matched wild-type mice (Figure 10). *Nphs2*$^{\Delta ipod}$**plg*$^{+/+}$ mice (n=8) and *nphs2*$^{\Delta ipod}$**plg*$^{-/-}$ mice (n=8) received doxycycline treatment at 8 weeks of age for induction of NS. On days 3, *nphs2*$^{\Delta ipod}$**plg*$^{+/+}$ mice and *nphs2*$^{\Delta ipod}$ **plg*$^{-/-}$ mice randomly assigned to either the aprotinin (n=4) or placebo group (n=4). Mice received 2 sustained release-aprotinin pellets/ mouse containing the dose of aprotinin of 1mg/ day which were implanted subcutaneously during isoflurane narcosis. Mice receiving placebo pellets were used as control. Bodyweight and spot urine were collected before doxycycline induction and every day from day 0. Mice were sacrificed on day 8 (5 days after pellets implantation), blood samples, and kidneys were harvested (Figure 10).

2.1.5 Section V: Long-term effect of plasminogen deficiency in experimental NS

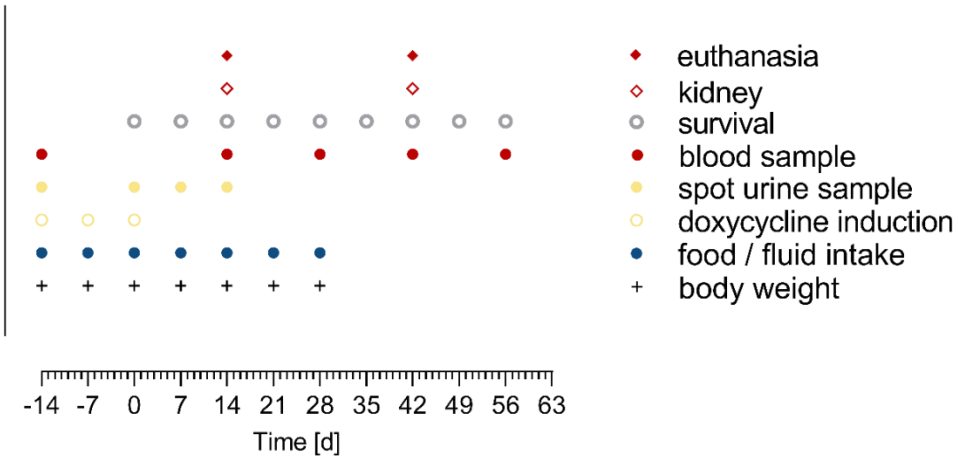

Figure 11 Timeline for Section V

A cohort observation of nephrotic mice in both *nphs2*$^{\Delta ipod}$**plg*$^{+/+}$ mice (n=14) and *nphs2*$^{\Delta ipod}$**plg*$^{-/-}$ mice (n=12) was followed up for 63 days after induction to study the lasting influence of plasminogen deficiency on kidney function (Figure 11). Among them, 16 mice (8 *nphs2*$^{\Delta ipod}$**plg*$^{+/+}$ mice and 8 *nphs2*$^{\Delta ipod}$**plg*$^{-/-}$ mice) were observed for two weeks to obtain a normal growth curve in both genotypes before induction. Mice then received doxycycline induction at 8-week old. Food, fluid intake, and weight of mice were daily monitored from day -14 until day 28, and spot urine samples were collected.

Blood samples (75µl) were taken from day -14 and were collected every two weeks thereafter for evaluating kidney function by plasma urea measurement. Another 100µl of blood samples were drawn for blood gas analysis (BGA) on day 14. Survival of mice were followed up until day 63 when all experimental mice died or euthanized, except for control mice. Mice were euthanized, and kidneys were removed when the prespecified score reached a value of more than 7, according to National Institutes of Health Guide for the Care and Use of Laboratory Animals and the German law for the welfare of animals.

2.2 Animal experiments

2.2.1 Genotyping

Ear tissues were collected from the offspring at 3 weeks of age. Genotyping of the offspring was performed as described in a standard protocol:

- *DNA extraction.* Ear tissues were stored at -20ºC in a 1.5ml/reaction tube before process. Tissue lysis, digestion and g-DNA extraction were processed by using a commercial kit (EchoLUTION Tissue DNA Micro Kit, AIM GmbH, Germany). A pre-mixed buffer contained 5 µl turbolyse T protease and 90 µl tissue lysis buffer per sample was pipetted to each sample. This mixture was kept at 60ºC for 30 minutes with maximum agitation. After that, the temperature was further increased to 80ºC for 10 minutes. During the incubation, the g-DNA-binding column was prepared and placed in a 1.5ml EP tube.

- *Purification of g-DNA.* After tissue lysis, 1 µl Rnase A and 10 µl Clearance buffer were added respectively to each sample. The mixture was centrifugated for 2 minutes at a maximum speed (13000 g) by centrifuge (Biofuge 13, Heraeus, Germany). Supernatant (90 µl) was collected and transferred to the g-DNA-binding column. Centrifuged the column for 1 minute at the speed of (1000 g). Subsequently, purified g-DNA was collected in the 1.5ml EP tube and stored at 4ºC if not used immediately, or at -20ºC for long term storage.

- *Polymerase chain reaction (PCR).* Primers and conditions used for genotyping of each genes were listed in Table 1 and Table 2 respectively.

- *Agarose gel electrophoresis.* Agarose-gels with 3%, 1.5% or 1.75% were prepared according to the amplicon size of each gene (standard-agarose mixed into 1x TAE buffer). Loading marker (1 µl 100 bp DNA Ladder, peQ Lab, Germany + 1 µl 6x DNA loading Dye, VWR International, Lithuania + 4 µl Ampuwa, Fresenius Kabi GmbH, Germany)

and PCR-product was pipetted into the well of agarose-gel. Electrophoresis was performed by Electrophoresis Power Supply (EPS 600, Bio Rad, USA) under 120 voltage for 40-60 minutes. The gel was stained by Nucleic Acid Gel Stain solution (GelRed, Biotium, USA) for 10-20 minutes, and results were observed under a gel-imaging system (Bio Rad, USA). Examples of genotyping images from each gene was shown in Figure 12.

- *Mice selection.* In total, sixty-two of *nphs2*$^{\Delta ipod}$**plg*$^{+/+}$ mice, forty-four of *nphs2*$^{\Delta ipod}$**plg*$^{-/-}$ mice, and ten control mice were included in this project.

Mice were kept on a 12:12-h light-dark cycle and fed a standard diet (ssniff, sodium content 0.24% corresponding to 104 µmol/g, Soest, Germany)[74]. Mice were free for access of tap water and food. All animal experiments were conducted under the regulation of the National Institutes of Health Guide for the Care and Use of Laboratory Animals, and followed the German law for the welfare of animals. Animal experiments were approved by local authorities (Regierungspraesidium Tuebingen, approval number M 15/17)[74].

Table 1 PCR conditions for genotyping[74]

Gene	Denaturation	Annealing	Extension	Cycles
Nphs2$^{tm3.1Antc}$[77]	94 ºC, 30 seconds	62 ºC, 45 seconds	72 ºC, 30 seconds	40
Tg(Nphs1-rtTA*3G)^{8Jhm}[77]	94 ºC, 30 seconds	57 ºC, 30 seconds	72 ºC, 45 seconds	40
Tg(tetO-cre)^{1Jaw}[77]	94 ºC, 30 seconds	57 ºC, 30 seconds	72 ºC, 60 seconds	35
Bl6-Plg^{tm1Jld}[78]	94 ºC, 30 seconds	60 ºC, 60 seconds	72 ºC, 60 seconds	30

Table 2 Primers used for genotyping[74]

Gene	sense/forward 5'→3' orientation	antisense/reverse 5'→3' orientation	amplicon	reference	Manufacturer
Nphs2$^{tm3.1Antc}$	CCAGCATCCCATTAGATAGATGAGG	GCATCCAAATGATCAGAGTTCCCAGG	236 / 286 bp (wild-type / floxed allele)	[31]	Eurofins Genomics
Tg(Nphs1-rtTA*3G)^{8Jhm}	GAAGCAGCAGAATGAGTTCACACTGGGTCC	ACTTTGCTCTTGTCCAGTCTAGACATGGTG	400	[79]	Eurofins Genomics
Tg(tetO-cre) ^{1Jaw}	GCATAACCAGTGAAACAGCATTGCTG	GGACATGTTCAGGGATCGCCAGGCG	280	[80]	Eurofins Genomics
Bl6-Plg$^{+/+}$ and Plg^{tm1Jld}	TCAGCAGGGCAATGTCACGG (wt) and GCACAGCTGCGCAAGGAACGCC (ko)	CTCTCTGTCTGCCTTCCATGG (wt) and AAGATGGATTGCACGCAGGTTCTC	450 / 230 (wild-type / ko allele)	[78]	Eurofins Genomics

(ko)

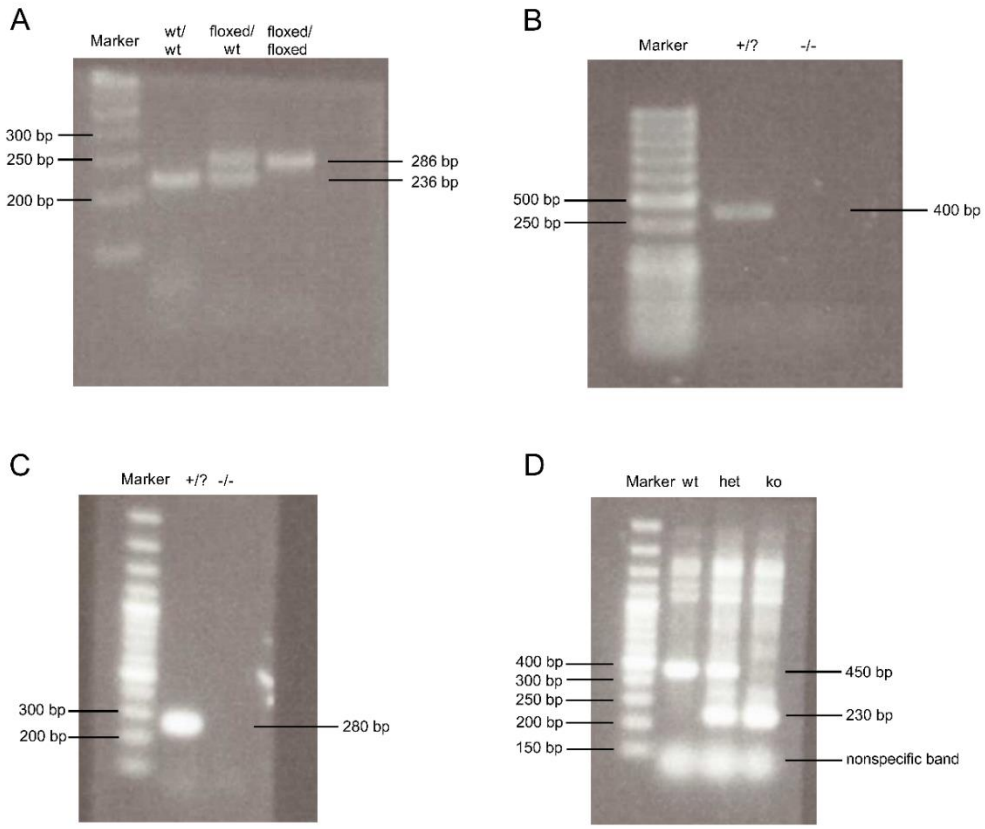

Figure 12 Examples of genotyping by PCR

(A) Genotyping of floxed *nphs2*. The expression of homozygote floxed *nphs2* was at 236 bp. Heterozygote floxed *nphs2* showed both bands at 236 and 286 bp, while homozygote wild type *nphs2* showed only one band at 286 bp.
(B) Genotyping of Nphs1-rtTA*3G^{8Jhm}. The result showed if the mouse contained at least one of nphs1-rtTA*3G)^{8Jhm} allele, it appeared at a single band at 400bp; if there was no band, the mouse did not express the transgene.
(C) Genotyping of tet-O cre. Presence of tet O-cre was observed at 280 bp.
(D) Genotyping of plasminogen showed the knock-out allele at 230 bp, and the wildtype allele at 450 bp.

Wt: wild type; het: heterozygote; ko: knock out; +/?: positive expression of the gene; -/- : negative expression of the gene

2.2.2 Induction of experimental nephrotic syndrome in nphs2$^{\Delta ipod}$ mice

As described in Chapter 1.2, *nphs2$^{\Delta ipod}$* mice were used to model experimental NS, which is based on a Tet O-Cre recombinase system and removes the floxed *nphs2* gene in the presence of doxycycline (Figure 13). All experimental animals including control mice, received a daily oral doxycycline treatment with a mixture of 2g doxycycline powder (Yancheng Suhai Pharmaceutical, China) and 50g sucrose in 1 L tap water for NS induction at the age of 8 weeks[74]. The duration of oral doxycycline

treatment was 2 weeks, and the water was changed every 3 days for preventing bacterial or fungus growth.

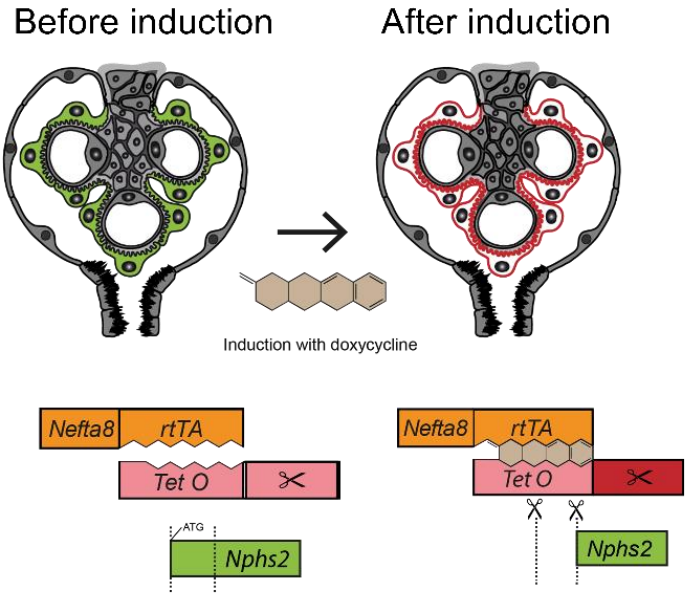

Figure 13 A schematic diagram of inducible *nphs2* (podocin, green) deletion in the podocyte before and after doxycycline initiation[74]

Upon exposure to doxycycline, the reverse tetracycline transactivator (rtTA) binds to the promotor (Tet O), which induces expression of Cre which in turn initiates the deletion of floxed *nphs2* gene. In *nphs2*$^{\Delta ipod}$ model, the rtTA is podocyte-specific (Nefta8), which means doxycycline induction of NS not affecting other cells and tissues (Figure was first published on May 2020 Acta Physiologica).

2.2.3 Daily monitoring of body weight, food and fluid intake, and the collection of spot urine samples

Spot urine samples were collected in clean Eppendorf-tubes by bladder massage individually during 8:00 – 9:00 every morning. Daily spot urine samples were used for monitoring the development of proteinuria, proteasuria and sodium retention, etc. Body weight of mice was obtained by keeping mouse individually inside a constraint container and weighing it on a balance. Due to the difficulties and inaccuracy in measurement of ascites, increase of body weight was taken as the parameter for the development of edema and ascites in nephrotic mice. The increase of body weight was a hint of ascites despite a stable food and fluid intake. The increase of body weight was calculated as the following: difference in BW (%) = (BW on day 0, 1,2… - baseline value of BW) / baseline value of BW *100%. Body weight on day 0 was used as baseline value.

Food and fluid intake were monitored by weighing the weight and recoding the

differences between two days. The calculation of the intake was: intake of food/fluid (g) = (weight of food/ fluid on the day before - weight of food/ fluid) / number of mice in the cage.

2.2.4 Blood sampling

Blood was drawn from the orbital sinus under anesthesia by isoflurane-inhalation[81] using a gas anesthesia machine, which contains an oxygen flow of 2 l/min and a precision vaporizer. The dose for induction anesthesia was 4-5 vol% of isoflurane as regulated by the animal warfare. A 125 µl of blood sample was drawn for blood gas analysis. A 75 µl blood sample was centrifuged for 20 min at a speed of 800 g, then the supernatant (plasma) was stored at -20 ºC for later measurements.

2.2.5 Implantation of extended release aprotinin pellets

The subcutaneous aprotinin pellets with a matrix-driven sustained release were custom-made by Innovative Research of America, Florida, USA[34]. The procedure of implantation was performed as following[34] (this surgery was performed by Dr. Bernhard N Bohnert):

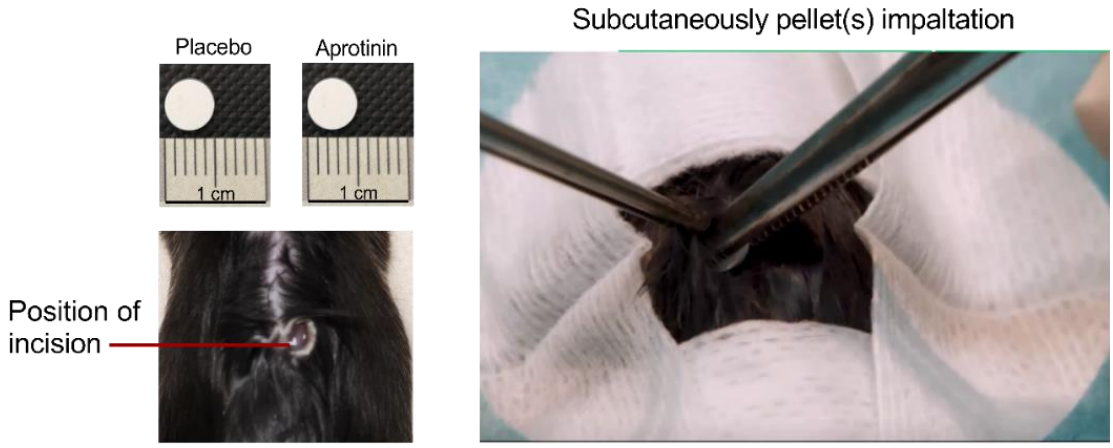

Figure 14 Aprotinin pellets implantation subcutaneously[34]

- The instruments and materials for the implantation were prepared, including a pair of hair scissors, a pair of skin preparation scissors, a surgical scalpel, surgical tweezers, two pairs of tissue tweezers, a needle holder, and 15 cm non resorbable monofil suture[34].
- Instruments were sterilized before the implantation in advance by using a heat sterilizer

for 5 min at 240 °C[34]. The instruments were needed to cool down until room temperature before using.

- The implantation was performed under isoflurane narcosis (5 vol% for induction and 1.5 vol% for maintenance)
- Mice were put in a prone position and were kept the temperature about 37 °C. Eyes of mice were protected with ointment during operation.
- Hair on the center back of mice was removed using hair scissors. After disinfection, the hairless skin was incised about 5 mm length with a surgical scalpel in a vertical direction (Figure 14)[34]. A left lateral pocket of about 1 cm depth in the subcutaneous connective tissue[34] was prepared using a dull tweezer. For interventional treatment, one 10-day release aprotinin pellet containing a dose of 10 mg was inserted into the pocket mentioned above by sterilized tweezers on day 7 after induction of NS. For preventive intervention, 2 aprotinin/ placebo pellets were implanted to each mouse on day 3 at the end of doxycycline treatment. The two pellets had to keep distance on each side at the back of mice, so that they did not overlap and influence the treatment effect.
- The wound was sutured, and mice were kept individually after the surgery.

2.2.6 24h urine samples collection in metabolic cages and calculation of sodium balance

Sodium excretion generally equals to sodium intake in human and mice with normal kidney function and sodium handling. Sodium handling was observed by calculating sodium balance in uninduced mice with both genotypes, under conditions with either a standard or a low-salt diet. Each mouse was weighed and put with an emptied bladder into metabolic cages individually from 8:00 until the next day at 8:00 (24h). Urine samples and feces were collected, and weighed 24h after hosing in metabolic cages. Mice were free for tap water and food during the whole observation.

A standard diet contains 106 µmol/g of sodium (C1000, Altromin, Lage, Germany), and a low salt diet contains 7 µmol/g of sodium (C1036, Altromin, Lage, Germany). Tap water contains 1µmol/g of sodium. Sodium balance was calculated as following:

Sodium balance [µmol/ml] = (sodium intake from food + sodium intake from fluid) – (24h urinary sodium excretion + 24h fecal sodium excretion)

2.2.7 Natriuretic response to amiloride

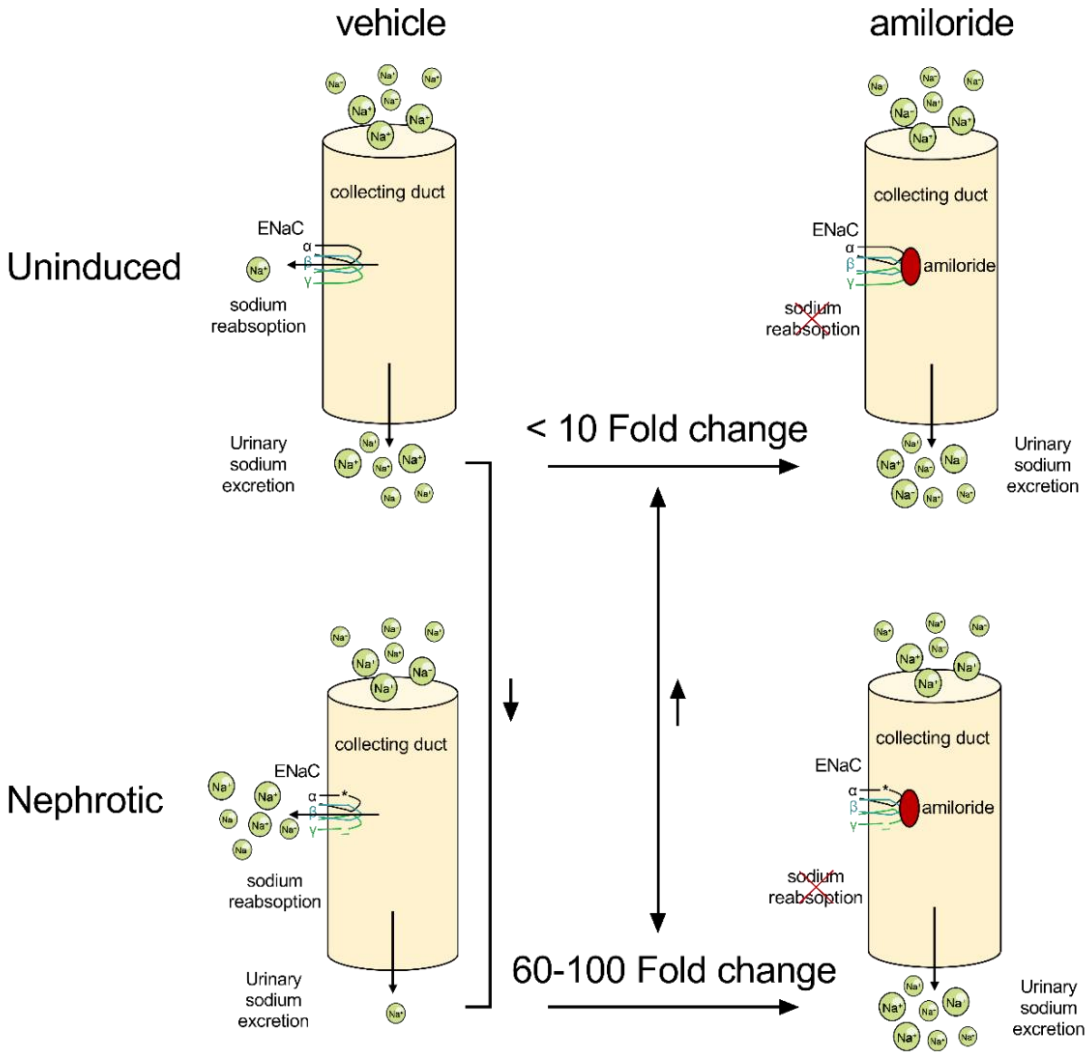

Figure 15 The schematic diagram of amiloride-natriuresis experiment

Urinary Na^+ excretion after a vehicle injection was taken as baseline value in uninduced mice. In principle, there would be an increase in urinary Na^+ excretion after a high dose of amiloride injection, even in mice with normal sodium handling. After NS was established in mice, urinary Na^+ excretion would be extremely low with vehicle injection, while amiloride injection could markedly increase the excretion of sodium indicating ENaC activation in nephrotic animals.

Amiloride-induced natriuresis was determined to assess ENaC activity in both uninduced and nephrotic *nphs2*$^{\Delta ipod}$**plg*$^{+/+}$ mice and *nphs2*$^{\Delta ipod}$**plg*$^{-/-}$ mice. The urinary sodium excretion in uninduced mice after a vehicle injection reflected baseline natriuresis. The response to amiloride obtained in uninduced animals was compared to the response in the same animal after induction of NS. The expectation was that urinary Na^+ excretion after

a vehicle injection during the nephrotic stage significantly decreased, indicating sodium retention. Since urinary Na^+ excretion was markedly increased by amiloride injection, this would be the strong evidence in favor of ENaC activation in nephrotic animals. The difference in amiloride-natriuresis between uninduced and nephrotic mice reflects the degree of ENaC activation (Figure 15).

For vehicle injection, mice received 5 µl/g bw injectable water; and for amiloride injection, mice were injected with a dose of 10 µg/g bw amiloride intraperitoneally[74]. Injection was given at 8:00 in the morning of the experiment day. Urine was voided before injection. Mice were kept individually in regular cages after injection. Urine samples were collected, and weighed (g) 6h later to determine the volume.

Urinary sodium excretion in 6 hours was calculated for each mouse as following:

Urinary sodium excretion /* 6h [µmol/6h] = urinary sodium concentration $_{\text{measured by flame-photometer}}$ [µmol/ml] * weight of urine [≈ml]

2.2.8 Euthanasia and kidneys collection

At the end of observation, if blood samples were not needed, mice were euthanized mice by exposing them to isoflurane with a dose of 5 vol% for a minimum of 2 minutes. The vaporizer was stopped when the movement and respiration of mice were not observed anymore. A cervical dislocation was applied to ensure euthanasia and death of the mice. If blood samples were needed from the animals, after 90 seconds of Isoflurane-induced anesthesia, blood was drawn from the retro-orbital sinus as much as possible. For kidneys collection, mice were placed on the table in the supine position. A midline laparotomy from the top of the pubic bone to the sternum was performed, and the abdominal skin and the muscles were cut with scissors. The blood vessels connected to the left kidney were clamped. The right kidney was then perfused by injecting 5 ml of Phosphate-Buffered Saline (PBS) (Sigma-Aldrich, Germany) to remove excess blood, and was fixed successively with an injection of 5 ml 4% Paraformaldehyde (PFA, Otto Fischer GmbH & Co.KG, Germany) for histology study. The left kidney without perfusion was then removed and stored at -80 ºC for WB analysis.

2.3 Laboratory measurements

2.3.1 Urinary protein

Urinary protein was measured using a colorimetric method according to Bradford[74,82]. Urine samples were measured undiluted before induction of NS and were diluted 10-20 folds during proteinuria. Undiluted/diluted urine (2 µl) was added into a 1ml 1x Bradford working solution (Bio-Rad Laboratories, Germany) and was incubated at room temperature (RT) for 8 minutes. Absorbance was obtained at a photometer at a wavelength of 595 nm. Distilled water (ddH2O)/Ampuwa (2 µl) was used as blank control. The photometer was calibrated with bovine serum albumin (BSA) from 1-10 mg/ml. Data were recorded in a laboratory book entitled with date, series number, mouse ID, and results with the unit as mg/ml (and so as all the other measurements). Data from diluted samples were multiplied with the dilution factor accordingly. The ratio of urinary protein and urinary creatinine (urinary protein [mg/ml]/ creatinine [mg/dl]) was used as the parameter of proteinuria evaluation [mg/mg crea].

2.3.2 Urinary creatinine

Urinary creatinine was measured using the colorimetric Jaffé method (Labor+Technik, Berlin, Germany). DdH_2O/ Ampuwa (10 µl), standard solution (2 mg/ml), and 10- or 20-fold diluted urine sample were added into cuvettes with a 1 cm light path, respectively. Working solution (picric acid + NaOH, 200 µl) was pipetted into cuvettes before reading. The cuvettes were put into a photometer with a wavelength of 492 nm and the first absorbance (A1) was read 10 seconds later. After exactly 8 minutes, the second absorbance (A2) was obtained. The creatinine concentration (C_{crea}) was calculated according to the following formula:

Delta A = Absorbance A1 – Absorbance A2

C_{crea} [mg/dl] = (Delta A_{sample} - Delta A_{blank}) / (Delta $A_{standard}$ - DeltaA_{blank}) * $Conc._{Standard}$ * DF

2.3.3 Urinary/ fecal sodium concentration

Urinary and fecal Na^+ concentration was measured using an automated flame photometer (Eppendorf EFUX 5057, Germany). Urine samples were directly measured by flame photometer undiluted, and values were normalized to the urinary creatinine concentration. The linear range of Na^+ measurement was 10-200 mM. Feces were collected over 24 h in metabolic cages and were dried at 80ºC for 3 hours, dry feces were weighed and dissolved

in 3 ml of 0.75 M HNO_3 overnight to generate a creamy mass. After centrifugation at 683 g by an universal table top refrigerated centrifuge (Megafuge 2.0R, Heraeus, Germany) for 10 min, 1 ml of the supernatant was measured directly by the flame photometer[83]. Fecal sodium content in µmol/24 was calculated by multiplication with 3.

2.3.4 Urinary plasmin activity

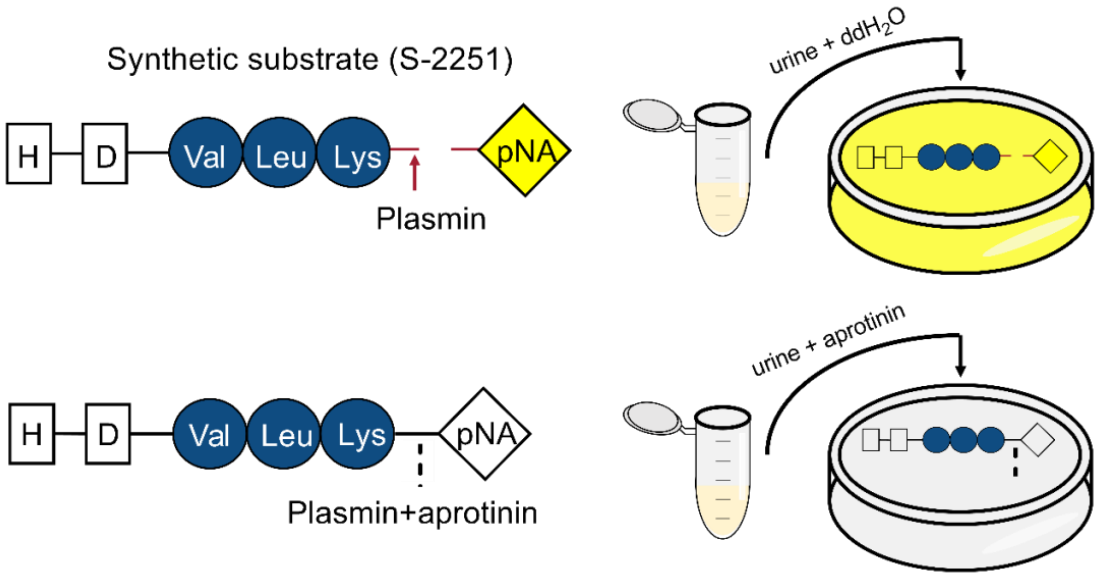

Figure 16 Illustration of the principle of urinary amidolytic activity measurement by using a synthetic substrate (S-2251)

The substrate S-2251 (H-D-Valyl-L-leucyl-L-lysine-p-Nitroaniline dihydrochloride) is a synthetic tripeptide substrate coupled to a chromophore pNA. When pNA is liberated from the substrate by cleavage of plasmin (↑ indicating the cleavage of substrate by plasmin), an increased absorbance at 405 nm will be detected and will be proportional to the plasmin activity. Aprotinin is a wide spectrum serine protease inhibitor that can inhibit plasmin activity (¦indicating the inhibition effect of the substrate cleavage by plasmin) and is added into urine samples to calculate the aprotinin-sensitive activity which represents plasmin activity in this assay.

The urinary activity of plasmin was measured by the proteolysis of the amid bond of the chromogenic substrate S-2251 releasing the chromophore p-Nitroaniline dihydrochloride ne dihydrochloride (pNA), so called urinary amidolytic activity (Figure 16). S-2251 is a preferred tripeptide substrate of plasmin (Haemochrom, Germany). 3 µL urine and 50 µL 2 mM substrate was incubated for 60 minutes at 37°C with or without the plasmin inhibitor aprotinin (final concentration 20 µg/ml)[74]. The values of optical density (OD) of blank and samples were obtained at 405 nm on a 96-well plate reader (Biotek EL800, VT, USA). The difference between the OD_{405} with or without aprotinin reflected the

predominant activity of plasmin[74]. Values were expressed as relative units.
Calculation of urinary amidolytic (plasmin) activity as the following formula:
Urinary amidolytic activity [OD/60*1000] = ($OD_{405\ without\ aprotinin}$ - $OD_{405\ with\ aprotinin}$) / 60 *1000

2.3.5 Plasma/ urinary albumin

In NS, concentration of plasma albumin decreases as a consequence of large proteinuria, and leads to hypoalbuminemia. Plasma albumin concentration was measured with a fluorescent ligand (Albumin blue, Carlsbad, USA). The standard curve was prepared using mouse plasma albumin (Sigma, stock solution with 1000 µg/ml in Ampuwa) in the range of 10 - 500 µg/ml. Urine or plasma samples were briefly centrifugated (at 1000 g, for 5 min,) before measurements. Plasma samples were diluted 100-200 fold, while urine samples were directly measured. Mouse standard albumin or samples (20 µl) were pipetted into each well of a 96-well microcuvette. After addition of 100 µl dye reagent, wells were incubated for 5 min RT. The fluorescence was measured at an excitation wavelength of 560 nm and emission wavelength of 620 nm. Calculation of the concentration was done using a linear standard curve (Y= a x + b) in Excel which had to have an R^2 value of > 0.95.

2.3.6 Plasma cholesterol

Hyperlipidemia or hypercholesterolemia is also one of typical characters of NS. Total plasma cholesterol was measured by a colorimetric kit (Labor+Technik, Berlin, Germany) to fully characterize the experimental NS in this study. DdH_2O/ standard solution or undiluted sample (3 µl) was pipetted into a cuvette. After addition of 300 µl reagent and mixing, the samples were incubated for 60 min RT. Subsequently, OD value was read at a wavelength of 546 nm. Calculation of the concentration was according the following formula:

$C_{cholesterol}$ [mg/dl] = ($E_{sample} - E_{blank}$) / ($E_{standard} - E_{blank}$) * $C_{standard}$ (standard concentration is 200 mg/dl, E_{sample} stands for measured value of sample; E_{blank} stands for measured value of ddH_2O; $E_{standard}$ stands for measured value of standard)

2.3.7 Plasma urea

Plasma urea is a marker of kidney function, which reflects glomerular filtration rate. The increase of plasma urea indicates the decrease in GFR and the damage of kidney function. Concentration of plasma urea was measured using a colorimetric kit (Labor+Technik, Berlin, Germany). DdH2O/ standard solution or sample (3 µl) was added into a cuvette. Samples were undiluted or diluted into 3 folds, depending on the kidney impairment. After pipetting, additional 300 µl reagent was added and mixed up and down for 30 sec. Samples were incubated for 8 min at RT and measured by a photometer at a wavelength of 334 nm. Calculation of the concentration was according to the following formula:

C_{urea} [mg/dl] = ($E_{sample} - E_{blank}$) / ($E_{standard} - E_{blank}$) * $C_{standard}$ * dilution factor (standard concentration is 2 mg/dl)

2.3.8 Plasma creatinine

Creatinine is one of the products that mostly eliminated through kidneys, and the increase of plasma creatinine indicates the decline of kidney function. Plasma creatinine could be measured reliably by HPLC in mice, however, was not available. Therefore plasma creatinine was measured by an enzymatic kit (Labor+Technik, Berlin, Germany) in this study. DdH_2O/ standard solution or undiluted samples (10 µl) were pipetted into cuvettes. An additional of 250 µl reagent 1 was added into the cuvette and mixed by up and down subsequently. The mixture was incubated at RT for 5 min. After incubation, 125 µl reagent 2 was pipetted into the cuvette, mixed and incubated for 1 min. OD values were obtained at a wave length of 490 nm. The concentration of plasma creatinine was calculated as following:

C_{crea} [mg/dl] = ($E_{sample} - E_{blank}$) / ($E_{standard} - E_{blank}$) * $C_{standard}$ ($C_{standard}$ = 2.00 mg/dl)

2.3.9 Plasma aldosterone

The underfill theory claims a low osmotic plasma pressure caused by hypoalbuminemia, which activates the RAAS and causes the increase of plasma aldosterone as described in Chapter 1.3. Besides, there is good evidence demonstrating that the number of ENaC expressed on the tubular membrane is related to plasma aldosterone level. Thus, to investigate the change of plasma aldosterone in the experimental NS model, and the difference between nephrotic $nphs2^{\Delta ipod}$*$plg^{+/+}$ mice and $nphs2^{\Delta ipod}$*$plg^{-/-}$ mice, plasma aldosterone concentration was measured by a competitive ELISA kit (IBL, Germany)

(Figure 17).

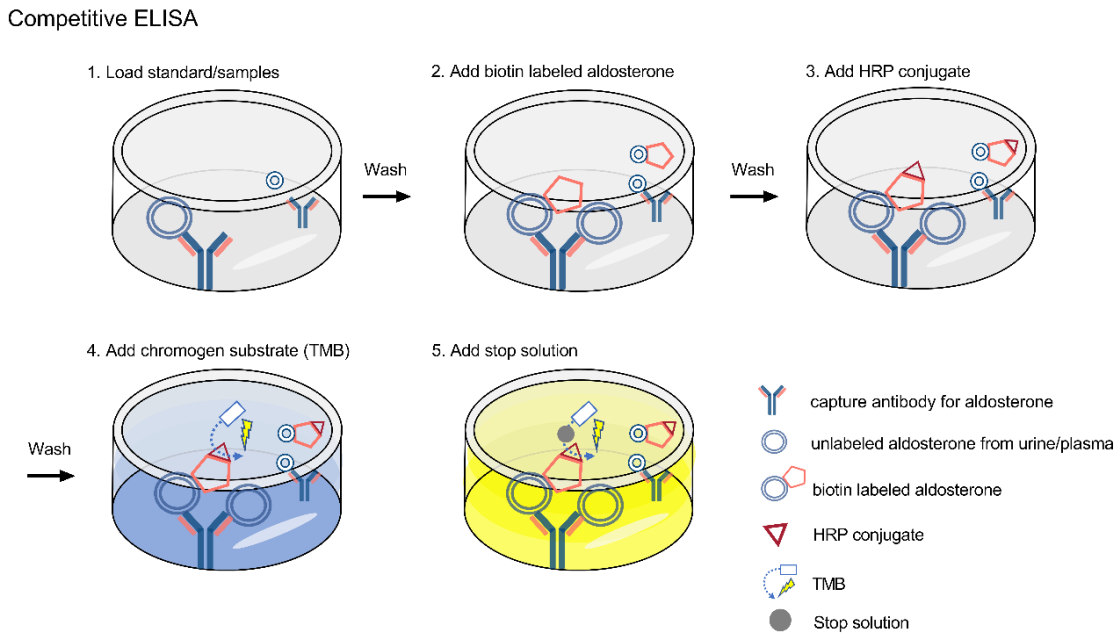

Figure 17 Diagram of the principle and steps of plasma aldosterone concentration measurement by using an ELISA kit based on competitive technique

Calibration was made using standards with the following concentrations: 0, 20, 80, 200, 500, 1000 [pg/ml] and checked by the use of positive/ negative controls. Plasma samples were measured undiluted by pipetting 25 µl into the micro plate coated with anti-aldosterone antibodies. After incubation for 30 min at RT 100 µl, the biotin-conjugated aldosterone was added as a tracer and mixed thoroughly for 10 sec. After another incubation for 60 min at RT, each well was washed with 400 µl of 1x wash buffer (1:40) for 5 times and removed excess solution. 200 µl of TMB substrate was added to each micro cuvette by a multiple channel pipette, and incubated for 30 min at RT. The reaction was stopped by adding 100 µl of TMB stop solution. OD values were obtained with a microplate reader at 450 nm. The obtained OD values (y-axis, linear) of the standard were plotted against their concentrations (x-axis, logarithmic) on a sigmoidal, four-parameter logistic graph (Figure 18, GraphPad Prism 8, GraphPad Software, San Diego, CA, www.graphpad.com). The equation of calculation the aldosterone concentration (X values [pg/ml]) was:

Y = Bottom + (X^ Hillslope) * (Top - Bottom) / (X ^ Hillslope + IC50 ^ Hillslope)[84]

(Y was the obtained OD value; values of Bottom, Top, Hillslope, and IC 50 were all reported by Prism). The interpolated X values then were multiplied by the dilution factor

to get the final concentrations.

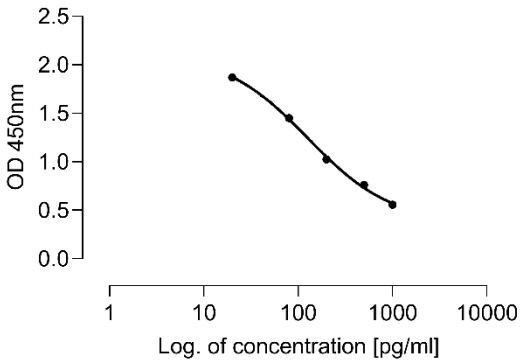

Figure 18 Standard curve of plasma aldosterone measurement

2.3.10 Plasma plasminogen/ urinary plasmin concentration

To investigate the development of plasminuria in nephrotic *nphs2*$^{\Delta ipod}$**plg*$^{+/+}$ mice, urinary plasminogen concentration was measured in *nphs2*$^{\Delta ipod}$**plg*$^{+/+}$ mice by using a commercial ELISA kit (AssayPro, USA) which is based on a quantitative sandwich enzyme immunoassay technique (Figure 19). The influence of plasma plasminogen concentration in nephrotic *nphs2*$^{\Delta ipod}$**plg*$^{+/+}$ mice was measured by this ELISA kit as well.

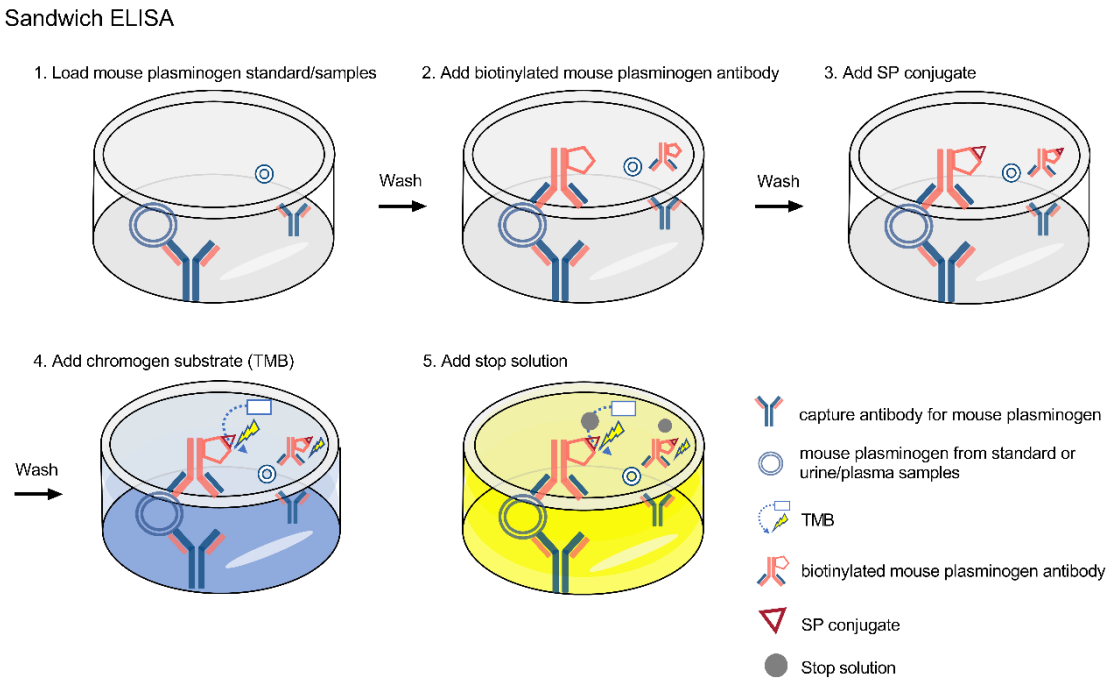

Figure 19 Diagram of the principle and steps of plasma/urinary plasmin(ogen) activity measurement by using a sandwich ELISA kit

Calibration was made using standards with the following concentrations: 6.0, 3.0, 1.5, 0.75, 0.375, 0.188, 0.094, 0 [ng/ml]. Plasma samples were diluted 50000 – 100000 fold according to the development of proteinuria and proteasuria. Urine samples collected from uninduced mice were diluted 100 fold, while the nephrotic urine samples were diluted into 5000 – 100000 folds. 50 µl of each standard/ sample was pipetted into the micro cuvettes and incubated for 120 min at RT. The plate was washed with 200 µl of 1x wash buffer for 5 times and excess solution was removed. 50 µl of biotinylated mouse plasminogen antibody was added and incubated for 60 min at RT. After washing as stated above, 50 µl of SP conjugate was added and incubated for 30 min at RT. After another wash procedure, 50 µl of chromogen substrate was added and incubated at RT for 10 min. 50 µl of the stop solution was added to stop the reaction, and the absorbance was immediately read at 450 nm using by a microplate reader. The standard curve was drawn by plotting the absorbance (on a Y-axis) against the concentrations of standard on the X-axis on a log-log paper (Graphpad Prism 8)(Figure 20). The unknown plasma/urinary plasmin concentration from the sample was determined from the standard curve and multiplied with the dilution factor. The calculation of concentration (X values [µg/ml]) was following the equation below:

Y (OD values) = 10 ^ (slope * log(X) + $Y_{intercept}$) * DF / 1000 (OD values were obtained; slope and $Y_{intercept}$ were reported by Prism)

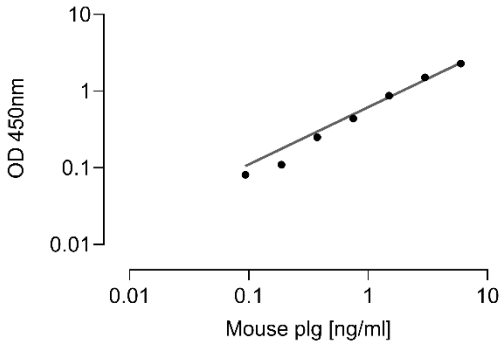

Figure 20 Standard curve of plasma/ urinary plasmin(ogen) measurement

2.3.11 Plasma/ urinary aprotinin concentration

To investigate the achieved concentration of aprotinin in both plasma and urine, plasma and urinary aprotinin were measured by a commercial competitive ELISA kit (Cloud-clone corp, China). Standard solution using the same aprotinin as given to the mice (Loxo,

Germany), was prepared with the following concentration: 100, 33.33, 11.11, 3.70, 1.23, 0 [ng/ml] was prepared in advance. Plasma samples were diluted 50-100 fold, while urine samples were 10-20 fold diluted using PBS as the dilution solution. Pipette 50 µl of each standard/ sample into each microcuvettes, respectively. 50 µl of detection reagent A was pipetted and the incubation at 37°C lasted for 60 min. The incubation was followed by a wash step with 350 µl of 1x wash buffer for 3 times. 100 µl of detection reagent B working solution was added into each microplate and incubated for 30 min at 37°C. The wash procedure was repeated for 5 times. Subsequently, 90 µl of substrate solution was added and incubated for 10 – 20 min at 37°C. The reaction was ended by Adding 50 µl of the stop solution, and OD values were immediately obtained at 450 nm by using by a microplate reader. The standard curve draw by plotting the obtained OD values on the X-axis, and the log concentration of the diluted standards on the Y-axis by using a Semi-log regression fit (Graphpad Prism 8)(Figure 21). The concentration of plasma/urinary aprotinin was calculated by using the following equation:

Y [µg/ml] = 10 ^ (Slope * X + $Y_{intercept}$) * DF / 1000 (X was the obtained OD value; Slope, $Y_{intercept}$ were reported by Prism;)

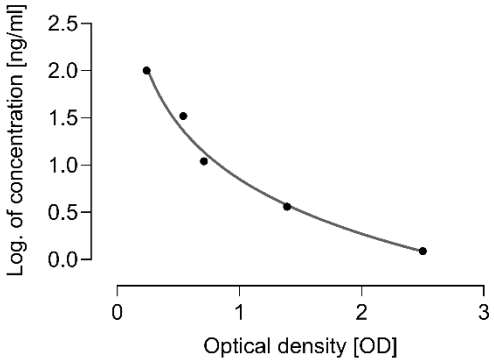

Figure 21 Standard curve of plasma/ urinary aprotinin concentration measurement

2.3.12 Plasma cystatin C concentration

Plasma cystatin C or cystatin 3, is a biomarker of kidney function, which is more accurate and sensitive than plasma creatinine and plasma urea. Unlike plasma creatinine and plasma urea, plasma cystatin C is less dependent on age, gender, muscle mass and protein intake. The increase of plasma cystatin C indicates the decline of kidney function and GFR[85]. Urinary cystatin C was reported as a sensitive marker of renal tubular injury[86-89]. Concentration of plasma or urinary cystatin C was measured by using a sandwich-ELISA

kit (R&D Systems, Inc, USA). Calibrations were prepared as the following concentration: 8000, 4000, 2000, 1000, 500, 250, 125, 0 [pg/ml]. Plasma samples were diluted 200 – 1000 fold depending on the development of renal impairment. 50 µl of standards or samples was pipetted into each well of the 96-plate, and mixed with 50 µl of Assay Diluent RD1W. The samples were incubated at RT for 120 min. The solution in each well was removed and the plate was washed by 1x Wash Buffer (400 µl/ well) for 5 times. 100 µl of Mouse Cystatin C conjugate was pipetted into each well after washing. Incubated for 12 min at RT. Repeated the wash step for 5 times after incubation. 100 µl of substrate Solution was added and incubated for 30 min at RT (notice that light protection was needed in this step). 100 µl of the stop solution was pipetted into each wells to end the reaction, and the absorbances were read at 450 nm within 10 min using a microplate reader. The standard curve was drawn by plotting the absorbance (on a Y-axis) against the concentration of standard on the X-axis on a four-parameter logistic paper (Graphpad Prism 8)(Figure 22). The unknown concentration of plasma/urinary Cystatin C was calculated using the equation described in plasma aldosterone measurement.

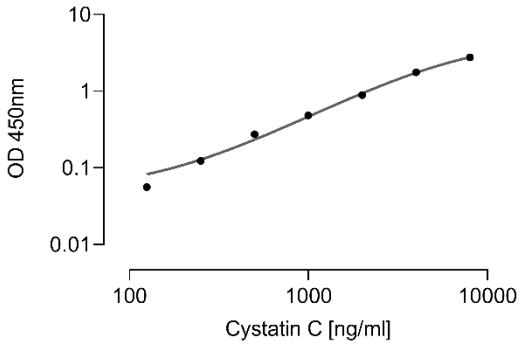

Figure 22 Standard curve of plasma Cystatin C measurement

2.3.13 Venous blood gas analysis (BGA)

Venous BGA provided the values of pH, standard HCO_3^-, plasma electrolytes including Na^+, K^+, and Ca^{2+}, haematocrit (hct), and calculated haemoglobin concentration (cHb), etc. Alkalemia or acidemia in nephrotic mice could be determined by plasma pH and standard HCO_3^-. Patients or animal models with kidney disease could have plasma electrolytes disorders, such as hypernatremia, hyponatremia, hyperkalemia, and hypocalcemia. Thus, plasma electrolytes should be monitored. Hct, and cHb concentration could determine if mice had anemia, which is a common complication of

CKD. A blood sample of about 125 µl was collected in a capillary glass tube, and BGA was done immediately using an IL GEM® Premier 3000 blood gas analyzer[74] (Instrumentation Laboratory, Munich, Germany).

2.4 Periodic acid–Schiff (PAS) from kidney tissue

Histology study is essential for diagnosing of NS in both clinical practice and model-study. By using PAS method, the structural damage of glomeruli and tubuli, as well as proteinuria could be observed. The kidneys were immersed in 10% formalin and embedded in paraffin. Formalin-fixed, paraffin-embedded sections (5 µm) were deparaffinized and hydrated to deionized water. The tissue sections of control mice and nephrotic *nphs2*$^{\Delta ipod}$ mice with both plasminogen wild type and deficiency were processed on the same slide. Slides were oxidized in 0.5% periodic acid solution for 5 min, RT. Slides were stained with Schiff solution for 15 min, RT, after rinsing in ddH_2O from the last step. Slides were washed by running tap water for at least 5 min and were counterstained afterward in Hematoxylin solution for 1.5 min, RT. After repeating the rinsing step, slides were dehydrated, cleared and sealed by toluene for light-microscopy observation (technology and images were provided by III. Department of Medicine, University Medical Center Hamburg-Eppendorf, Hamburg, Germany)[74].

2.5 Western blot (WB) from urine samples and kidney tissue of mice

WB detected Semi-quantitatively albuminuria and the expression of plasminogen excretion in mouse-urine samples. 10 µg of urine protein (or maximum volume when urine protein was less than 10µg)[74] was loaded into each lane of an 8% gel for SDS-PAGE. A rabbit antibody directly against for the heavy chain of plasminogen (ab154560, abcam, England), amino acid residues 84-434, was applied to detect plasminogen expression. Plasminogen (zymogen) can be cleaved at 105 kDa. After the cleavage, a heavy chain of 80 kDa released and could be detected by the antibody mentioned above[74]. Albumin was detected using an antibody from R&D systems (AF3329)[74] (the method and data analysis from this part was provided by Mr. Matthias Wörn).

Glomeruli isolation was done by using a biotinylation approach and cell sorting[74,90]. For protein detection of podocin, an antibody from Sigma, Germany, was applied (P0372)[74] (technology and images were provided by Dr. Grahammer, III. Department of Medicine,

University Medical Center Hamburg-Eppendorf, Hamburg, Germany).

The cortex of one kidney of each mouse was dissected using a scalpel. The cortex tissue was homogenized by a Dounce homogenisator in 1ml lysis buffer, which consist of 250 mM sucrose, 10 mM triethanolamine HCl, 1.6 mM ethanolamine, and 0.5 ethylenediamine tetraacetic acid at pH 7.4[35] (all Sigma-Aldrich, Germany). The homogenate was then centrifuged at 300,000 g for 1 hour, at 4 ºC. The pellet from last step was resuspended and boiled in Laemmli buffer (Sigma-Aldrich, Germany) at 70 ºC for 10 minutes[35]. Note: to prevent the cleavage of γ-ENaC, aprotinin (40mg/ml) and a mixture of other protease inhibitors (final concentration 0.1 x stock; cOmplete, Roche Diagnostics, Germany)[35] were added during the preparation.

Electrophoresis was performed by loading 40 mg of homogenate from last step on a 7.5 % polyacrylamide gel for detection of γ-ENaC[35]. For electrophoresis of α-ENaC and β-ENaC, a polyacrylamide gel of 7%, and 8% was used respectively. The blocking of blots was performed after transferring to nitrocellulose membranes, by incubation with the antibodies in a 1:500 dilution overnight, at 4 ºC.

For this study, the antibodies used to detect ENaC subunits were obtained from rabbits against the amino acids at 45-68 for α-ENaC, 617-638 for β-ENaC 634–655 for γ-ENaC (Pineda, Germany), respectively[74,91,92]. Besides, the detection of γ-ENaC was verified by an antibody directed against the same immunogenic peptide (SPC-405, Stressmarq)[74]. Subsequently, blots were incubated with the secondary antibody labelled with fluorescent infrared dyes (fluorescent donkey anti-rabbit, LI-COR Biosciences, Lincoln, USA) with a dilution ratio of 1:20,000 for 1hour, at 4 ºC. Finally, blots were scanned by a fluorescence scanner (Odyssey, LI-COR Biosciences, Lincoln, USA)[74]. For loading control, total protein was measured using Revert Total Protein Stain (Licor, Lincoln, USA)[74] (the method and data analysis from this part was provided by Ms. Andrea Janessa).

2.6 Immunohistochemistry and immunofluorescence from kidney tissue

One kidney was removed from each mouse. Kidney tissue for immunohistochemistry with a size of 1.0 cm x 1.0cm x 0.2cm was fixed by formalin and embedded with paraffin and was sliced into 2μm sections. Sections were deparaffinized and rehydrated using a standard protocol[74], and were blocked with normal goat serum for 15 minutes[74]. The dilution of the goat serum was with 50 mM of tris (hydroxymethyl)-aminomethane (Tris)

into 1:5, pH 7.4, supplemented with 1% (w/v) skim milk (Bio-Rad Laboratories, Munich, Germany)[35,74]. Incubation was performed by the primary antibodies, rabbit anti-γ-ENaC, 1:50 or rabbit anti-α-ENaC, 1:1000, for 1 hour, at 37 °C. Subsequently, a wash step was done by using Tris buffer (50 mM Tris, pH 7.4, supplemented with 0.05% (v/v) Tween 20 (Sigma-Aldrich, Munich, Germany; 3 x 5 minutes)[74]. Sections were incubated for another 30 minutes with the secondary antibody (a biotinylated goat anti-rabbit, Vector Laboratories, Burlingame, CA USA; 1:500[74]). Under the manufacturer's instructions (DABImmpact, Vector Laboratory), sections were then processed using the VectaStain ABC kit as substrate[74]. Finally, the sections were observed using an Olympus Bx60 upright microscope after the counterstaining in hemalaun and dehydration (technology and images were provided by Institute of Nephropathology, Friedrich-Alexander University Erlangen-Nürnberg (FAU), Erlangen, Germany)[74].

Kidneys were frozen in OCT compound for immunofluorescence. Sliced kidneys with a thickness of 5 µm were obtained by Leica Kryostat (Wetzlar, Germany). The sections were then fixed with 4% paraformaldehyde or Methanol. Blocking of slices were done by a mixture containing PBS, 5% BSA, and 5% Normal Donkey Serum[35]. Several times of rinse by PBS then followed the incubation of the sections with primary antibodies (as described above) for 45 min. After an additional incubation with fluorophore-conjugated secondary antibodies for 30 minutes (LifeTechnology, Karlsruhe, Germany), images were obtained by a Zeiss fluorescence microscope[35] (Zeiss, Oberkochen, Germany)(technology and images were provided by Dr. Grahammer, III. Department of Medicine, University Medical Center Hamburg-Eppendorf, Hamburg, Germany).

2.7 Electron microscopy

For the ultrastructural study, a cubic piece of mouse renal cortex (about $1mm^3$) was immersed in 4% PFA and 1% (v/v) glutaraldehyde in 0.1M PB[74]. Fixation was lasted for over-night with the same solution at 4°C. Before tissue blocks were treated with 0.5% OsO_4 for 1 hour, washing step was done by 0.1 M PB solution. Kidneys were then stained with uranyl acetate (1% w/v in 70% v/v Ethanol)[74]. The tissue blocks were embedded in epoxy resin (Durcupan ACM, Sigma-Aldrich, Gillingham, UK)[74] after dehydration. Sections with the thickness no more than 40nm were cut on an UC6 ultramicrotome (Leica, Wetzlar, Germany) and analyzed using an 80kV Philipps CM100 transmission

electron microscope and Olympus ITEM software (technology and images were provided by III. Department of Medicine, University Medical Center Hamburg-Eppendorf, Hamburg, Germany)[74].

2.8 Statistical analysis

Data in this thesis are presented as means with SEM. The Normality of data was tested by using the Kolmogorov-Smirnov-Test, D'Agostino, and Pearson omnibus normality test and Shapiro-Wilk-Test respectively[74]. Variances test were run by the Bartlett´s test for equal variances[74]. Analysis for significant difference for repeated measurements were tested by one-way ANOVA (multiple comparisons). A considerable difference between genotypes with two time points was tested by one-way ANOVA (multiple comparisons). Data analysis mentioned above was done by GraphPad Prism 8, GraphPad Software (San Diego, CA, www.graphpad.com)[74]. Densitometric analysis of western blots was obtained by Image Studio Version 3.1.4 (Licor)[74]. It would be considered to reach a statistically significant when the p-value <0.05 by two-tailed testing[74].

3 Results

3.1 Characterization of a new mouse model with inducible *nphs2* deficiency (*nphs2*$^{\Delta ipod}$ mouse model)

3.1.1 Deletion of the nphs2 gene in podocytes after doxycycline induction

Podocin encoded by the nphs2 gene is expressed on the foot process of podocyte and is a critical molecular for preserving a regular function and structure of podocyte in humans and mice. To establish a genetic model of experimental NS with podocyte-specific, tetracycline-sensitive *nphs2* deletion in adult mice in this study, the triallelic mice were yielded[31]. Firstly, mice with two *nphs2*-modified by two flox alle (*nphs2fl/fl*) were intercrossed with mice carrying podocyte-specific nephrin promoter to make sure that the specificity expression of a reverse tetracycline transactivator (rTA[75]) in podocyte. These mice were then intercrossed with mice carrying a transgene for expression of Cre recombinase to initiate *nphs2* deletion after binding of rTA in the podocytes. This model was first established by Dr. Grahammer (III. Department of Medicine, University Medical Center Hamburg-Eppendorf, Hamburg, Germany) and were imported to our facility. The Cre-recombinase was not activated before doxycycline induction, and the *nphs2* gene was functional. Once doxycycline was given, the Cre-recombinase was activated and the deletion of *nphs2* was initiated in *nphs2*$^{\Delta ipod}$ mice (n=5-16) (see methods). On the contrary, the *nphs2* gene was preserved in mice have two floxed tag on *nphs2* but lacking either Cre-recombinase or nephrin promotor. Those mice were taken as control (n=5-10).

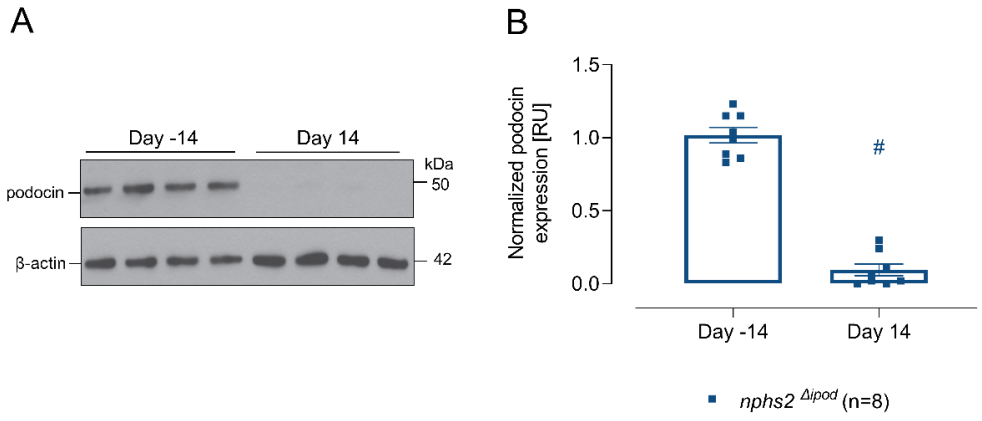

Figure 23 Western blot revealed *nphs2* deletion in adult *nphs2*$^{\Delta ipod}$ mice by using a doxycycline-sensitive Cre lox-P system

Protein was prepared from an isolated podocyte of uninduced and nephrotic *nphs2*$^{\Delta ipod}$ mice. Actin expression used as a loading control. WB showed the expression of podocin was deleted on day 14 (A-B). Arithmetic means ± SEM, # indicates a significant difference to the baseline value (Figures A-B were first published on May 2020 Acta Physiologica)

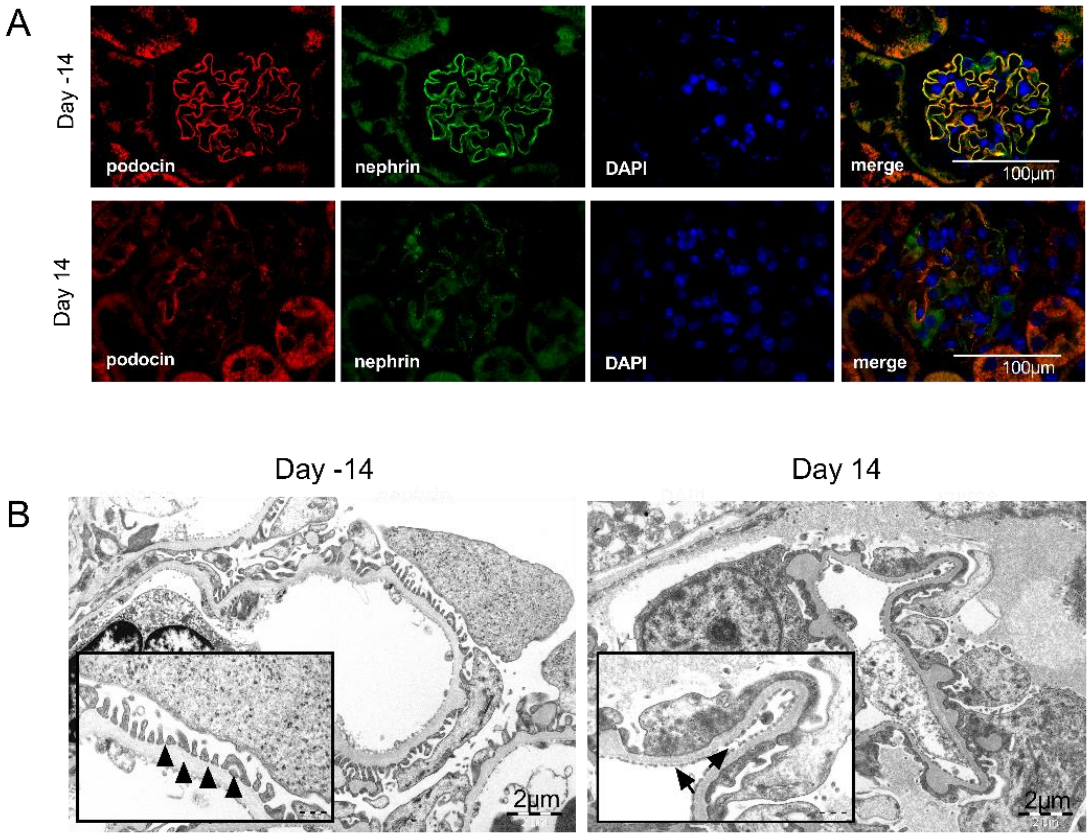

Figure 24 Immunofluorescence and ultrastructure study of *nphs2*$^{\Delta ipod}$ mice before and after induction

(A) Podocin expression (red) was almost lost in nephrotic *nphs2*$^{\Delta ipod}$ mice on day 14 compared with uninduced mice. In contrast, nuclei expression (blue) was constant in podocytes from both uninduced and nephrotic mice. Scale bar: 100 µm.
(B) In the uninduced animals, podocytes had normal foot processes (arrowheads), while in the nephrotic mice, foot process were effacement (arrows). Scale bar: 2 µm. (Figures A-B were first published on May 2020 Acta Physiologica)

All of *nphs2*$^{\Delta ipod}$ mice and control mice received an oral doxycycline treatment in daily drinking water for 14 days. The beginning of doxycycline induction was designated as day -14, and the end of doxycycline-water intake was day 0. The duration of observation for this cohort of mice ended on day 14 after induction. Expression of podocin was not detectable in glomeruli 14 days after induction according to Western blot (Figure 23 A). The *nphs2* expression was 1.02 ± 0.05 relative units in uninduced animals (n=8) and decreased to 0.10 ± 0.04 relative units in nephrotic mice on day 14 (n=8, $P < 0.0001$, Figure 23 B[74]). This corresponds to a down-regulation by about 90% after a 14-day doxycycline treatment, which indicates a very high efficiency. These results were further confirmed by immunofluorescence, which demonstrated the disappearance of podocin in

podocytes in kidney harvested on day 14. Interestingly, besides the downregulated expression of podocin, the expression of another podocyte protein nephrin was also found to be lost in nephrotic mice (Figure 24 A). Ultrastructural studies using electron microscopy revealed the fused foot processes on day 14 after induction (Figure 24 B).

3.1.2 Characterization of proteasuria and sodium retention in doxycycline induced nphs2$^{\Delta ipod}$ mice

Nphs2$^{\Delta ipod}$ mice (n=19) were induced for experimental NS by doxycycline. It has been shown that Na^+ retention could be inhibited by aprotinin in a doxorubicin-induced experimental nephrotic model[35]. To study the effects of aprotinin in *nphs2$^{\Delta ipod}$* mice, nephrotic *nphs2$^{\Delta ipod}$* mice were separated into an aprotinin treatment group, which received an aprotinin pellet implantation (1 mg/ day) on day 7, and an untreated group. Mice lacking tet O Cre or nephrin-driven promoter were used as control. Urinary protein concentration was measured every day, and plasma samples were collected every 7 days after induction of NS for albumin concentration measurement. In control mice, proteinuria remained constant through the entire observation (3.7 ± 0.7 on day 7, p=0.9702; 4.6 ± 0.7 on day 14, p=0.7928, Figure 25 A). On the contrary, all *nphs2$^{\Delta ipod}$* mice developed massive proteinuria reaching a nephrotic range (> 100 mg/mg crea) after induction of NS (Figure 25 A). Compared to the value from day -14, proteinuria increased > 20 fold on day 7 (from 2.8 ± 0.8 mg/mg crea to 64.3 ± 7.6 mg/mg crea, p=0.0001) and was further increasing until day 14 (146.0 ± 20.0 mg/mg crea, compared to baseline, p=0.0009). There was no significant difference in proteinuria between day -14 and day 0 in *nphs2$^{\Delta ipod}$* mice (P=0.9998), indicating that the development of NS did not start before the end of induction. Compared the aprotinin treated mice with untreated ones, there was no significant difference in maximum proteinuria (143.4 ± 13 mg/mg Crea vs. 116.4 ± 8.9 mg/mg Crea, p=0.4818), indicating aprotinin had no effects on protein excretion quantitatively. However, aprotinin suppressed urinary amidolytic activity immediately from day 8, which measured with the chromogenic substrate S-2251 (Figure 25 B).

As a consequence of massive urinary protein loss, plasma albumin concentration dropped from 31.2 ± 0.8 mg/ml on day -14 to 11.0 ± 2.3 mg/ml in nephrotic *nphs2$^{\Delta ipod}$* mice on day 7 (Figure 25 C, P<0.0001). It continued to drop thereafter to 7.3 ± 0.5 mg/ml until day 14 in *nphs2$^{\Delta ipod}$* mice (P<0.0001).

Plasma aldosterone concentration was measured by ELISA. Results revealed an increased

tendency of plasma aldosterone concentration in nephrotic *nphs2*$^{\Delta ipod}$ mice on day 14, however, the difference was not statistically significant, indicating that sodium retention and edema was not regulated by aldosterone (Figure 25 D). The measured results from plasma aldosterone were 271 ± 33 pg/ml on day -14, 295 ± 18 pg/ml on day 7 and 333 ± 69 pm/ml on day 14.

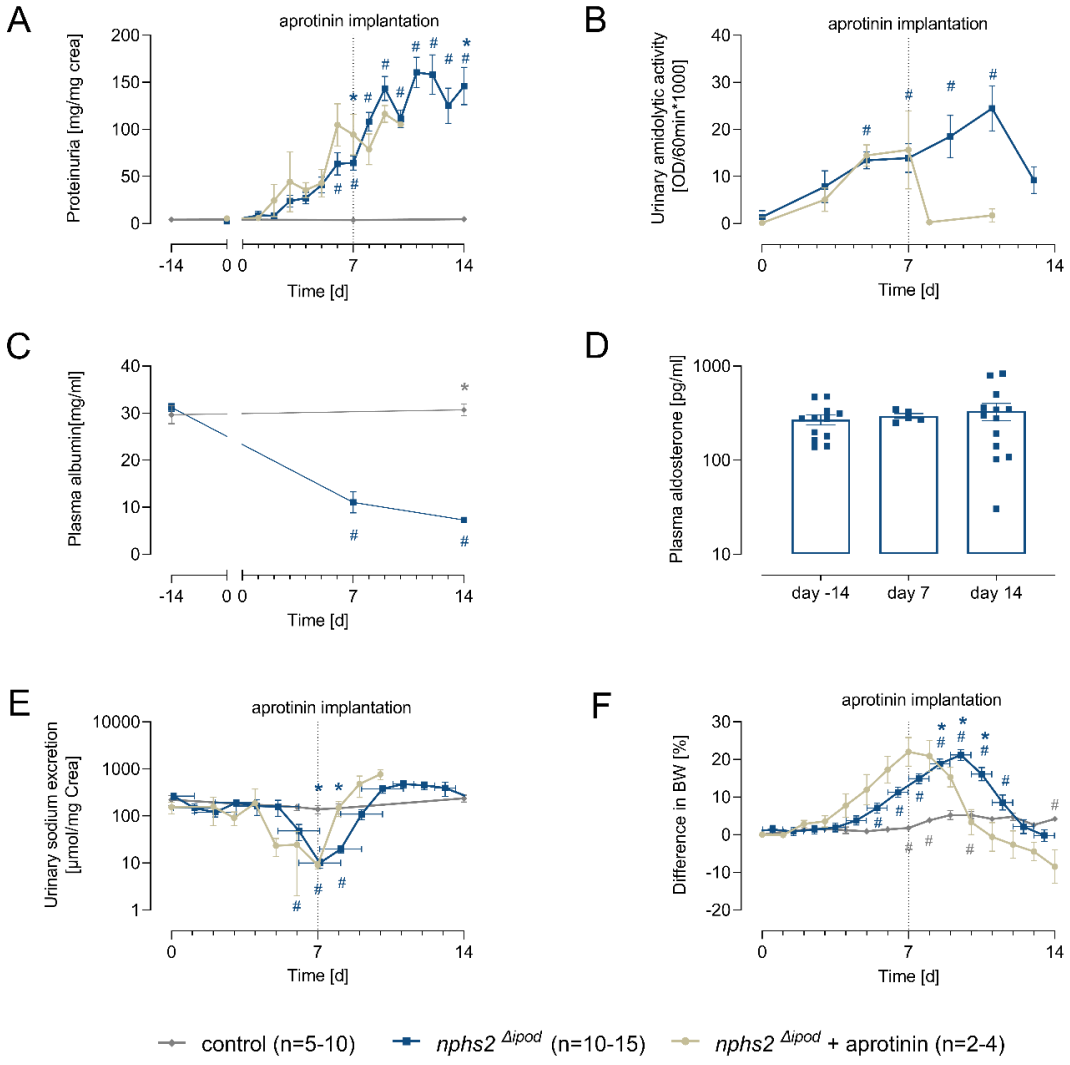

Figure 25 *Nphs2*$^{\Delta ipod}$ mice developed massive proteinuria, proteasuria, hypoalbuminemia, sodium retention and edema after induction of experimental nephrotic syndrome

(A) Course of urinary protein, in nephrotic *nphs2*$^{\Delta ipod}$ mice with or without aprotinin pellet implantation on day 7, and control mice.
(B) Course of urinary amidolytic activity in nephrotic *nphs2*$^{\Delta ipod}$ mice with or without aprotinin pellet implantation.
(C) Plasma albumin concentration in nephrotic *nphs2*$^{\Delta ipod}$ mice and control mice.
(D) Concentration of plasma aldosterone.
(E-F) Course of urinary Na^+ excretion and difference in BW in *nphs2*$^{\Delta ipod}$ mice with aprotinin treatment or untreated, as well as control mice.
Arithmetic means ± SEM, # indicates significant difference to baseline value; * indicates significant difference between *nphs2*$^{\Delta ipod}$ mice and control mice.

Sodium retention and edema are typical characters of NS, and were monitored by urinary Na^+ excretion in spot voided urine daily and body weight difference during a constant food and drink intake. In nephrotic *nphs2*$^{\Delta ipod}$ mice without aprotinin treatment, urinary sodium concentration dropped from 206 ± 59 to a minimum of 10 ± 2 µmol/mg Crea (p=0.0001), and as a consequence, body weight increased to a maximum by 21 ± 1% from the baseline value on day 10 (p=0.0143) and was paralleled with the development of ascites which was easily visible by extruded flanks (Figure 25 E-F, Figure 40). Urinary Na^+ excretion immediately increased from 9 ± 2 µmol/mg Crea to 150 ± 53 µmol/mg Crea after aprotinin pellet implantation, indicating reversion of sodium retention by aprotinin (Figure 25 E). This led to a prompt decrease in body weight and resolution of ascites in aprotinin-treated nephrotic *nphs2*$^{\Delta ipod}$ mice (Figure 25 F). In control mice, the excretion of sodium, and body weight was constant during the 14-day observation.

Periodic acid–Schiff (PAS) staining of kidneys of nephrotic *nphs2*$^{\Delta ipod}$ mice displayed sclerosis of segments in some glomeruli with protein casts in the tubule which is the typical manifestation of focal-segmental glomerulosclerosis (FSGS, Figure 26). Aprotinin implantation did not show any effects on kidney damage and proteinuria.

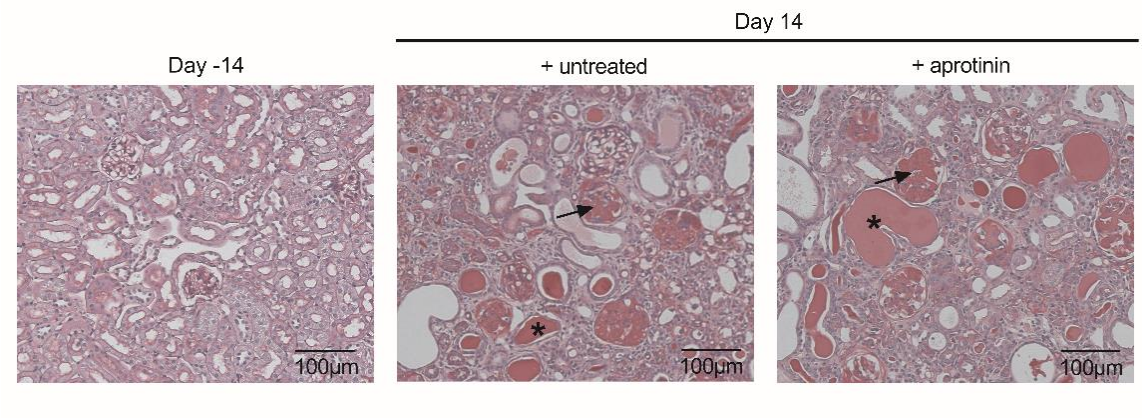

Figure 26 PAS of uninduced and nephrotic *nphs2*$^{\Delta ipod}$ mice

Kidneys harvested from uninduced (day -14) and nephrotic (day 14) *nphs2*$^{\Delta ipod}$ mice. Light microscopy of kidney in uninduced mice showed normal structure of glomeruli and tubules, while in *nphs2*$^{\Delta ipod}$ mice showed segments of sclerosis in some glomeruli and protein droplets (arrow) in dilated tubules of nephrotic mice. Scale bar: 100 µm.

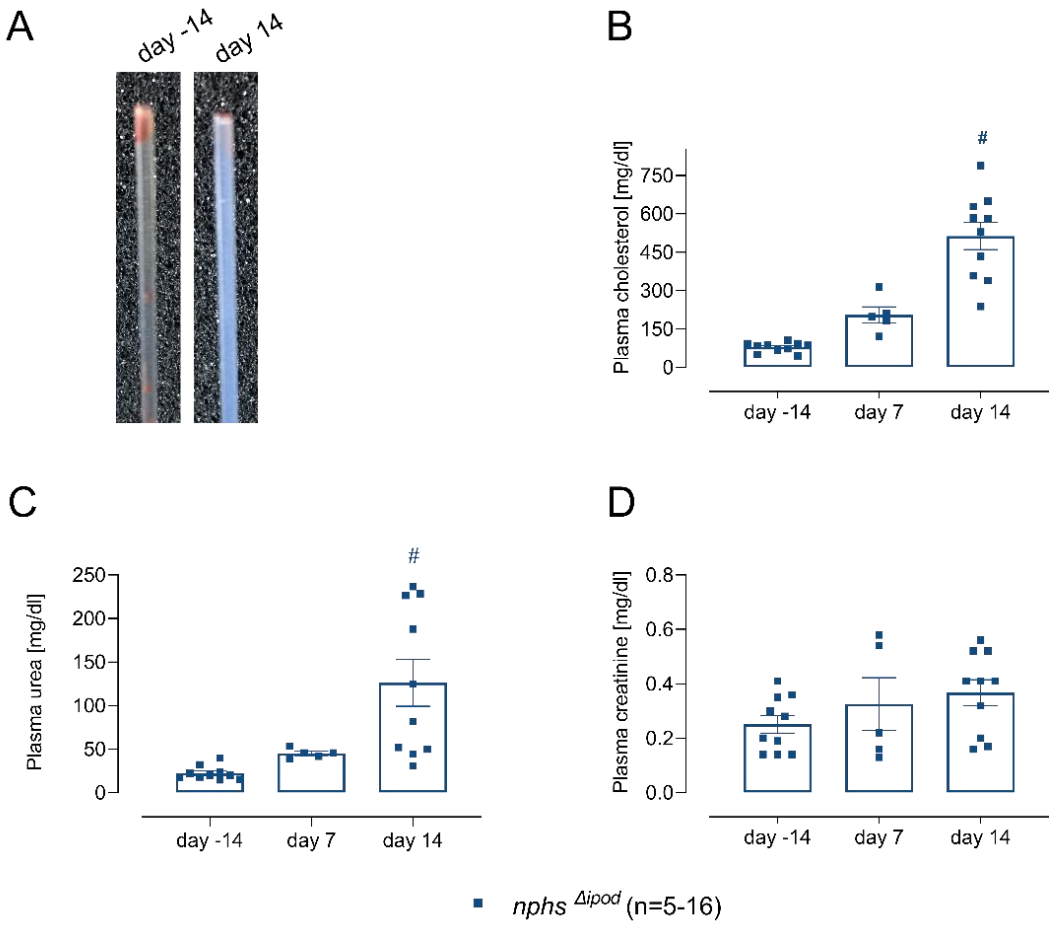

Figure 27 Plasma cholesterol and kidney function before and after induction of NS in *nphs2*$^{\Delta ipod}$ mice

(A-B) Plasma was obtained after centrifugation of the blood samples collected on day -14, day 7 and day 14, respectively. On day -14, a clear plasma was observed, whereas it turned whitish 14 days after induction of NS indicating hyperlipidemia. Measurement of plasma cholesterol showed an increasing tendency on day 7 after initiation of NS and reached a significance on day 14.
(C-D) Concentrations of plasma urea, and plasma creatinine on day -14, day 7 and day 14 respectively. Arithmetic means ± SEM, # indicates significant difference to baseline value.

Hyperlipidemia is another complication of NS and manifests as an elevated plasma level of cholesterol and triglycerides. Thus, plasma cholesterol concentration was evaluated in this study to validate the model of nephrotic syndrome. The results of plasma cholesterol in *nphs2*$^{\Delta ipod}$ mice increased subsequently from 79 ± 6 mg/dl on day -14, to 205 ± 31 g/dl on day 7, and 513 ± 53 g/dl on day 14 (day -14 vs day 7, p=0.1004; day -14 vs day 14, p<0.0001)(Figure 27 A-B). This result indicated that nephrotic *nphs2*$^{\Delta ipod}$ mice developed massive hypercholesterolemia. To investigate the kidney function in *nphs2*$^{\Delta ipod}$ mice, plasma urea and plasma creatinine were measured on day 7 and day 14, respectively. Plasma urea concentration was significantly increased on day 14, compared to day -14

(126 ± 27 mg/dl vs 22 ± 2 mg/dl, p=0.0007), however it was not significantly increased on day 7 (45 ± 2 mg/dl vs 22 ± 2 mg/dl, p=0.7034, Figure 27 C). There was an increased tendency in plasma creatinine of *nphs2*$^{\Delta ipod}$ mice after induction, however the differences did not reach statistical significance. The values were 0.25 ± 0.03 mg/dl on day -14, 0.33 ± 0.10 mg/dl on day 7 and 0.36 ± 0.05 mg/dl on day 14 (Figure 27 D).

3.2 Role of plasminogen in a genetic mouse model of experimental nephrotic syndrome with plasminogen deficiency

3.2.1 Nphs2$^{\Delta ipod}$**plg*$^{-/-}$ *mice have growth retardation but normal kidney function*

Nphs2$^{\Delta ipod}$ mice were intercrossed with the mice which were constitutively absent of plasminogen (Bl6-Plg^{tm1Jld} or *plg*$^{-/-}$) to generate double knockout mice (*nphs2*$^{\Delta ipod}$**plg*$^{-/-}$). *Nphs2*$^{\Delta ipod}$**plg*$^{-/-}$ mice had a reduced body weight and often developed rectal prolapse compared to the wild-type littermates (*nphs2*$^{\Delta ipod}$**plg*$^{+/+}$) (Figure 28 A-B[74,93]). Since lacking of plasminogen could lead to damage to the liver and gastrointestinal tract due to fibrin deposition, which has been reported in a mouse model previously[94]. The retarded bodyweight in uninduced *nphs2*$^{\Delta ipod}$**plg*$^{-/-}$ mice could be as a consequence of plasminogen deficiency. At day -21, the body weight was 21.02 ± 0.63 g in *nphs2*$^{\Delta ipod}$**plg*$^{+/+}$ mice (n=8) and 19.65 ± 1.10 g in *nphs2*$^{\Delta ipod}$**plg*$^{-/-}$ mice. This difference however, did not reach statistical significance (p=0.3051).

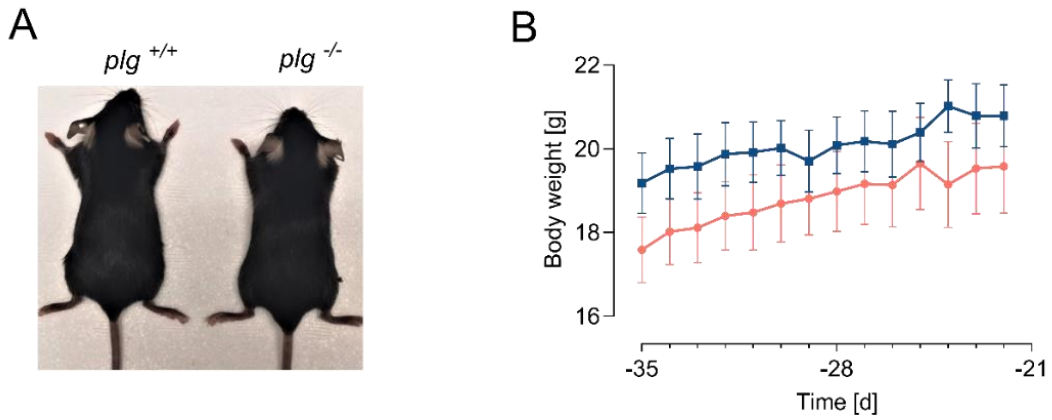

Figure 28 Comparison of the uninduced *nphs2*$^{\Delta ipod}$**plg*$^{+/+}$ and *nphs2*$^{\Delta ipod}$**plg*$^{-/-}$ mice

(A) Phenotype of uninduced *nphs2*$^{\Delta ipod}$**plg*$^{+/+}$ and *nphs2*$^{\Delta ipod}$**plg*$^{-/-}$ mice.
(B) Growth curve of *nphs2*$^{\Delta ipod}$**plg*$^{+/+}$ and *nphs2*$^{\Delta ipod}$**plg*$^{-/-}$ mice from day -35 until day -22 (First published on May 2020 Acta Physiologica).
Arithmetic means ± SEM.

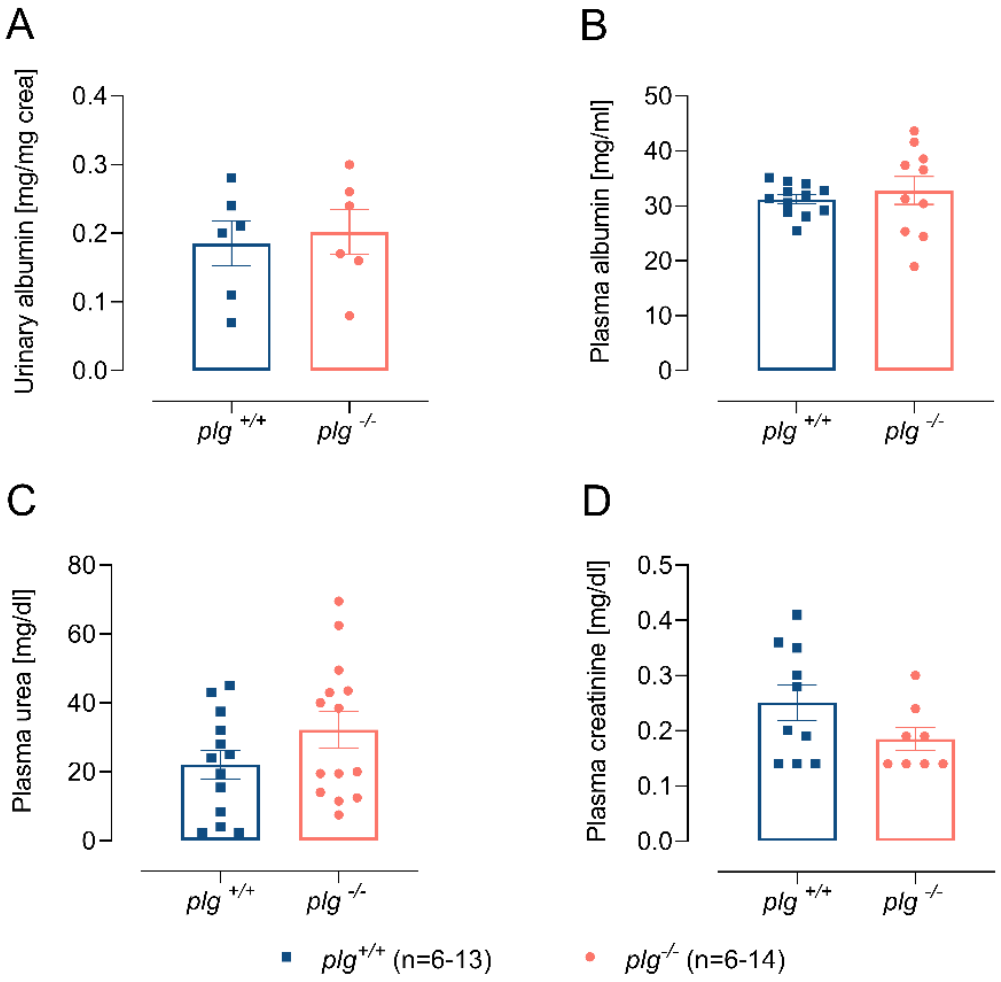

Figure 29 Kidney function in the uninduced *nphs2*$^{\Delta ipod}$**plg*$^{+/+}$ and *nphs2*$^{\Delta ipod}$**plg*$^{-/-}$ mice[74]

(A-B) Absence of albuminuria and hypoalbuminemia in uninduced *nphs2*$^{\Delta ipod}$**plg*$^{+/+}$ and *nphs2*$^{\Delta ipod}$**plg*$^{-/-}$ mice.
(C-D) Similar extent of plasma urea and plasma creatinine concentrations in uninduced mice with both genotypes.
Arithmetic means ± SEM.

Despite the possible damage of other organs, the kidney function was normal in uninduced *nphs2*$^{\Delta ipod}$**plg*$^{-/-}$ mice. As shown in Figure 29 A, urinary albumin excretion on day -35 was 0.19 ± 0.03 mg/mg crea vs. 0.20 ± 0.03 mg/mg crea in uninduced *nphs2*$^{\Delta ipod}$**plg*$^{+/+}$ and *nphs2*$^{\Delta ipod}$**plg*$^{-/-}$ mice respectively (p=0.7254). Plasma albumin concentration was similar in both genotypes (P=0.5266, Figure 29 B) indicated *nphs2*$^{\Delta ipod}$**plg*$^{-/-}$ mice were not hypoalbuminemic. There was also no significant difference between *nphs2*$^{\Delta ipod}$**plg*$^{+/+}$ and *nphs2*$^{\Delta ipod}$**plg*$^{-/-}$ mice in plasma urea and creatinine concentrations (Figure 29 C-D). Concentration of plasma urea was 22 ± 4 mg/dl vs 32 ± 5 mg/dl in *nphs2*$^{\Delta ipod}$**plg*$^{+/+}$ vs. *nphs2*$^{\Delta ipod}$**plg*$^{-/-}$ mice on day -14

(p=0.1501). Plasma creatinine concentration was 0.25 ± 0.03 mg/dl vs. 0.19 ± 0.02 mg/dl in uninduced *nphs2*$^{\Delta ipod}$**plg*$^{+/+}$ and *nphs2*$^{\Delta ipod}$**plg*$^{-/-}$ mice (p=0.1246). Histology of kidneys from uninduced mice of both genotypes also revealed a normal glomerular structure (Figure 30). In conclusion, these findings demonstrated that the kidneys were spared from the detrimental effects of plasminogen deficiency as seen in the liver, lungs or the gastrointestinal tract [73].

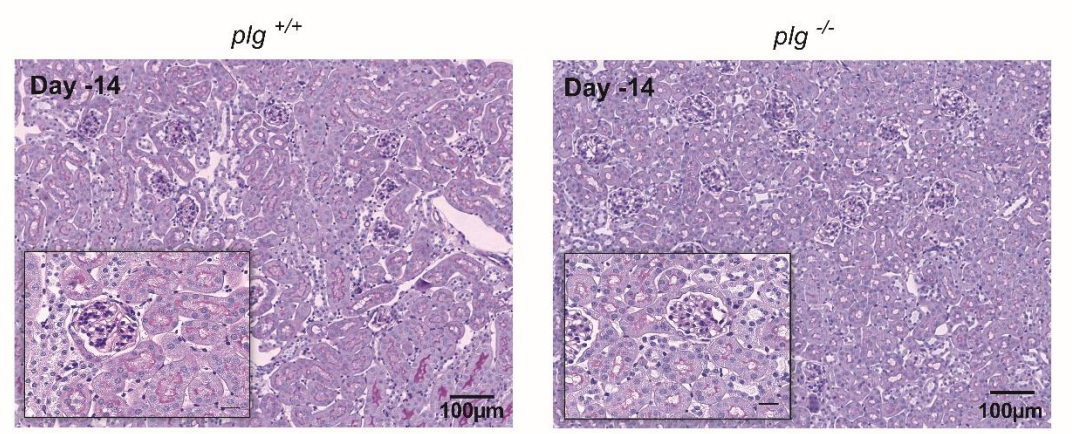

Figure 30 Histology of the uninduced *nphs2*$^{\Delta ipod}$**plg*$^{+/+}$ and *nphs2*$^{\Delta ipod}$**plg*$^{-/-}$ mice showed the normal renal structure[74]

3.2.2 Uninduced nphs2$^{\Delta ipod}$**plg*$^{-/-}$ *mice have normal sodium handling*

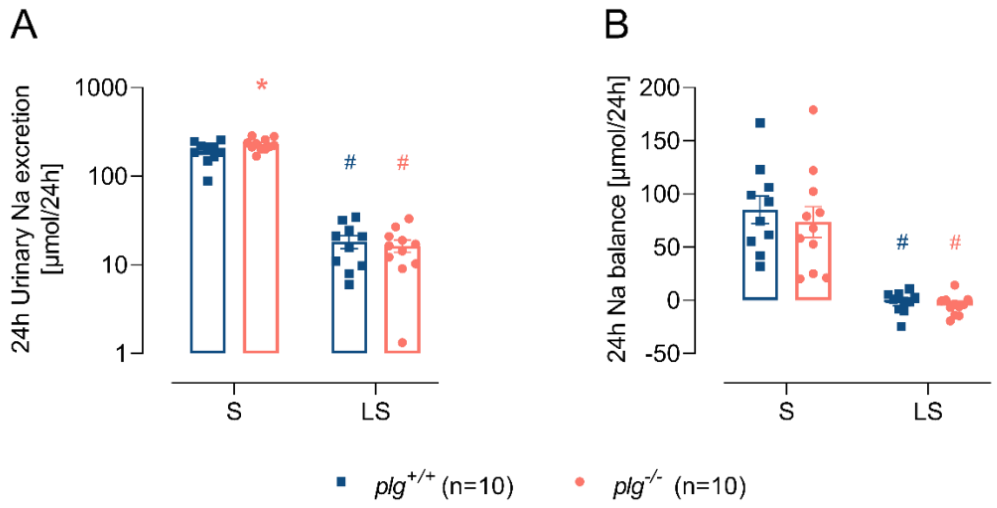

Figure 31 Sodium handling in uninduced *nphs2*$^{\Delta ipod}$**plg*$^{+/+}$ and *nphs2*$^{\Delta ipod}$**plg*$^{-/-}$ mice under a standard and a low salt diet condition

(A-B) 24h Urinary sodium excretion and sodium balance in uninduced *nphs2*$^{\Delta ipod}$**plg*$^{+/+}$ and *nphs2*$^{\Delta ipod}$**plg*$^{-/-}$ mice[74].
S: standard diet; LS: low salt diet.
Arithmetic means ± SEM, # indicates significant difference to baseline value, * indicates significant

difference between genotypes.
Uninduced *nphs2*$^{\Delta ipod}$**plg*$^{-/-}$ mice had a slightly higher urinary sodium excretion than uninduced *nphs2*$^{\Delta ipod}$**plg*$^{+/+}$ mice due to a higher food intake (Table 3). After a 5-day of low salt diet, 24h urinary sodium excretion was similarly decreased in both genotypes, compared to the Na^+ excretion under a standard diet (Figure 31 A-B, Table 3). In both control and low salt diet, sodium balance was not different between uninduced *nphs2*$^{\Delta ipod}$**plg*$^{+/+}$ and *nphs2*$^{\Delta ipod}$**plg*$^{-/-}$ mice excluding the abnormal sodium handling in *nphs2*$^{\Delta ipod}$**plg*$^{-/-}$ mice.

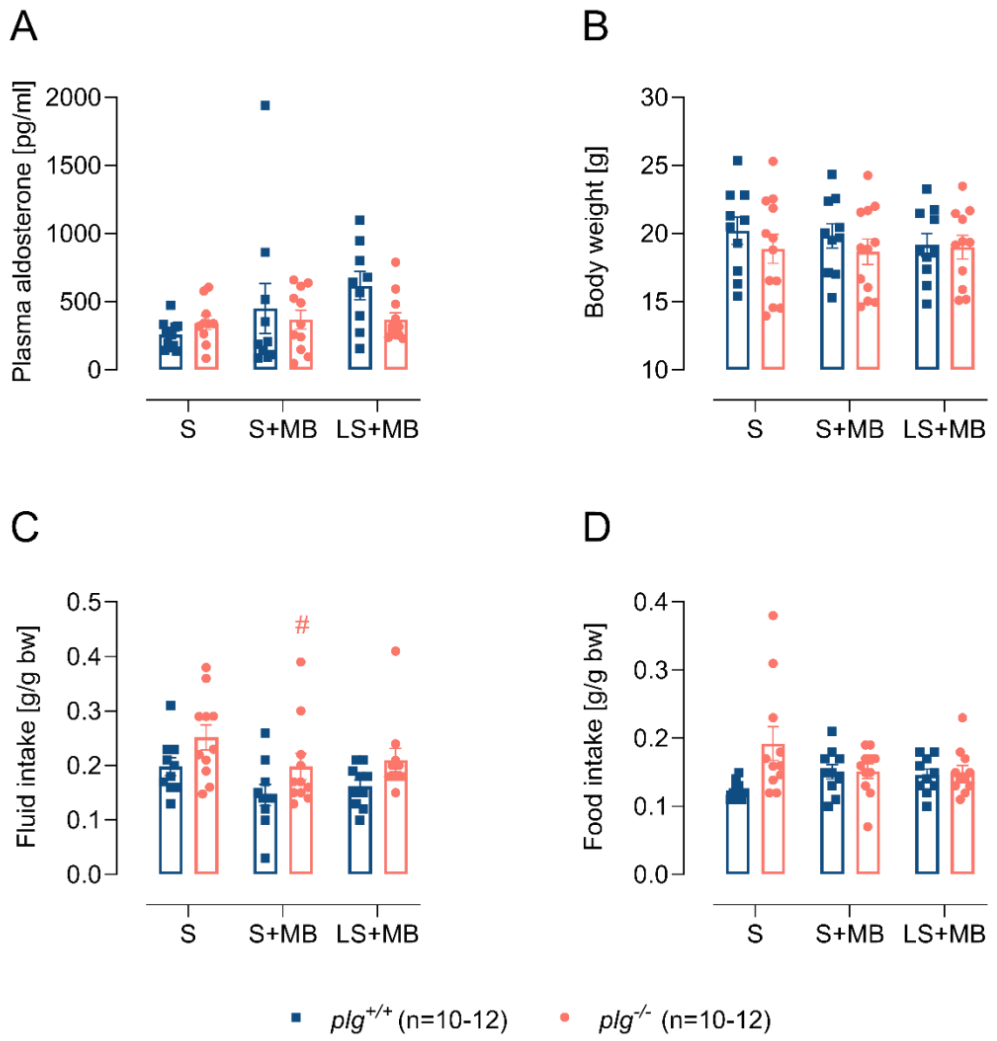

Figure 32 The change of plasma aldosterone concentration, body weight, as well as the intake in uninduced *nphs2*$^{\Delta ipod}$**plg*$^{+/+}$ and *nphs2*$^{\Delta ipod}$**plg*$^{-/-}$ mice under either a standard or a low salt diet condition

(A-B) Plasma aldosterone concentration and body weight verified under different conditions in uninduced *nphs2*$^{\Delta ipod}$**plg*$^{+/+}$ and *nphs2*$^{\Delta ipod}$**plg*$^{-/-}$ mice.
(C-D) Fluid and food intake in both genotypes under different conditions.
S: standard diet (housing in a regular cage); S + MB: standard diet + housing in a metabolic cage; LS + MB: low salt diet + housing in a metabolic cage.

Arithmetic means ± SEM, # indicates significant difference to baseline value.

Plasma aldosterone concentration was similar in uninduced *nphs2*$^{\Delta ipod}$**plg*$^{+/+}$ and *nphs2*$^{\Delta ipod}$**plg*$^{-/-}$ mice under control or low salt diet, indicating plasma aldosterone regulation is not altered in uninduced *nphs2*$^{\Delta ipod}$**plg*$^{-/-}$ mice (Figure 32 A). There was a small influence on the individual values depending on the maintenance of the mice (standard cage vs. metabolic cage). However, the large scatter precluded the detection of significant differences. The body weight was almost constant in uninduced *nphs2*$^{\Delta ipod}$**plg*$^{+/+}$ and *nphs2*$^{\Delta ipod}$**plg*$^{-/-}$ mice under a low salt diet in metabolic cages (Figure 32 B). Fluid intake in *nphs2*$^{\Delta ipod}$**plg*$^{-/-}$ mice was decreased after housing in metabolic cages (0.37 ± 0.07 g/g bw in standard cages vs. 0.20 ± 0.02 g/g bw in metabolic cages, p=0.0373, Figure 32 C) while food intake was not affected by the different housing conditions (Figure 32 D).

3.2.3 Nphs2$^{\Delta ipod}$**plg*$^{-/-}$ *mice develop nephrotic-range proteinuria with the absent of urinary plasminogen excretion*

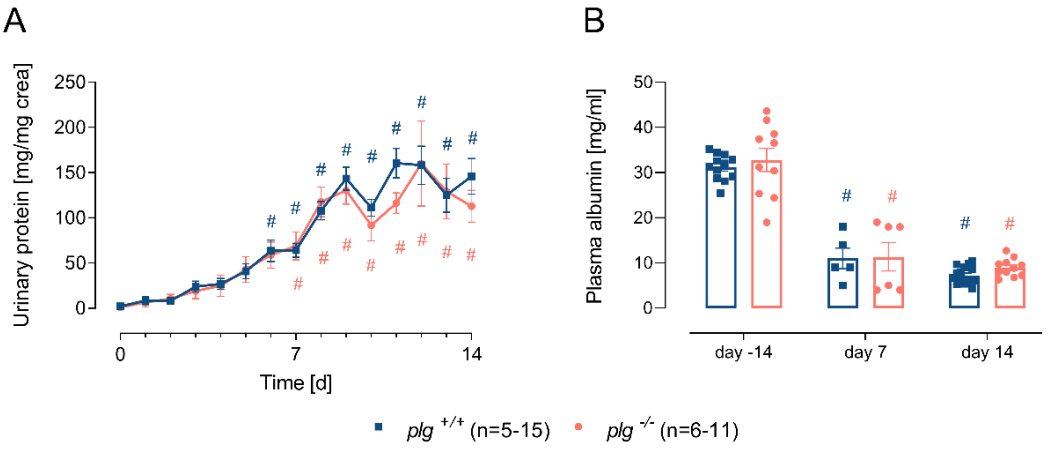

Figure 33 *Nphs2*$^{\Delta ipod}$**plg*$^{+/+}$ mice and *nphs2*$^{\Delta ipod}$**plg*$^{-/-}$ mice were successfully induced similar extent of massive proteinuria and hypoalbuminemia after doxycycline treatment.

(A) Course of proteinuria in nephrotic *nphs2*$^{\Delta ipod}$ mice with both plasminogen wild type or plasminogen deficiency.
(B) Concentration of plasma albumin in both *nphs2*$^{\Delta ipod}$**plg*$^{+/+}$ mice and *nphs2*$^{\Delta ipod}$**plg*$^{-/-}$ mice before and after induction of nephrotic syndrome.
Arithmetic means ± SEM, # indicates significant difference to baseline value (Figures A-B were first published on May 2020 Acta Physiologica).

Development of proteinuria was similarly in both *nphs2*$^{\Delta ipod}$**plg*$^{+/+}$ and *nphs2*$^{\Delta ipod}$**plg*$^{-/-}$ mice after doxycycline induction (Figure 33 A). Urinary protein excretion increased from 2.2 ± 0.4 mg/mg crea to 23.9 ± 6.1 mg/mg crea in *nphs2*$^{\Delta ipod}$**plg*$^{+/+}$ mice, and increased

from 1.1 ± 0.5 mg/mg crea to 19.1 ± 8.4 mg/mg crea in *nphs2*$^{\Delta ipod}$**plg*$^{-/-}$ mice on day 3. Proteinuria increased further on day 6 in both genotypes (63.5 ± 11.9 mg/mg crea in *nphs2*$^{\Delta ipod}$**plg*$^{+/+}$ mice and 68.8 ± 15.4 mg/mg crea in *nphs2*$^{\Delta ipod}$**plg*$^{-/-}$ mice). Maximum of urinary protein excretion was 161 ± 16 mg/mg crea in *nphs2*$^{\Delta ipod}$**plg*$^{+/+}$ mice and was 160 ± 47 mg/mg crea in *nphs2*$^{\Delta ipod}$**plg*$^{-/-}$ mice which was almost identical difference (P>0.9999).

Accordingly, plasma albumin concentration decreased significantly in both genotypes on day 7 compared to their baseline values (10.9 ± 2.2 mg/ml vs. 31.2 ± 0.8 mg/ml, p<0.0001 in *nphs2*$^{\Delta ipod}$**plg*$^{+/+}$ mice; 11.2 ± 3.1 mg/ml vs. 32.8 ± 2.6 mg/ml, p<0.0001 in *nphs2*$^{\Delta ipod}$**plg*$^{-/-}$ mice). Minimum plasma albumin concentration was observed in both genotypes on day 14 and there was no significant difference between genotypes (7.3 ± 0.5 mg/ml in *nphs2*$^{\Delta ipod}$**plg*$^{+/+}$ mice vs. 9.0 ± 0.6 mg/ml in *nphs2*$^{\Delta ipod}$**plg*$^{-/-}$ mice, p=0.9696, Figure 33 B).

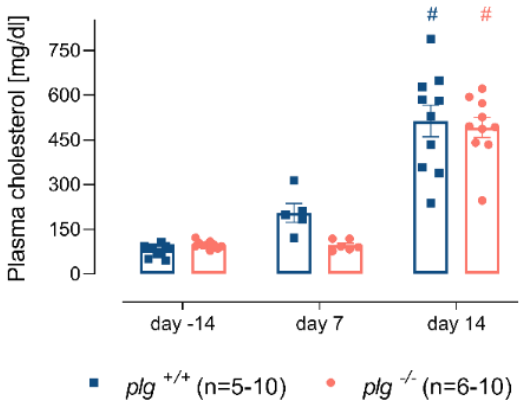

Figure 34 Plasma cholesterol concentration in *nphs2*$^{\Delta ipod}$**plg*$^{+/+}$ and *nphs2*$^{\Delta ipod}$**plg*$^{-/-}$ mice before and after induction of NS

Arithmetic means ± SEM, # indicates significant difference to baseline value (Figure was first published on May 2020 Acta Physiologica).

In addition, plasminogen deficiency did not influence the development of hyperlipidemia in nephrotic *nphs2*$^{\Delta ipod}$**plg*$^{-/-}$ mice compared to their wild-type littermates (Figure 34[74]). The increase of plasma cholesterol concentration was similar in both genotypes on day 14 (456.3 ± 81.0 mg/dl in *nphs2*$^{\Delta ipod}$**plg*$^{+/+}$ mice vs. 490.9 ± 33.5 mg/dl *nphs2*$^{\Delta ipod}$**plg*$^{-/-}$ mice, p=0.9856).

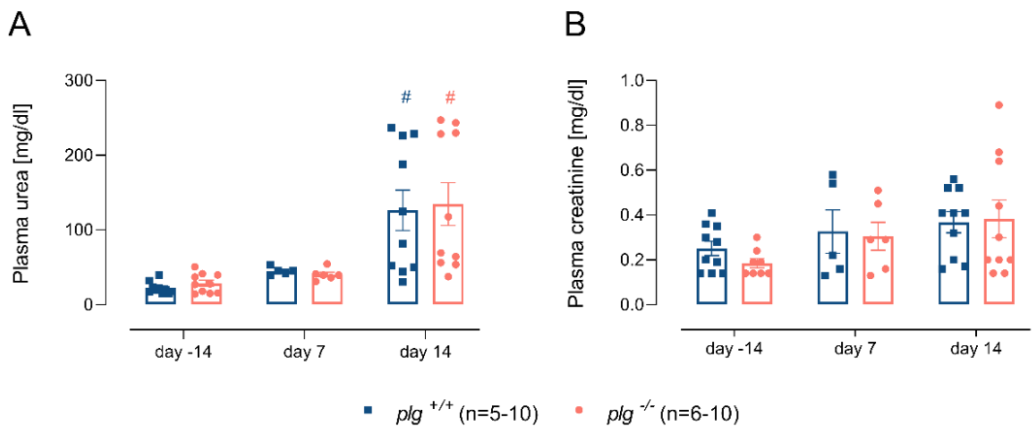

Figure 35 Plasma urea (A) and plasma creatinine (B) concentrations in *nphs2*$^{\Delta ipod}$**plg*$^{+/+}$ mice and *nphs2*$^{\Delta ipod}$**plg*$^{-/-}$ mice

Arithmetic means ± SEM, # indicates significant difference to baseline value (Figure was first published on May 2020 Acta Physiologica).

Kidney function was evaluated in both genotypes every 7 days after induction of NS. A decreased renal function was suggested by an increase in plasma urea concentration (Figure 35 A[74]) on day 14 compared to the values measured on day -14 (126 ± 27 mg/dl vs. 22 ± 3 mg/dl in *nphs2*$^{\Delta ipod}$**plg*$^{+/+}$ mice, p=0.0002; and 135 ± 29 vs. 29 ± 4 in *nphs2*$^{\Delta ipod}$**plg*$^{-/-}$ mice, p=0.0005). There was no significant difference between genotypes (p>0.9999). When analyzing plasma creatinine concentration, there was no significant change over the course of NS in both genotypes (Figure 35 B[74]).

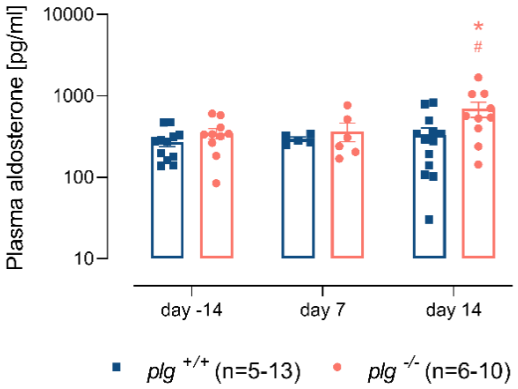

Figure 36 Plasma aldosterone concentrations in nephrotic *nphs2*$^{\Delta ipod}$**plg*$^{+/+}$ and *nphs2*$^{\Delta ipod}$**plg*$^{-/-}$ mice

Arithmetic means ± SEM, # indicates significant difference to baseline value, * indicates significant difference between genotypes (Figure was first published on May 2020 Acta Physiologica).

Plasma aldosterone concentration was not significantly different in uninduced

nphs2$^{\Delta ipod}$**plg*$^{+/+}$ mice *and* *nphs2*$^{\Delta ipod}$**plg*$^{-/-}$ mice. Plasma aldosterone concentration increased significantly in nephrotic *nphs2*$^{\Delta ipod}$**plg*$^{-/-}$ mice on day 14 (day -14 vs. day 14 in *nphs2*$^{\Delta ipod}$**plg*$^{-/-}$ mice, 346 ± 50 pg/ml vs. 693 ± 146 pg/ml, p=0.0277, Figure 36[74]) which were also significantly higher than in the nephrotic wild type-mice (693 ± 146 pg/mL vs. 333 ± 69 pg/ml, p=0.0112). However, the measured values of plasma aldosterone on day 7, did not increase significantly in both genotypes compared to day -14 (day -14 vs. day 7 in *nphs2*$^{\Delta ipod}$**plg*$^{+/+}$ mice, 271 ± 33 pg/ml vs. 295 ± 18 pg/ml, p>0.9999; day -14 vs. day 7 in *nphs2*$^{\Delta ipod}$**plg*$^{-/-}$ mice 346 ± 50 pg/ml vs. 368 ± 94 pg/ml, p>0.9999).

Plasminogen expression in plasma and urine samples was detected using Western blot from uninduced as well as nephrotic mice (Figure 37[74,93]). Albumin (69 kDa) was barely observed in the urine from uninduced *nphs2*$^{\Delta ipod}$**plg*$^{+/+}$ mice, as well as plasminogen (105 kDa). However, urine samples collected on day 7 contained abundant albumin, plasminogen (105 kDa), and the heavy chain (80 kDa) indicating the activation of plasminogen by uPA[36]. There was no significant change in the expression of plasma plasminogen on day 7, compared to the baseline. Massive albumin was observed in urine from nephrotic *nphs2*$^{\Delta ipod}$**plg*$^{-/-}$ mice, whereas plasminogen was not detectable in both plasma and urine samples[74].

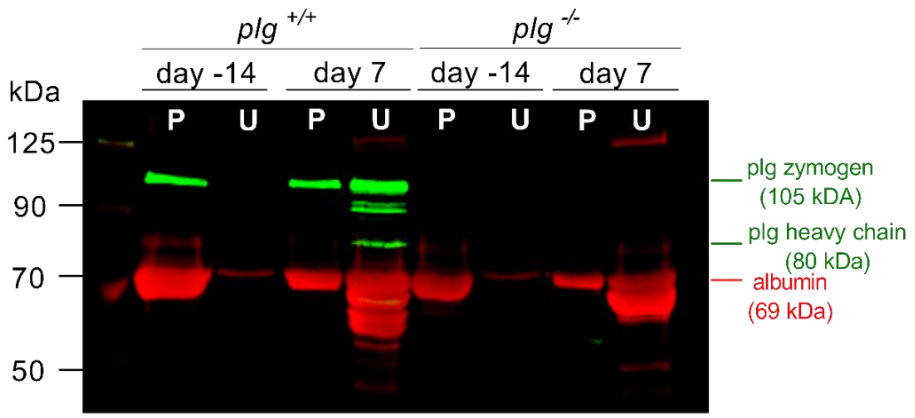

Figure 37 Qualitative study of plasmin(ogen) expression in *nphs2*$^{\Delta ipod}$**plg*$^{+/+}$ and *nphs2*$^{\Delta ipod}$**plg*$^{-/-}$ mice

Detection of plasminogen and albumin by Western blot from both plasma (P) and urine (U) samples of *nphs2*$^{\Delta ipod}$ mice with both plasminogen wild type or knock out, before and after induction of NS (Figure was provided by Mr. Matthias Wörn and first published on May 2020 Acta Physiologica).

Quantification of plasmin(ogen) excretion in the urine of *nphs2*$^{\Delta ipod}$**plg*$^{+/+}$ mice using ELISA showed a massive increase from 0.41 ± 0.22 µg/mg crea on day 0 to 2005 ± 493

µg/mg crea on day 11 (p<0.0001, Figure 38[74]). Plasma concentration of plasmin(ogen) slightly increased on day 14, compared to the results on day 0 (278 ± 16 µg/ml on day 0 vs. 440 ± 37 µg/ml on day 14, p=0.0263), and this result was consistent with the result had shown by western blot (Figure 37).

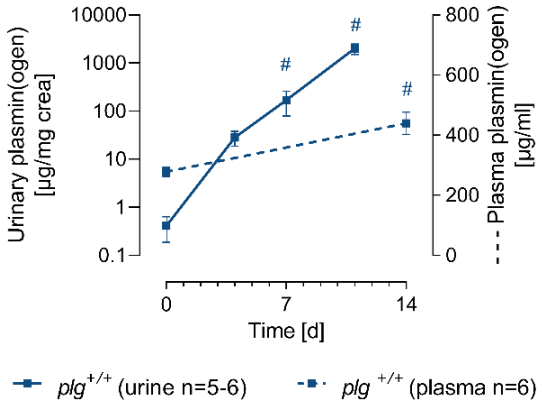

Figure 38 Qualification of urinary plasmin(ogen) excretion in *nphs2*$^{\Delta ipod}$**plg*$^{+/+}$ mice

Course of urinary and plasma plasmin(ogen) concentration in *nphs2*$^{\Delta ipod}$**plg*$^{+/+}$ mice[74]. Urinary plasmin(ogen) excretion increased heavily after induction of NS, while the plasma plasminogen concentration was also slightly elevated.
Arithmetic means ± SEM, # indicates significant difference to baseline value (Figure was first published on May 2020 Acta Physiologica).

3.2.4 Nephrotic nphs2$^{\Delta ipod}$**plg*$^{+/+}$ *and nphs2*$^{\Delta ipod}$**plg*$^{-/-}$ *mice undergo ENaC activation and sodium retention*[74]

To assess ENaC activity, the natriuretic response to amiloride (10 µg/g bw i.p.) was determined in *nphs2*$^{\Delta ipod}$**plg*$^{+/+}$ and *nphs2*$^{\Delta ipod}$**plg*$^{-/-}$ mice sequentially in both the uninduced and nephrotic state[74]. The baseline of natriuresis was determined by injecting mice with the injectable water (5 µl/g bw, vehicle injection)[74].

As shown in Figure 39 A, the response to amiloride was similar in *nphs2*$^{\Delta ipod}$**plg*$^{+/+}$ (n=10) and *nphs2*$^{\Delta ipod}$**plg*$^{-/-}$ mice (n=11) before induction of NS (*nphs2*$^{\Delta ipod}$**plg*$^{+/+}$ vs. *nphs2*$^{\Delta ipod}$**plg*$^{-/-}$, 93 ± 11 µmol/6 h vs. 91 ± 11 µmol/6 h), presenting a close ENaC function in both genotypes[74]. After treatment of doxycycline, the response to amiloride injection increased significantly in both genotypes to a similar extent. In nephrotic *nphs2*$^{\Delta ipod}$**plg*$^{+/+}$ mice (n=9) and *nphs2*$^{\Delta ipod}$**plg*$^{-/-}$ mice (n=8) urinary sodium excretion was significantly reduced (3 ± 1 µmol/6 h and 5 ± 1 µmol/6 h, respectively) after a vehicle injection, indicating sodium retention[74]. After amiloride injection, urinary sodium excretion increased to 110 ± 26 µmol/6 h and 159 ± 27 µmol/6 h[74], in nephrotic

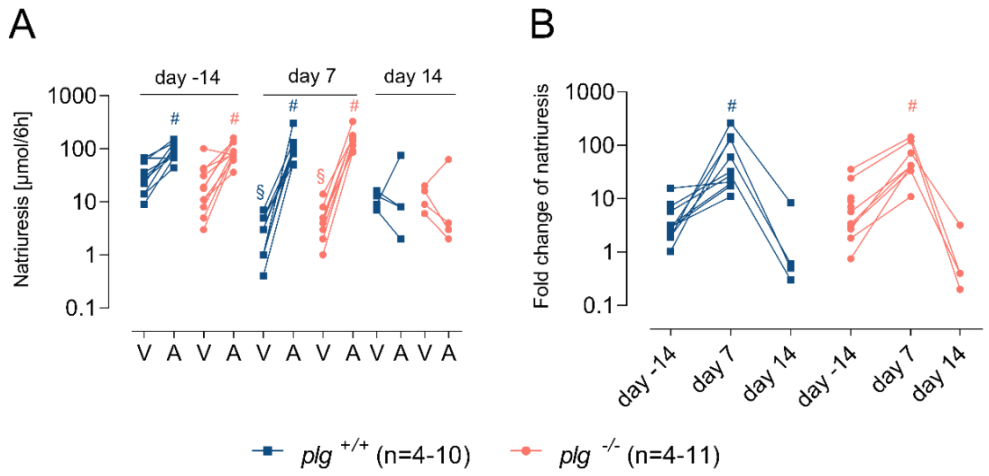

Figure 39 ENaC activation and sodium retention in nephrotic *nphs2*$^{\Delta ipod}$**plg*$^{+/+}$ and *nphs2*$^{\Delta ipod}$**plg*$^{-/-}$ mice[74]

(A) Natriuretic response to vehicle or amiloride injection in *nphs2*$^{\Delta ipod}$**plg*$^{+/+}$ and *nphs2*$^{\Delta ipod}$**plg*$^{-/-}$ mice before and after induction of NS, respectively[74].
(B) ENaC activation was presented as an increased ratio between amiloride and vehicle injection in nephrotic mice on day 7. The ratio was decreased on day 14, indicating the inactivation of ENaC. Arithmetic means ± SEM, # indicates significant difference to baseline value, * indicates significant difference between genotypes, § indicates significant difference between uninduced and nephrotic state. A: amiloride; U: uninduced; N: nephrotic. V: vehicle[74] (Figures A-B were first published on May 2020 Acta Physiologica).

nphs2$^{\Delta ipod}$**plg*$^{+/+}$ and *nphs2*$^{\Delta ipod}$**plg*$^{-/-}$ mice, respectively. The ratio of the natriuretic response between vehicle and amiloride injection (amiloride response/ vehicle response, A/V) was calculated and showed a significant increase in both genotypes after induction of NS (Figure 39 B). In *nphs2*$^{\Delta ipod}$**plg*$^{+/+}$ mice, the A/V ratio was 4 ± 1 (n=10) before induction, and it was increased to 72 ± 26 after induction of NS (p=0.0328). In uninduced *nphs2*$^{\Delta ipod}$**plg*$^{-/-}$ mice the ratio was 9 ± 3 (n=11) and in nephrotic mice the ratio was 63 ± 16 (p=0.0070). This was the clearest evidence of ENaC activation in nephrotic mice of both genotypes. However, there was no significant difference between two genotypes in A/V ratio before or after induction of NS (difference comparison the A/V ratio between uninduced *nphs2*$^{\Delta ipod}$**plg*$^{+/+}$ and *nphs2*$^{\Delta ipod}$**plg*$^{-/-}$ mice, p=0.9952; difference comparison the A/V ratio between nephrotic *nphs2*$^{\Delta ipod}$** plg*$^{+/+}$ and *nphs2*$^{\Delta ipod}$**plg*$^{-/-}$ mice, p=0.3468). Because of an unexpected reversely increase in urinary Na^+ excretion and a loss of body weight around 8-10 days after induction of NS in *nphs2*$^{\Delta ipod}$ mice as described previously (Figure 25 E-F). To investigate ENaC activity after reverse loss of sodium retention and edema in both *nphs2*$^{\Delta ipod}$**plg*$^{+/+}$ and *nphs2*$^{\Delta ipod}$**plg*$^{-/-}$ mice, four mice per genotype were received the vehicle and amiloride injection respectively on day 13 and on day 14. Results

showed that there was a tendency in the decrease of response to amiloride on day 14 in each genotype. The 6h urinary sodium excretion after an amiloride injection was 23 ± 17 µmol/6 h in *nphs2*$^{\Delta ipod}$**plg*$^{+/+}$ mice and was 18 ± 15 µmol/6 h in *nphs2*$^{\Delta ipod}$**plg*$^{-/-}$ mice. And the A/V ratio was also decreased in both genotypes on day 14 (2 ± 2 in *plg*$^{+/+}$ mice, and 1± 1 in *plg*$^{-/-}$ mice, Figure 39 A-B). The difference was not significant compared to the values on day 8 because of the low sample size.

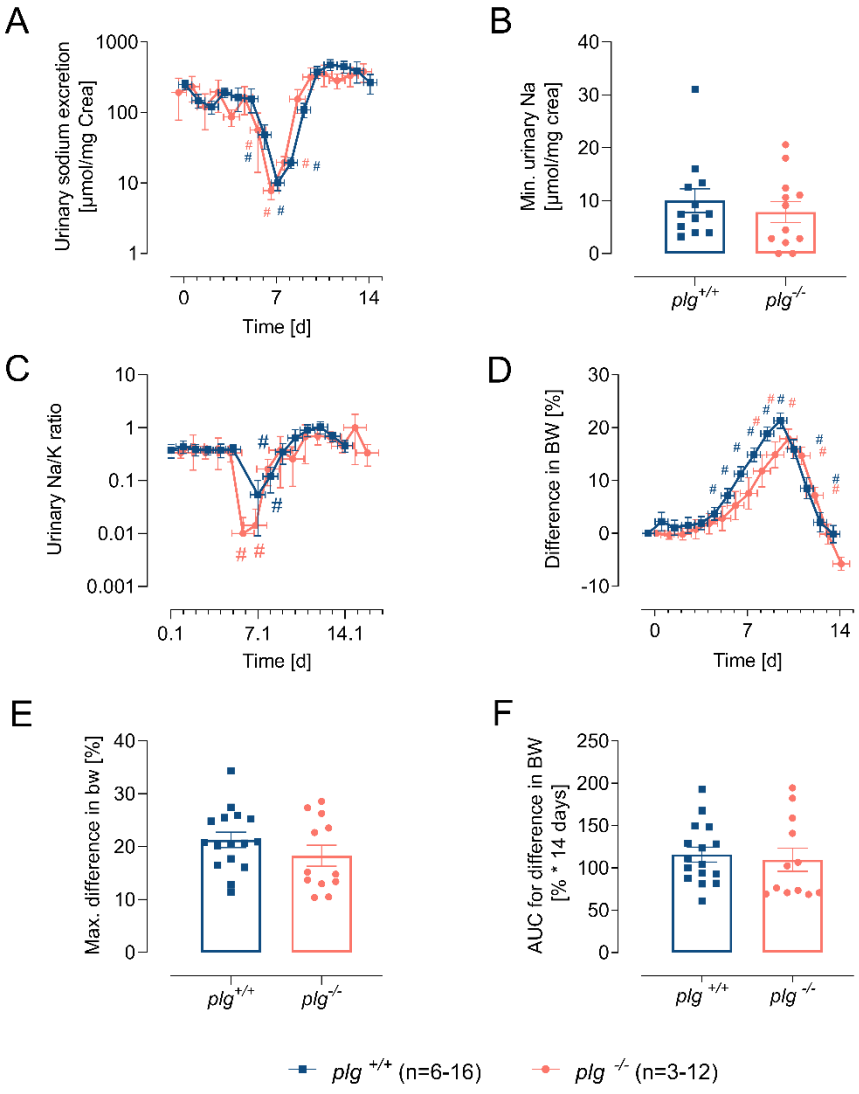

Figure 40 Sodium retention and edema in nephrotic *nphs2*$^{\Delta ipod}$**plg*$^{+/+}$ and *nphs2*$^{\Delta ipod}$**plg*$^{-/-}$ mice[74]

(A-B) Course of sodium concentration in spot urine and the minimum values of *nphs2*$^{\Delta ipod}$**plg*$^{+/+}$ and *nphs2*$^{\Delta ipod}$**plg*$^{-/-}$ mice[74].
(C-D) Course of body weight and the maximum increase in both genotypes indicating the development of edema.
(E) Course of Na^+/K^+ ratio in spot urine.
(F) Area under the curve (AUC) of difference in body weight in nephrotic mice of both genotypes[74].
Arithmetic means ± SEM, # indicates significant difference to baseline value (Figures A, C and F were first published on May 2020 Acta Physiologica).

As a consequence of increased ENaC activity within the first 7 days after induction of NS, sodium concentration from daily collected spot urine samples dropped to minimal values of 6 ± 1 mM (10 ± 2 µmol/mg crea) and 5 ± 1 mM (7 ± 2 µmol/mg crea) in *nphs2*$^{\Delta ipod}$***plg*$^{+/+}$ and *nphs2*$^{\Delta ipod}$** plg*$^{-/-}$ mice respectively (Figure 40 A-B)[74], despite a constant sodium intake (Figure 54 A-B). The results indicated both *nphs2*$^{\Delta ipod}$***plg*$^{+/+}$ and *nphs2*$^{\Delta ipod}$***plg*$^{-/-}$ mice underwent sodium retention, and there was no significant difference between the two genotypes (p>0.9999). Urinary Na^+/K^+ which excluded the influence of intake and urinary creatinine, was consistent with the result of urinary sodium concentration (Figure 40 C). The evidence of a significantly decreased 24h-urinary sodium excretion (Table 3) also showed sodium retention in nephrotic mice of both genotypes (a decrease from 193 ± 16 µmol/24 h to 15 ± 6 µmol/24 h in *nphs2*$^{\Delta ipod}$***plg*$^{+/+}$ mice, p=0.0002; and a decrease from 229 ± 11 µmol/24 h to 25 ± 7 µmol/24 h in *nphs2*$^{\Delta ipod}$***plg*$^{-/-}$ mice, p=0.0202). Besides, the positive sodium balance (Table 3) was also evidence supported for sodium retention.

Table 3 Sodium balance in *nphs2*$^{\Delta ipod}$***plg*$^{+/+}$ and *nphs2*$^{\Delta ipod}$***plg*$^{-/-}$ mice during various conditions[74]

Values of 'low salt diet' were obtained in uninduced mice 5 days after a low salt diet. Nephrotic mice received the standard diet and data were collected on day 7.
Arithmetic means ± SEM (n= 8-11 each).
$^{\#}$ significant difference compared to uninduced mice of the same genotype under a control diet, * significant difference between genotypes (Data were first published on May 2020 Acta Physiologica)

	Day -28 (control diet)		Day -21 (low salt diet)		Day 7 (control diet)	
	plg$^{+/+}$	*plg*$^{-/-}$	*plg*$^{+/+}$	*plg*$^{-/-}$	*plg*$^{+/+}$	*plg*$^{-/-}$
total Na^+ intake, µmol 24/h	290 ± 14	322 ±16	23 ± 1 $^{\#}$	24 ± 1 $^{\#}$	258 ± 15	304 ± 13
urinary Na^+ excretion, µmol/24 h	193 ± 16	229 ± 11 *	18 ± 3 $^{\#}$	16 ± 3 $^{\#}$	15 ± 6 $^{\#}$	25 ± 7 $^{\#}$
fecal Na^+ excretion, µmol/24 h	13 ± 1	19 ± 3	7 ± 1	13 ± 2	11 ± 2	21 ± 2 *
Na^+ balance, µmol/24 h	84 ± 13	74 ±14	-2 ± 3 $^{\#}$	-5 ± 3 $^{\#}$	232 ± 18 $^{\#}$	258 ± 15 $^{\#}$

Subsequently, nephrotic mice of both genotypes developed a visible ascites (Figure 41) which was accompanied by body weight gain (Figure 40 D-F). To correct for the smaller size of *nphs2*$^{\Delta ipod}$***plg*$^{-/-}$ mice, the relative difference in body weight increase (%) was calculated. The maximal difference in body weight was 21 ± 1% in *nphs2*$^{\Delta ipod}$***plg*$^{+/+}$ mice whereas 18 ± 2% in *nphs2*$^{\Delta ipod}$***plg*$^{-/-}$ mice[74]. There was no significant difference in body weight increase between genotypes (p=0.2192, Figure 40 E). In addition, the area under the curve (AUC) of the bodyweight difference was calculated in each mouse during the 14-day observation (Figure 40 F[74]). The AUC values from *nphs2*$^{\Delta ipod}$***plg*$^{+/+}$ mice (116 ±

9 % * 14 days) were similar to those from *nphs2*$^{\Delta ipod}$**plg*$^{-/-}$ mice (110 ± 14 % * 14 days) without showing a significant difference (p=0.6951).

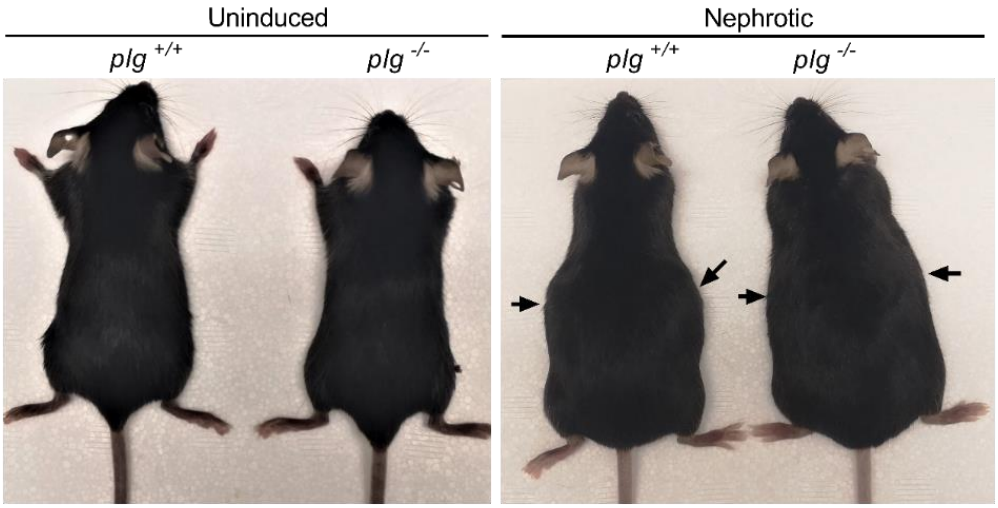

Figure 41 Phenotypes of *nphs2*$^{\Delta ipod}$**plg*$^{+/+}$ and *nphs2*$^{\Delta ipod}$**plg*$^{-/-}$ mice before and after induction of NS

The mice developed an identical ascites (the arrow pointed) after the induction of NS in both genotypes.

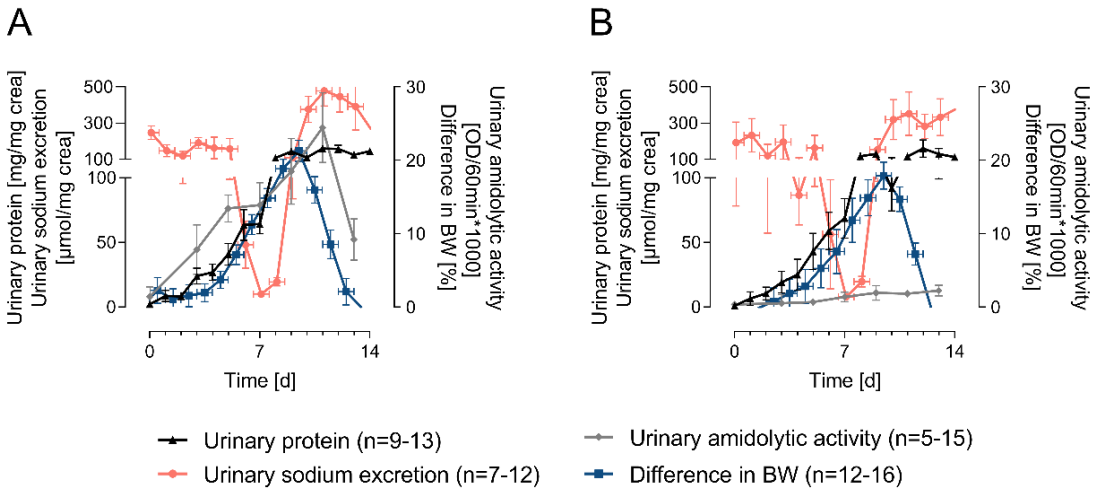

Figure 42 Chronological features of experimental NS development in *nphs2*$^{\Delta ipod}$**plg*$^{+/+}$ and *nphs2*$^{\Delta ipod}$**plg*$^{-/-}$ mice

Arithmetic means ± SEM (Figures A-B were first published on May 2020 Acta Physiologica)

Both *nphs2*$^{\Delta ipod}$**plg*$^{+/+}$ and *nphs2*$^{\Delta ipod}$**plg*$^{-/-}$ mice displayed the symptoms of experimental NS in a chronological order. Proteinuria was the first noticed symbol of NS in nephrotic *nphs2*$^{\Delta ipod}$** plg*$^{+/+}$ and *nphs2*$^{\Delta ipod}$**plg*$^{-/-}$ mice (Figure 42 A-B[74]). Surprisingly, the development of urinary amidolytic activity was even ahead of proteinuria in nephrotic

nphs2$^{\Delta ipod}$**plg*$^{+/+}$ mice. This finding indicated urinary amidolytic activity maybe more sensitive in investigating glomerular damage than urinary protein, and perhaps could be used as a promising biomarker in diagnosing proteinuric diseases. The decrease of sodium excretion in urine was observed after an increased urinary amidolytic activity and proteinuria, indicating sodium retention. Maximum of body weight increase in nephrotic *nphs2*$^{\Delta ipod}$**plg*$^{+/+}$ mice was a delay of one to two days than sodium retention. Unexpectedly, sodium retention and edema were spontaneously reversed on day 9-10 in *nphs2*$^{\Delta ipod}$**plg*$^{+/+}$ mice. The same results have been reported previously in doxorubicin-induced nephrotic mice[32] and in PAN induced nephropathy-rats[95]. The pathophysiological process in *nphs2*$^{\Delta ipod}$**plg*$^{-/-}$ mice was generally the same as *nphs2*$^{\Delta ipod}$**plg*+/+ mice, except for the urinary amidolytic activity which constantly remained at a very low level during the entire time course.

Table 4 Plasma parameters of venous blood gas analysis in *nphs2*$^{\Delta ipod}$**plg*$^{+/+}$ and *nphs2*$^{\Delta ipod}$**plg*$^{-/-}$ mice before and 14 days after induction of nephrotic syndrome[74]

Arithmetic means ± SEM (n=8-11 each)

$^{\#}$ significant difference between uninduced and nephrotic mice of the same genotype;* significant difference between genotypes

Abbreviations: std standard, Hct haematocrit, cHb calculated haemoglobin concentration (Data were first published on May 2020 Acta Physiologica)

	Day -14		Day 7		Day 14	
	plg$^{+/+}$	*plg*$^{-/-}$	*plg*$^{+/+}$	*plg*$^{-/-}$	*plg*$^{+/+}$	*plg*$^{-/-}$
venous pH	7.28± 0.02	7.24 ± 0.01	7.24± 0.01	7.23 ± 0.02	7.31±0.01	7.23 ± 0.02 *
std HCO_3^-, mM	22 ± 0.9	21 ± 0.8	26 ± 1.4 $^{\#}$	25 ± 1.5 $^{\#}$	25 ± 0.6 $^{\#}$	22 ± 0.8
Na^+, mM	147 ± 0	150 ± 1	146 ± 1	147 ± 1	144 ± 1 $^{\#}$	149 ± 2 *
K^+, mM	4.1 ± 0.07	4.2 ± 0.13	4.3 ± 0.24	4.7 ± 0.25	4.9 ± 0.15 $^{\#}$	5.1 ± 0.19 $^{\#}$
Ca^{++}, mM	1.00± 0.01	1.13 ± 0.02 *	1.00± 0.05	1.10 ± 0.07	1.03 ± 0.01	1.05 ± 0.04
Hct, %	44 ± 1	44 ± 1	41 ± 4	46 ± 1	42 ± 1	42 ± 1
cHb, g dL^{-1}	14.6 ± 0.3	14.4 ± 0.2	16.3 ± 1.4	18.7 ± 1.9 $^{\#}$	14.0 ± 0.5	13.8 ± 0.4

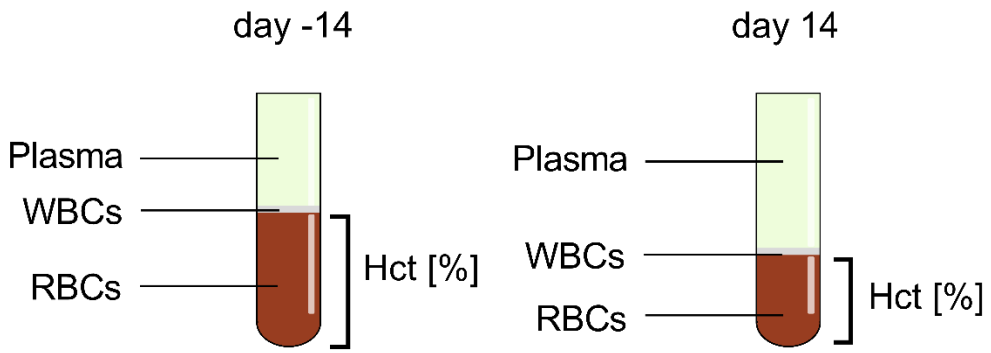

Figure 43 An illustration of hematocrit in uninduced and nephrotic mice

Whole blood was divided into three parts after centrifugation, including plasma, white blood cells (WBCs), and red blood cells (RBCs). In uninduced mice, the hematocrit (Hct) value (%) was about 44% of the whole-blood, while the Hct value tended to decrease in nephrotic mice on day 14.

Plasma parameters measured by a blood gas analyzer before and after induction of NS in *nphs2*$^{\Delta ipod}$**plg*$^{+/+}$ and *nphs2*$^{\Delta ipod}$**plg*$^{-/-}$ mice were listed in Table 4[74]. Venous pH values were lower in *nphs2*$^{\Delta ipod}$**plg*$^{-/-}$ mice on day 14 than in *nphs2*$^{\Delta ipod}$**plg*$^{+/+}$ mice (p=0.0009). However, the values of venous pH from *nphs2*$^{\Delta ipod}$**plg*$^{-/-}$ mice were not significantly different from baseline values (p>0.9999). Standard bicarbonate concentration tended to be higher in both genotypes on day 7, as well as in *nphs2*$^{\Delta ipod}$**plg*$^{-/-}$ mice on day 14 (day 7 vs. day -14 in *nphs2*$^{\Delta ipod}$**plg*$^{+/+}$ mice, p=0.0349; day 14 vs. day -14 in *nphs2*$^{\Delta ipod}$**plg*$^{+/+}$ mice, p=0.0275; day 7 vs. day -14 in *nphs2*$^{\Delta ipod}$**plg*$^{-/-}$ mice, p=0.0194). Plasma concentration of Na^+ significantly decreased in *nphs2*$^{\Delta ipod}$**plg*$^{+/+}$ mice on day 14 compared to baseline values, while did not decrease in *nphs2*$^{\Delta ipod}$**plg*$^{-/-}$ mice (day 14 vs. day -14 in *nphs2*$^{\Delta ipod}$**plg*$^{+/+}$ mice, p=0.0184; *nphs2*$^{\Delta ipod}$**plg*$^{+/+}$ vs. *nphs2*$^{\Delta ipod}$**plg*$^{-/-}$ mice on day 14, p=0.0007). Notably, plasma K^+ concentration was significantly elevated in both genotypes on day 14 (day 14 vs. day -14 in *nphs2*$^{\Delta ipod}$**plg*$^{+/+}$ mice, p=0.0005; day 14 vs. day -14 in *nphs2*$^{\Delta ipod}$**plg*$^{-/-}$ mice, p=0.0070), but not on day 7, indicating a hyperkalemia which has been analogously shown in nephrotic rats[38]. Plasma calcium concentration was slightly higher in *nphs2*$^{\Delta ipod}$**plg*$^{+/+}$ mice than in *nphs2*$^{\Delta ipod}$**plg*$^{-/-}$ mice before induction (*nphs2*$^{\Delta ipod}$**plg*$^{+/+}$ vs. *nphs2*$^{\Delta ipod}$**plg*$^{-/-}$ mice on day -14, p=0.0008). There was a decreased tendency in hematocrit values in both genotypes on day 14, indicating either anemia or plasma volume retention (Figure 43). Changes of cHb was in parallel with the result of hematocrit in both genotypes. In both *nphs2*$^{\Delta ipod}$**plg*$^{+/+}$ and *nphs2*$^{\Delta ipod}$**plg*$^{-/-}$ mice, histology of kidneys presented a manifestation of FSGS (Figure

44).

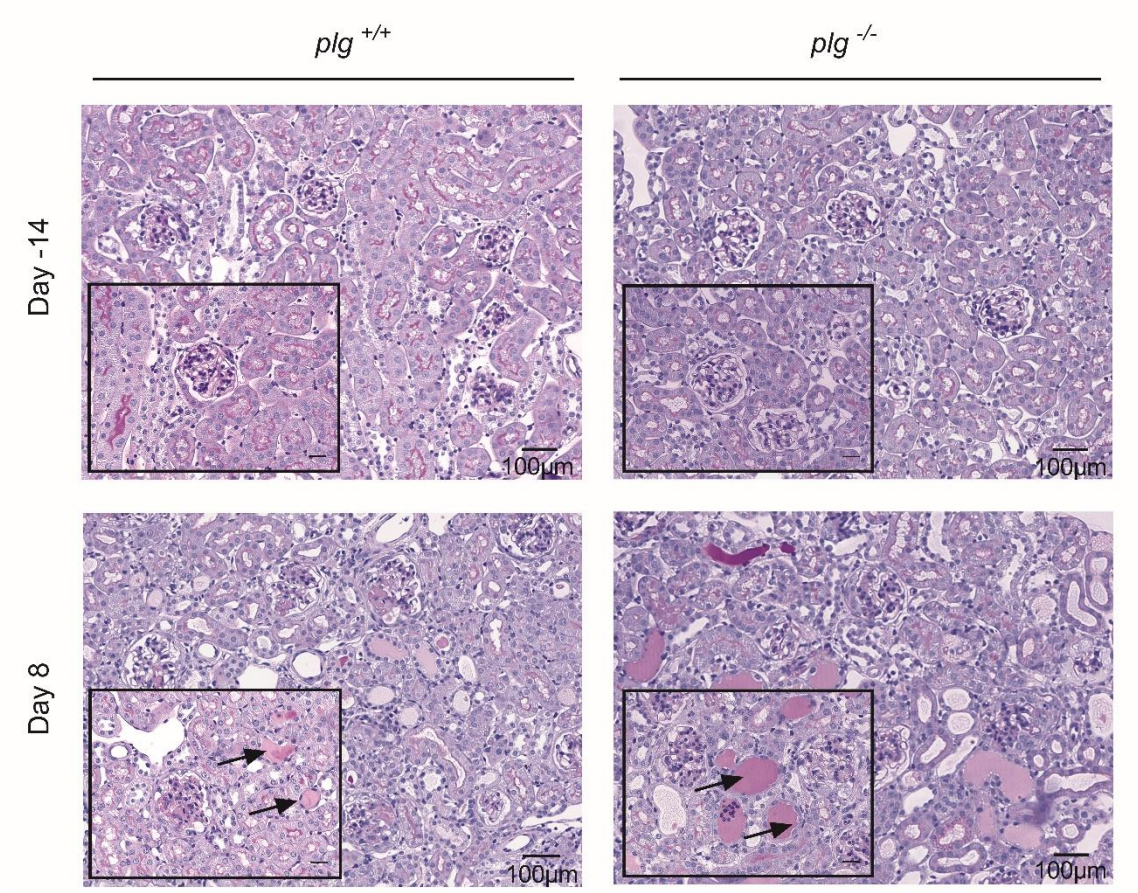

Figure 44 Histology of *nphs2*$^{\Delta ipod}$**plg*$^{+/+}$ and *nphs2*$^{\Delta ipod}$**plg*$^{-/-}$ mice before doxycycline induction and 14 days after induction of NS

The uninduced mice of both genotypes had normal structure of podocyte and tubular. Glomerulosclerosis in some glomerular, and protein cast in tubular (error) was observed on day 8 in both genotypes. Histology results showed mice developed FSGS in *nphs2*$^{\Delta ipod}$**plg*$^{+/+}$ and *nphs2*$^{\Delta ipod}$**plg*$^{-/-}$ mice. Scalar bar: 100 µm.

3.3 Aprotinin prevents sodium retention in nephrotic *nphs2*$^{\Delta ipod}$**plg*$^{+/+}$ and *nphs2*$^{\Delta ipod}$**plg*$^{-/-}$ mice[74]

3.3.1 Dose finding study for aprotinin pellet to nephrotic nphs2$^{\Delta ipod}$**plg*$^{+/+}$ *and nphs2*$^{\Delta ipod}$**plg*$^{-/-}$ *mice on day 0*

In doxorubicin-induced experimental NS, sodium retention and ascites were completely prevented by the serine protease inhibitor aprotinin[35]. The data presented in 3.1.2 showed that aprotinin treatment in nephrotic *nphs2*$^{\Delta ipod}$**plg*$^{+/+}$ mice starting from day 7 inhibited proteolytic activation of ENaC and edema. To analyze if proteasuria accounted for the sodium retention in mice lacking plasminogen (*nphs2*$^{\Delta ipod}$**plg*$^{-/-}$), we planned to preventively implant sustained-release pellets containing aprotinin to both *nphs2*$^{\Delta ipod}$***

plg$^{+/+}$ and *nphs2*$^{\Delta ipod}$**plg*$^{-/-}$ mice. At the beginning of this study, there was no data on aprotinin treatment in C57BL/6J mice. Based on the preliminary data with pellet implantation on day 7 and the previous study in 129S1/SvImJ mice [34,35] we began with the dose of 1 mg aprotinin per day to 4 mice of each genotype on day 0, the other 4 mice received placebo treatment on the same day. Compared to mice with placebo treatment, three out of four nephrotic *nphs2*$^{\Delta ipod}$**plg*$^{-/-}$ mice were completely protected from the decrease of urinary sodium excretion and body weight increase by 1 mg/day aprotinin treatment, however, one mouse failed to be protected. On the contrary, aprotinin implantation with a dose of 1 mg/day could not inhibit the development of sodium retention and edema in *nphs2*$^{\Delta ipod}$**plg*$^{+/+}$ mice. It was concluded that with the dose of 1 mg/day, treatment effect for sodium retention and edema by aprotinin was not sufficient for C57BL/6J mice, and the dose had to be increased.

3.3.2 Effect of aprotinin on sodium retention in nphs2$^{\Delta ipod}$**plg*$^{+/+}$ *and nphs2*$^{\Delta ipod}$**plg*$^{-/-}$ *mice*[74]

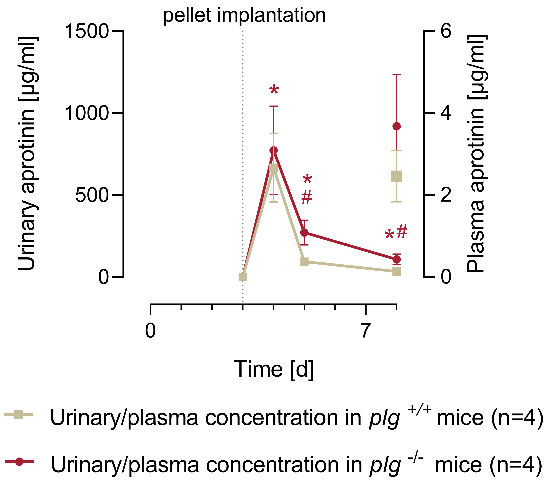

Figure 45 Investigation of effective concentration of aprotinin in urine and plasma samples of nephrotic *nphs2*$^{\Delta ipod}$**plg*$^{+/+}$ and *nphs2*$^{\Delta ipod}$**plg*$^{-/-}$ mice

Course of urinary aprotinin concentration. The excretion of aprotinin though urine was rapid in both genotypes after pellets implantation[74].
Arithmetic means ± SEM, # indicates significant difference to baseline value, * indicates significant difference between genotypes (Figure was first published on May 2020 Acta Physiologica).

After the dose-finding study, we decided to increase the dose of aprotinin to 2 x 1 mg per day (one pellet on each side of the back of each mouse) in both *nphs2*$^{\Delta ipod}$**plg*$^{+/+}$ mice or *nphs2*$^{\Delta ipod}$**plg*$^{-/-}$ mice which coincided with the development of proteinuria as well as amidolytic activity on day 3. The mice which were assigned to placebo group received

the same amount of matrix-only (placebo) pellets subcutaneously. Therefore, 3 days after of the end of doxycycline induction, 8 mice of each genotype were assigned equally to either placebo or aprotinin group (*nphs2*$^{\Delta ipod}$**plg*$^{+/+}$ + placebo, n=4; *nphs2*$^{\Delta ipod}$**plg*$^{+/+}$ + aprotinin, n=4; *nphs2*$^{\Delta ipod}$**plg*$^{-/-}$ + placebo, n=4; *nphs2*$^{\Delta ipod}$**plg*$^{-/-}$ + aprotinin, n=4).

The urinary aprotinin concentration on day 3 (the day of pellet implantation) was set as the negative control (Figure 45). The maximum value of urinary aprotinin concentrations reached to the maximum values between 667 ± 210 in *nphs2*$^{\Delta ipod}$**plg*$^{+/+}$ and 773 ± 269 µg/ml in *nphs2*$^{\Delta ipod}$**plg*$^{-/-}$ mice on day 4 (one day after pellets implantation)[74]. Thereafter, urinary aprotinin concentration dropped fast two days after pellets implantation to 94 ± 16 µg/ml in *nphs2*$^{\Delta ipod}$**plg*$^{+/+}$ mice and to 271 ± 75 in *nphs2*$^{\Delta ipod}$**plg*$^{-/-}$ mice. After 5 days of pellets implantation, urinary aprotinin concentration was further decreased to 35 ± 15 µg/ml in *nphs2*$^{\Delta ipod}$**plg*$^{+/+}$ mice and to 108 ± 32 µg/ml in *nphs2*$^{\Delta ipod}$**plg*$^{-/-}$ mice. Plasma aprotinin concentration 5 days after pellets implantation was only 2 ± 1 µg/ml and 4 ± 1 µg/ml in *nphs2*$^{\Delta ipod}$**plg*$^{+/+}$ and *nphs2*$^{\Delta ipod}$**plg*$^{-/-}$ mice, respectively. Notably, *nphs2*$^{\Delta ipod}$ *plg*$^{-/-}$ *mice* always had a higher aprotinin concentrations in both urine and plasma samples.

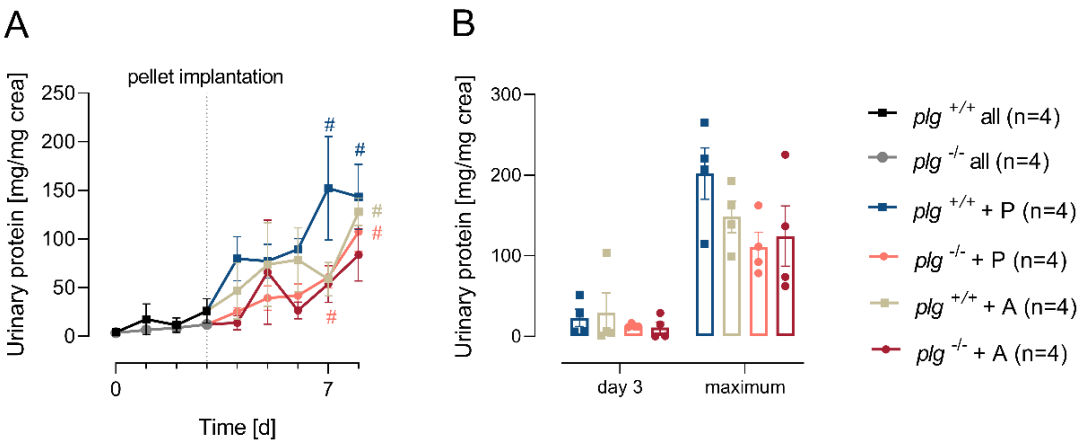

Figure 46 Proteinuria of in nephrotic *nphs2*$^{\Delta ipod}$**plg*$^{+/+}$ and *nphs2*$^{\Delta ipod}$**plg*$^{-/-}$ mice with aprotinin or placebo pellets implantation

(A-B) Course of proteinuria and the comparison of proteinuria before implantation and the maximum proteinuria after implantation.
Arithmetic means ± SEM, # indicates significant difference to baseline value. P: placebo pellets; A: aprotinin pellets (Figure A was first published on May 2020 Acta Physiologica).

The course of proteinuria was similar in all groups (Figure 46 A). The maximum of proteinuria after pellet implantation was 202 ± 32 mg/mg crea in *nphs2*$^{\Delta ipod}$* *plg*$^{+/+}$ + placebo group; 148 ± 20 mg/mg crea in *nphs2*$^{\Delta ipod}$ *plg*$^{+/+}$ + aprotinin group; 111 ± 18

mg/mg crea in *nphs2*$^{\Delta ipod}$**plg*$^{-/-}$ + placebo group and 112 ± 456 in *nphs2*$^{\Delta ipod}$**plg*$^{-/-}$ + aprotinin group, respectively. There was no significant difference in the maximum proteinuria among each group after pellet implantation (p=0.1798), indicating that aprotinin had no impact on urinary protein concentration (Figure 46 A-B).

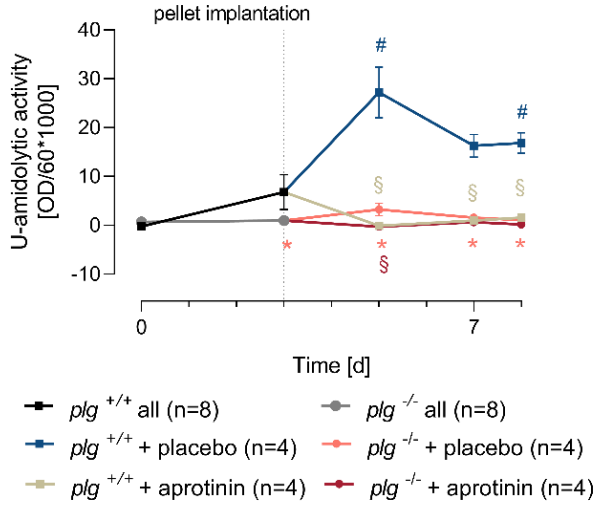

Figure 47 Urinary amidolytic activity in nephrotic *nphs2*$^{\Delta ipod}$**plg*$^{+/+}$ and *nphs2*$^{\Delta ipod}$**plg*$^{-/-}$ mice with placebo or aprotinin treatment

Arithmetic means ± SEM, # indicates significant difference to baseline value, * indicates significant difference between genotypes, § indicated significant difference between placebo and aprotinin-treated nephrotic mice[74] (Figure was first published on May 2020 Acta Physiologica).

However, the urinary amidolytic activity in aprotinin treated mice of both genotypes was utterly inhibited (Figure 47). In *nphs2*$^{\Delta ipod}$**plg*$^{+/+}$ + placebo group, urinary amidolytic activity increased significantly to a maximum value of 27 ± 5 OD/60*1000 on day 5 compared to the baseline. In contrast, the urinary amidolytic activity was zero in aprotinin treated mice of both genotypes on day 5. However, the urinary amidolytic activity was not completely abolished in *nphs2*$^{\Delta ipod}$**plg*$^{-/-}$ mice with placebo pellets implantation (the average value was 3 ± 1 OD/60*1000) on day 5. In *nphs2*$^{\Delta ipod}$**plg*$^{+/+}$ + placebo group, urinary amidolytic activity increased significantly to a maximum value of 27 ± 5 OD/60*1000 on day 5 compared to the baseline. In contrast, urinary amidolytic activity was completely suppressed in aprotinin treated mice of both genotypes.

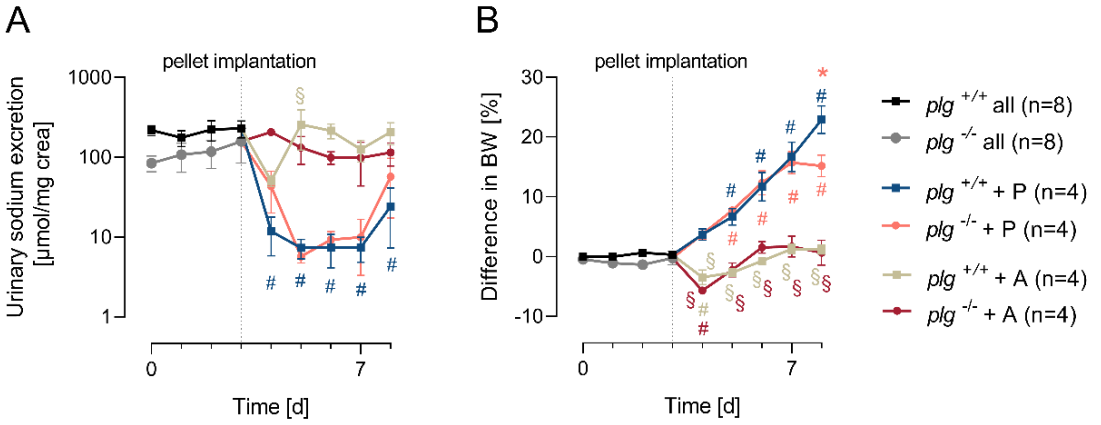

Figure 48 Inhibition effect of aprotinin in sodium retention and edema formation in nephrotic *nphs2*$^{\Delta ipod}$**plg*$^{+/+}$ and *nphs2*$^{\Delta ipod}$**plg*$^{-/-}$ mice[74]

(A-B) Course of urinary sodium excretion and difference in body wight in either aprotinin treated or placebo treated group with both genotypes.
Arithmetic means ± SEM, # indicates significant difference to baseline value, * indicates significant difference between genotypes, § indicated significant difference between placebo and aprotinin-treated nephrotic mice. P: placebo pellets; A: aprotinin pellets (Figures A-B were first published on May 2020 Acta Physiologica).

Urinary sodium excretion dropped in placebo-treated nephrotic *nphs2*$^{\Delta ipod}$**plg*$^{+/+}$ mice from 230 ± 55 µmol/mg crea on day 3 to a minimum value of 7 ± 3 µmol/mg crea on day 7[74] (values from day 3 vs. values on day 7, p=0.0068, Figure 48 A); in placebo-treated *nphs2*$^{\Delta ipod}$**plg*$^{-/-}$ mice urinary sodium excretion dropped from 158 ± 73 µmol/mg crea to 10 ± 7 µmol/mg crea (results on day 3 vs. results on day 7, p=0.0947). In contrast, urinary Na^+ concentration remained constant in aprotinin-treated nephrotic mice of both genotypes, indicating suppression of proteolytic ENaC activation by aprotinin[74]. Urinary sodium excretion in aprotinin-treated *nphs2*$^{\Delta ipod}$**plg*$^{+/+}$ mice was 230 ± 55 µmol/mg crea on day 3 and 207 ± 63 µmol/mg crea on day 8 (p=0.9914); in aprotinin-treated *nphs2*$^{\Delta ipod}$**plg*$^{-/-}$ mice urinary sodium excretion was 158 ± 73 µmol/mg crea on day 3 and 115 ± 37 µmol/mg crea on day 7 (p=0.9658). The inhibition effect of aprotinin in sodium retention led to a prevention of edema and ascites too, resulting in the non-increased bodyweight in nephrotic *nphs2*$^{\Delta ipod}$**plg*$^{+/+}$ and *nphs2*$^{\Delta ipod}$**plg*$^{-/-}$ mice. In contrast, placebo-treated nephrotic mice of both genotypes gained body weight and had edema[74] (Figure 48 B). The increased percentage of body weight in placebo group reached to a maximum of 23% ± 2 in *nphs2*$^{\Delta ipod}$**plg*$^{+/+}$ mice (p<0.0001, compared to the baseline value), and reached 15% ± 2 in *nphs2*$^{\Delta ipod}$**plg*$^{-/-}$ mice on day 8 (p<0.0001, compared to the baseline value), respectively. On the contrary, the difference in body weight on day 8,

was only 1 ± 1 % in aprotinin treated *nphs2*$^{\Delta ipod}$**plg*$^{+/+}$ mice (p=0.2679), and was 1 ± 2 % in *nphs2*$^{\Delta ipod}$**plg*$^{-/-}$ mice (p=0.8830) with aprotinin treatment[93].

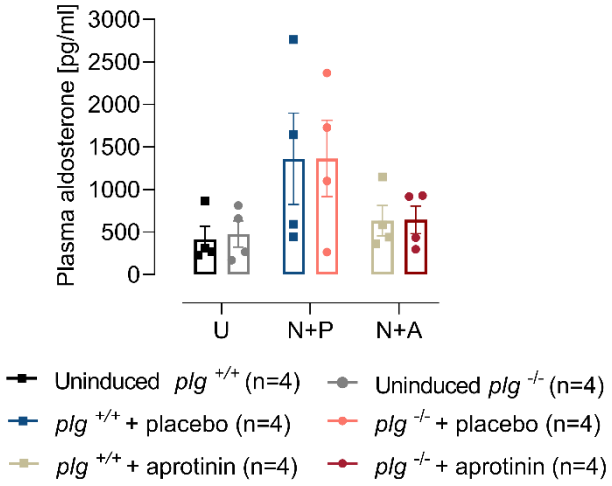

Figure 49 Change of plasma aldosterone concentration under different situation and treatment in *nphs2*$^{\Delta ipod}$**plg*$^{+/+}$ and *nphs2*$^{\Delta ipod}$**plg*$^{-/-}$ mice

Arithmetic means ± SEM, # indicates significant difference to baseline value, * indicates significant difference between genotypes, § indicated significant difference between placebo and aprotinin-treated nephrotic mice (Figure was first published on May 2020 Acta Physiologica).

Plasma aldosterone concentration was elevated in placebo-treated mice of both genotypes compared to the values from uninduced mice, however, there was a large scatter (1361 ± 538 pg/ml vs. 418 ± 151 pg/ml in *nphs2*$^{\Delta ipod}$**plg*$^{+/+}$ mice, p=0.3617; 1366 ± 449 pg/ml vs. 477 ± 154 pg/ml in *nphs2*$^{\Delta ipod}$**plg*$^{-/-}$ mice, p=0.4351), and was tended to be reduced by aprotinin treatment (634 ± 178 pg/ml, compared to baseline p=0.9999; 645 ± 163 pg/ml, p>0.9999 compared to baseline, Figure 49[74]).

3.3.3 Expression of ENaC subunits in kidney tissues from nephrotic nphs2$^{\Delta ipod}$**plg*$^{+/+}$ *and nphs2*$^{\Delta ipod}$**plg*$^{-/-}$ *mice*[74]

Expression of cleavage of α- and γ-ENaC in kidney cortex was studied using Western blot. Membrane protein samples were prepared from the kidney cortex of all 4 groups of mice treated with placebo or aprotinin-pellets. The used antibody against α-ENaC was directed against a N-terminal sequence, whereas the antibody against γ-ENaC bound to a C-terminal sequence (Figure 50 A-B[74]). Western blot revealed two specific bands for α-ENaC at 87 kDa and 26 kDa as expected as the full-length and the N-terminal fragment, and two bands for γ-ENaC at 84 kDa as the full-length, and 72 kDa as the C-terminal

fragment[74]. The specificity of the bands was confirmed by administration of the blocking-peptides to anti-α-ENaC and anti-γ-ENaC (Figure 50 C-D)[74].

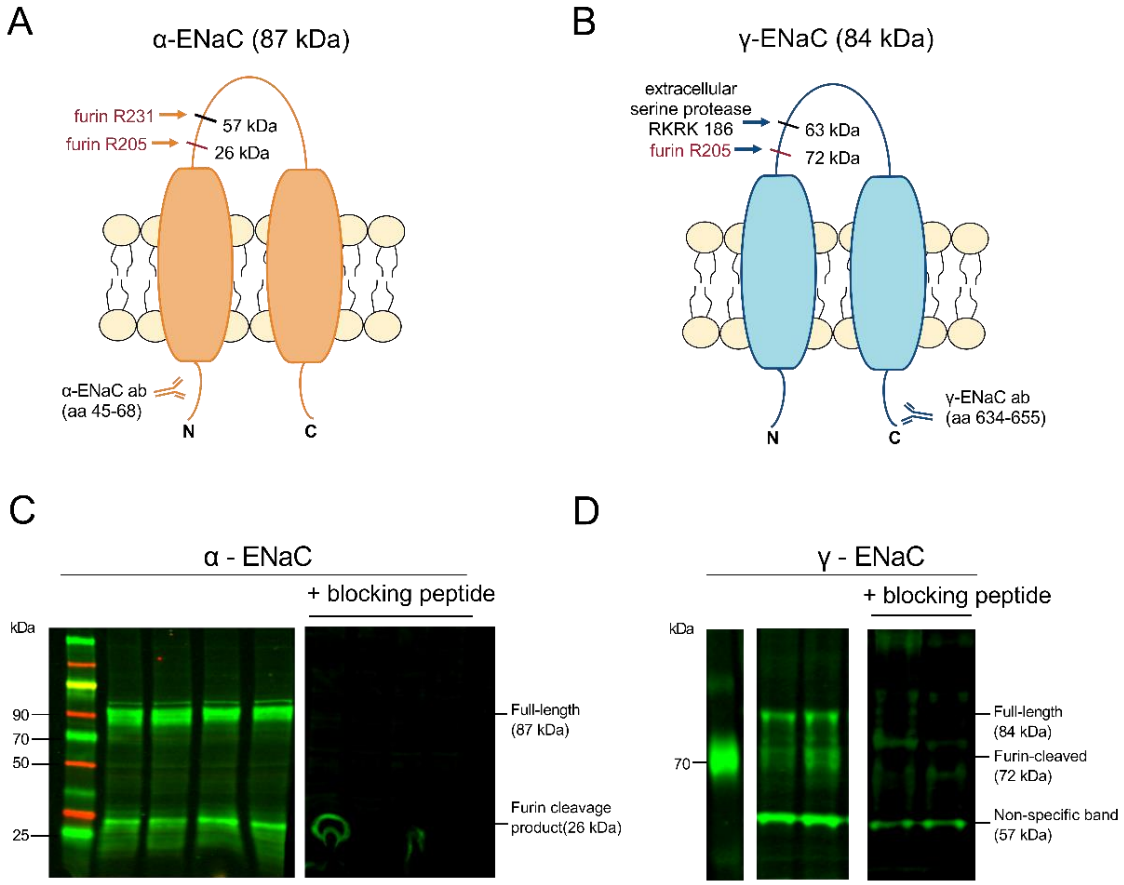

Figure 50 Specificity of the bands obtained with antibodies against α- and γ-ENaC subunits in kidney cortex from uninduced *nphs2*$^{\Delta ipod}$ mice[74]

(A) The antibody against α-ENaC is supposed to detect full-length α-ENaC and an N-terminal fragment with a mass of 26 kDa.
(B) The antibody against γ-ENaC is supposed to detect full-length γ-ENaC and a C-terminal fragment with a mass of 72 kDa after furin cleavage.
(C) Administration of the blocking peptide for α-ENaC attenuated the bands at 26 and 87 kDa.
(D) Administration of the blocking peptide for γ-ENaC (Stressmarq) attenuated bands at 84 and 72 kDa while the band at 57 kDa was only partially blocked.

The expression of the α- and β-ENaC subunits were not significantly changed in nephrotic *nphs2*$^{\Delta ipod}$**plg*$^{+/+}$ and *nphs2*$^{\Delta ipod}$**plg*$^{-/-}$ mice with either treatments, compared to uninduced animals, as presented in Figure 51 and as the densitometric analysis showed in Table 5[74]. However, there was an increased tendency of the 26 kDa α-ENaC fragment expressing in nephrotic *nphs2*$^{\Delta ipod}$**plg*$^{+/+}$ and *nphs2*$^{\Delta ipod}$**plg*$^{-/-}$ mice receiving placebo treatment. Detection of full-length γ-ENaC (84 kDa) by western blot was similar from uninduced mice in neither placebo nor aprotinin treated *nphs2*$^{\Delta ipod}$**plg*$^{+/+}$ and *nphs2*$^{\Delta ipod}$**plg*$^{-/-}$ mice (uninduced *nphs2*$^{\Delta ipod}$**plg*$^{+/+}$ mice vs. placebo mice, p=0.8641; uninduced *nphs2*$^{\Delta ipod}$**plg*$^{+/+}$ mice vs. aprotinin mice, p>0.9999).

However, there was a significant increase in γ-ENaC expression at 72 kDa, which indicated γ-ENaC cleaved by furin, in nephrotic *nphs2*$^{\Delta ipod}$**plg*$^{+/+}$ mice. And it was attenuated by aprotinin treatment (Table 5[74]) (uninduced *nphs2*$^{\Delta ipod}$**plg*$^{+/+}$ mice vs. placebo mice, p=0.0239, t-test; *nphs2*$^{\Delta ipod}$**plg*$^{+/+}$ + placebo mice vs. aprotinin mice, p=0.0165, t-test). The changing-tendency of the ENaC expression in nephrotic *nphs2*$^{\Delta ipod}$**plg*$^{-/-}$ mice, was not different from *nphs2*$^{\Delta ipod}$**plg*$^{+/+}$ mice. However, the individual variability in animals excluded the statistical differences (uninduced *nphs2*$^{\Delta ipod}$**plg*$^{-/-}$ mice vs. placebo mice, p=0.9998; uninduced *nphs2*$^{\Delta ipod}$**plg*$^{-/-}$ vs. aprotinin, p>0.9999).

Unfortunately, in the present study, we cannot detect the band of γ-ENaC between 65 to 67 kDa, which specifically corresponded to fully-cleavage of γ-ENaC, in renal cortex from nephrotic mice with both genotypes (Figure 50)[74].

Immunohistochemistry indicated an up-regulation of α- and γ-ENaC expression in both nephrotic *nphs2*$^{\Delta ipod}$**plg*$^{+/+}$ and *nphs2*$^{\Delta ipod}$**plg*$^{-/-}$ mice with placebo treatment[74]. The increasing tendency similarly and particularly at the luminal side of the principal cells (Figure 52[74]). Interestingly, the aprotinin treatment attenuated the up-regulation of α- and γ-ENaC expression to both genotypes and tended to prevent the apical targeting as described previously[35].

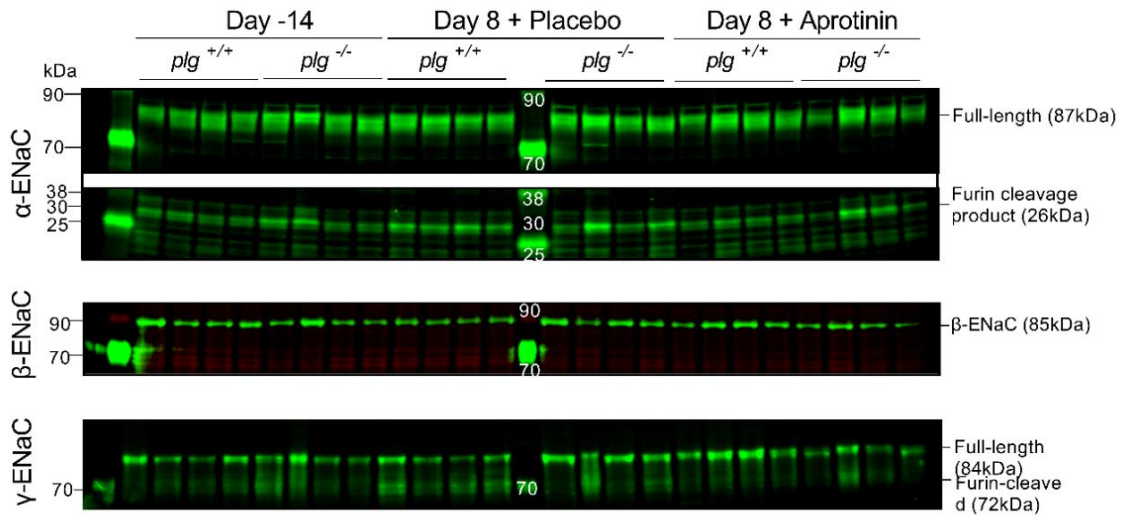

Figure 51 Expression of ENaC subunits in kidney cortex from *nphs2*$^{\Delta ipod}$**plg*$^{+/+}$ and *nphs2*$^{\Delta ipod}$**plg*$^{-/-}$ mice[74]

Detection of ENaC subunits by Western blots from uninduced, and nephrotic *nphs2*$^{\Delta ipod}$**plg*$^{+/+}$ and *nphs2*$^{\Delta ipod}$**plg*$^{-/-}$ mice with either placebo or aprotinin treatment. Kidneys were collected on day 8 as described in Figure 10 from mice in each group (n=4)[74].

Table 5 Densitometric analysis of ENaC subunits expression in kidney cortex from uninduced and nephrotic *nphs2*$^{\Delta ipod}$**plg*$^{+/+}$ and *nphs2*$^{\Delta ipod}$**plg*$^{-/-}$ mice with different treatments[74]

Signal intensity of the bands (relative units) was normalized for total protein expression of the respective lane[74].
Arithmetic means of expression in relative units ± SEM (n=4 each)
[#] significant difference between uninduced and nephrotic mice of the same genotype (t-test), § significant difference between placebo and aprotinin-treated nephrotic mice (t-test) (Data were first published on May 2020 Acta Physiologica).

		uninduced		nephrotic + placebo		nephrotic + aprotinin	
	molecular weight, kDa	*plg*$^{+/+}$	*plg*$^{-/-}$	*plg*$^{+/+}$	*plg*$^{-/-}$	*plg*$^{+/+}$	*plg*$^{-/-}$
α-ENaC	87	186 ± 16	252 ± 23	229 ± 40	237 ± 29	223 ± 58	183 ± 75
	26	64 ± 12	90 ± 31	110 ± 11	98 ± 53	69 ± 3	95 ± 21
β-ENaC	85	8 ± 1	10 ± 1	8 ± 0.3	10 ± 1	11 ± 1	9 ± 1
γ-ENaC	84	178 ± 36	183 ± 45	142 ± 28	254 ± 37	284 ± 42	188 ± 23
	72	110 ± 9	163 ± 55	187 ± 24 [#]	141 ± 62	97 ± 13 [§]	133 ± 48

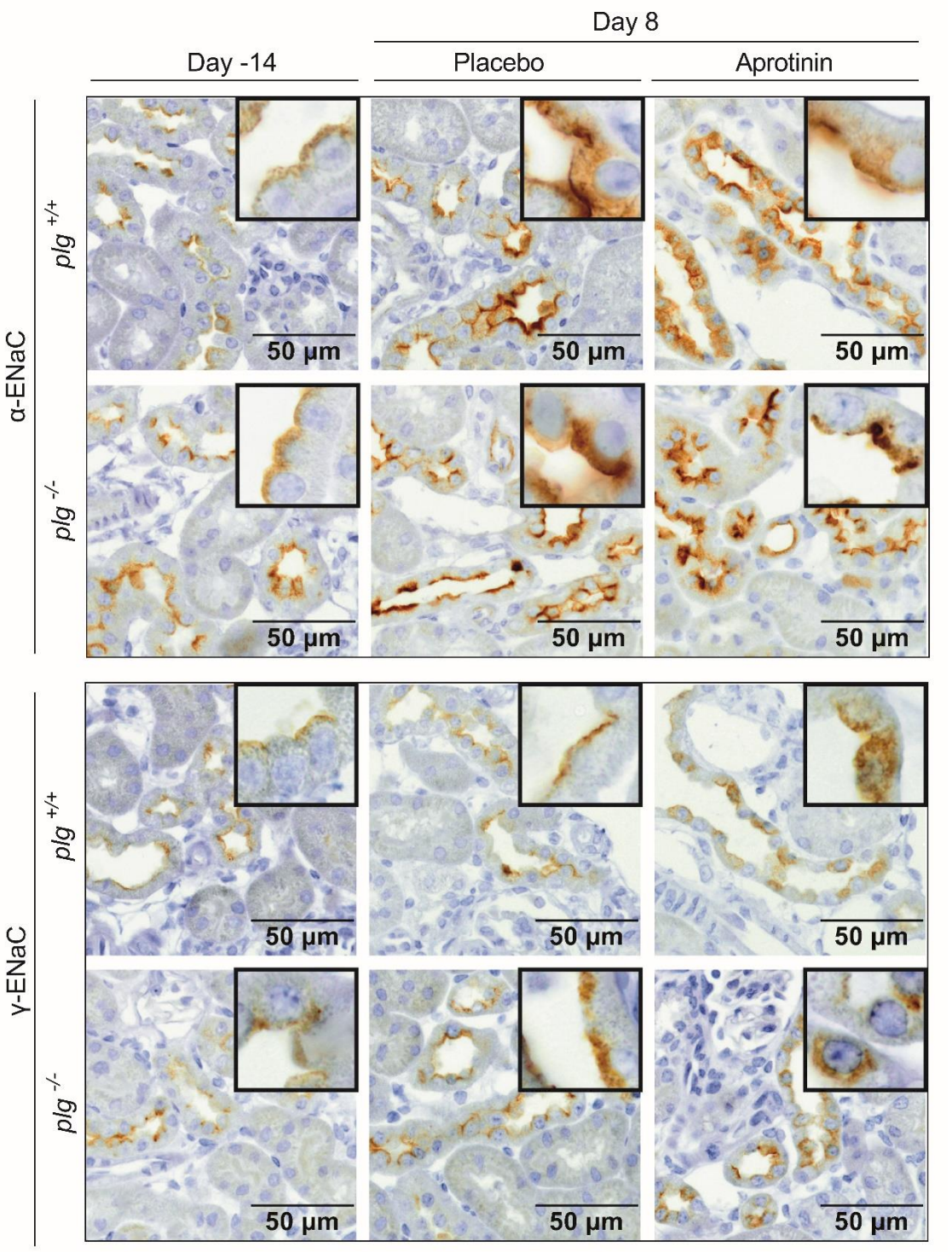

Figure 52 Expression of α-ENaC and γ-ENaC in kidney tissues from *nphs2*$^{\Delta ipod}$**plg*$^{+/+}$ and *nphs2*$^{\Delta ipod}$**plg*$^{-/-}$ mice[74]

Immunohistochemical staining of α-ENaC (brown) and γ-ENaC with formalin-fixed kidneys from uninduced, placebo-treated, or aprotinin-treated nephrotic *nphs2*$^{\Delta ipod}$**plg*$^{+/+}$ and *nphs2*$^{\Delta ipod}$**plg*$^{-/-}$ mice. Kidney-collections were performed on day 8 from the same mice as mentioned above[74]. Both α- and γ-ENaC were up-regulated on day 8 in both genotypes. The apical targeting was prevented in aprotinin-treated, both *nphs2*$^{\Delta ipod}$**plg*$^{+/+}$ and *nphs2*$^{\Delta ipod}$**plg*$^{-/-}$ mice (Figure was first published on May 2020 Acta Physiologica).

3.4 *Long-term course of nephrotic nphs2$^{\Delta ipod}$*plg$^{+/+}$ and nphs2$^{\Delta ipod}$*plg$^{-/-}$ mice*

After the spontaneous reversal of sodium retention and edema until day 14, body weight was lost thereafter in both genotypes (Figure 53 A[74]). Body weight loss was significantly faster in *nphs2$^{\Delta ipod}$*plg$^{-/-}$* mice than in *nphs2$^{\Delta ipod}$*plg$^{+/+}$* mice (Figure 53 B) reaching a significant difference on day 21 (*nphs2$^{\Delta ipod}$*plg$^{+/+}$* vs. *nphs2$^{\Delta ipod}$*plg$^{-/-}$*, -8 %± 2 vs. -20 % ± 3, p =0.0054).

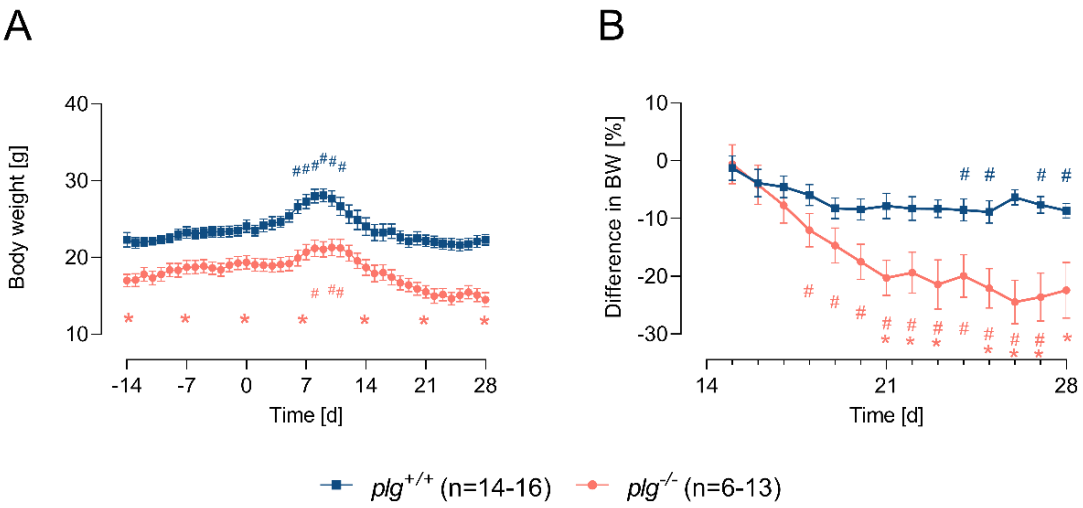

Figure 53 Long-term observation of the bodyweight

(A) Daily body weight was recorded from the beginning of doxycycline induction until 28 days after induction in *nphs2$^{\Delta ipod}$*plg$^{+/+}$* and *nphs2$^{\Delta ipod}$*plg$^{-/-}$* mice. An increasing bump of body weight was observed around day 10 in both genotypes, however, bodyweight was decreasing since then. Compared to *nphs2$^{\Delta ipod}$*plg$^{+/+}$*, *nphs2$^{\Delta ipod}$*plg$^{-/-}$* mice had a reduced body weight (Figure was first published on May 2020 Acta Physiologica).
(B) Changes of the percent body weight in *nphs2$^{\Delta ipod}$*plg$^{+/+}$* and *nphs2$^{\Delta ipod}$*plg$^{-/-}$* mice following from day 14 until day 28 after induction.
Arithmetic means ± SEM $^{\#}$ significant difference compared to the baseline within the same genotype, * significant difference between two genotypes

Body weight (g) was constant in *nphs2$^{\Delta ipod}$*plg$^{+/+}$* and *nphs2$^{\Delta ipod}$*plg$^{-/-}$* mice from day -14 until day 0 (until the end of doxycycline induction, Figure 53 A[74]). Six days after the end of doxycycline induction, body weight increased significantly in each genotype. Unexpectedly, bodyweight accumulation was reversed 14 days later after induction as previously described. Differences in bodyweight decrease (%) reached to a significant difference from day 24 in *nphs2$^{\Delta ipod}$*plg$^{+/+}$* mice and from day 17 in *nphs2$^{\Delta ipod}$*plg$^{-/-}$* mice compared to baseline value from day -14. There was a significant difference in body weight loss between two genotypes from day 21 (*nphs2$^{\Delta ipod}$*plg$^{+/+}$* vs. *nphs2$^{\Delta ipod}$*plg$^{-/-}$*, -8 ± 2 vs. -20 ± 3, p =0.0054).

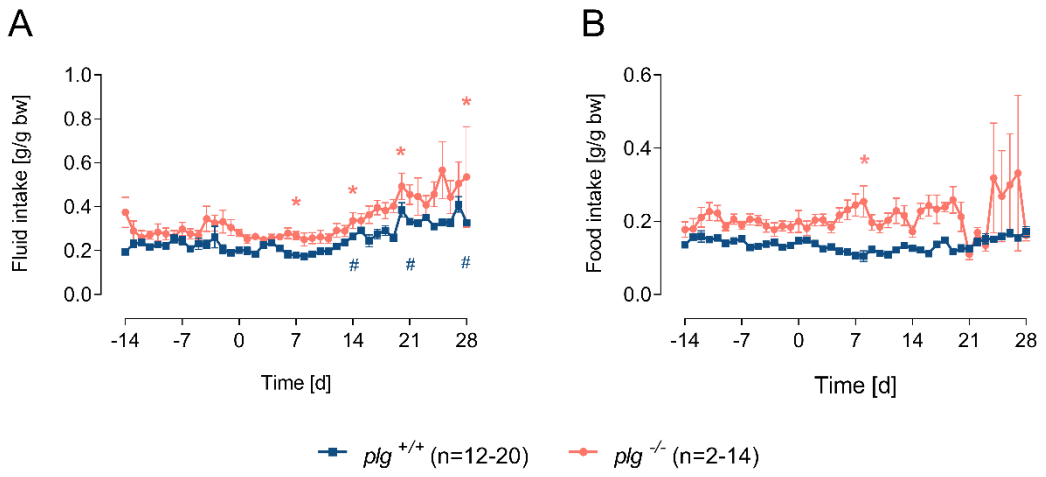

Figure 54 Food and fluid intake monitoring before and after induction[74]

There was an increase in fluid intake in both genotypes from day 14 to day 28, compared to uninduced mice. Whereas the amount of food intake was constant during the entire observation in both genotypes. It seemed the *nphs2*$^{\Delta ipod}$**plg*$^{-/-}$ mice had a higher fluid and food intake than *nphs2*$^{\Delta ipod}$**plg*$^{+/+}$ mice.
Arithmetic means ± SEM. $^{\#}$ significant difference between uninduced and nephrotic mice of the same genotype, * significant difference between genotypes (Figures A-B were first published on May 2020 Acta Physiologica).

Food and fluid intake was generally constant during the 6-week observation (from day -14 to day 28). Except for there was an increasing tendency in fluid intake in both genotypes from day 14 on, perhaps related to increases in body weight loss (Figure 54 A-B[74]). *Nphs2*$^{\Delta ipod}$**plg*$^{-/-}$ mice had a tendency of a higher intake than *nphs2*$^{\Delta ipod}$**plg*$^{+/+}$ mice during the entire observation that might indicate a increased energy demand (or expenditure) in *nphs2*$^{\Delta ipod}$**plg*$^{-/-}$ mice. Food and fluid intake was largely constant during the course of the model from day -14 to day 14 in *nphs2*$^{\Delta ipod}$**plg*$^{+/+}$ mice. Thereafter, there was a trend for increased fluid intake, perhaps related to development of renal failure. Kaplan-Meier curves for survival revealed a median survival of 42 days in *nphs2*$^{\Delta ipod}$** *plg*$^{+/+}$ mice and of 26 days in *nphs2*$^{\Delta ipod}$**plg*$^{-/-}$ mice (Figure 55 A). The difference in median survival between *nphs2*$^{\Delta ipod}$**plg*$^{+/+}$ mice and *nphs2*$^{\Delta ipod}$**plg*$^{-/-}$ mice was significant (log-rank P<0.0001). In contrast, no control mice died until day 63 (log-rank P<0.0001). Beginning after day 21, nephrotic mice deteriorated and experienced death or had to euthanized.

Concentration of plasma urea was increasing gradually after induction of NS in both *nphs2*$^{\Delta ipod}$**plg*$^{+/+}$ and *nphs2*$^{\Delta ipod}$**plg*$^{-/-}$ mice during the long term observation (Figure 55 B). The differences in plasma urea were not significant until day 7 compared to the

baseline values in each genotype whereas a substantial increase was evident from day 14 on. Plasma urea concentration significantly increased in nephrotic mice of both genotypes on day 28 (day 28 vs. day 0 in *nphs2*$^{\Delta ipod}$**plg*$^{+/+}$ mice, 231 ± 20 vs. 53 ± 9 mg/dl, p<0.0001; and 351 ± 167 vs. 29 ± 4 in *nphs2*$^{\Delta ipod}$**plg*$^{-/-}$ mice, p=0.0342). In control mice, plasma urea concentration remained stable after treatment with doxycycline until the end of observation.

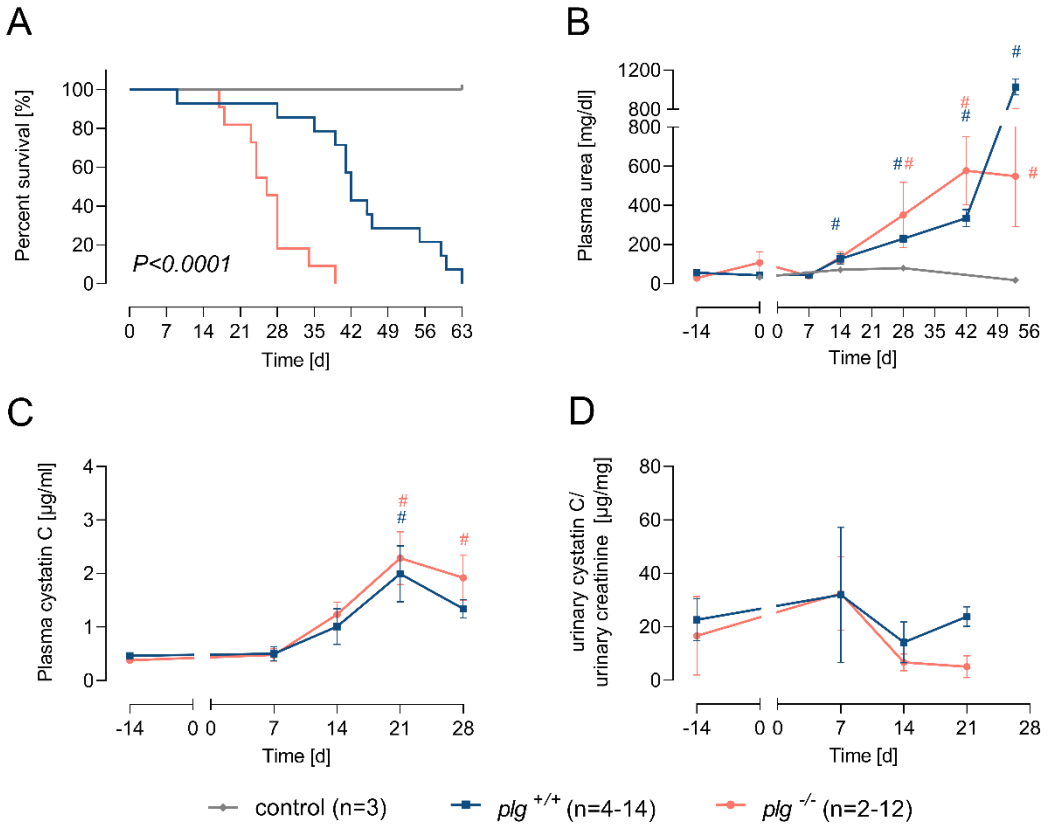

Figure 55 Long term study of survival and kidney function in *nphs2*$^{\Delta ipod}$**plg*$^{+/+}$ and *nphs2*$^{\Delta ipod}$**plg*$^{-/-}$ mice

(A) Kaplan-Meier survival curves of nephrotic and non-nephrotic mice following 63 days after doxycycline treatment.
(B) Course of plasma urea in *nphs2*$^{\Delta ipod}$**plg*$^{+/+}$ and *nphs2*$^{\Delta ipod}$**plg*$^{-/-}$ mice before and until day 53 after induction of NS.
(C-D) Concentration of plasma and urinary cystatin C. Plasma cystatin C had an increasing tendency 14 days after induction of NS in both genotypes, while the urinary cystatin C was increased slightly in both genotypes on day 7.
Arithmetic means ± SEM. # significant difference between uninduced and nephrotic mice of the same genotype.

Plasma cystatin C concentration which is a better biomarker for indicating kidney function than plasma urea was measured before doxycycline induction (on day -14) and was followed every 7 days after induction until day 28 in 4 mice of each genotypes

(Figure 55 C). There was an increasing tendency in plasma cystatin C concentration starting at 7 days after induction of NS in both genotypes, indicating a reduced kidney function in both genotypes overtime. The difference reached to a significance on day 21 compared to the baseline in both genotypes (2.00 ± 0.52 vs 0.47 ± 0.06 µg/ml in *nphs2*$^{\Delta ipod}$**plg*$^{+/+}$ mice, p=0.038; 2.29 ± 0.50 vs 0.38 ± 0.02 µg/ml in *nphs2*$^{\Delta ipod}$**plg-/-* mice, p=0.0037). However, the difference between genotypes did not reach to a statistical significance at any time point, which indicated a similar tendency of reduced kidney function in both genotypes. Urinary cystatin C was reported as a biomarker of renal disease. The increasing urinary cystatin C/ creatinine ratio especially indicated for tubular damage[88,89]. In this study, urinary cystatin C/ creatinine ratio was measured before induction of NS and was followed until 21 days after induction. Results showed no significant difference until 3 weeks after induction of NS, compared to the baseline in both genotypes, indicating tubular function was not much influenced in this model. Combining the results of plasma urea and plasma cystatin C, it indicated that the significant difference in survival between genotypes might not be caused by the decline of kidney function.

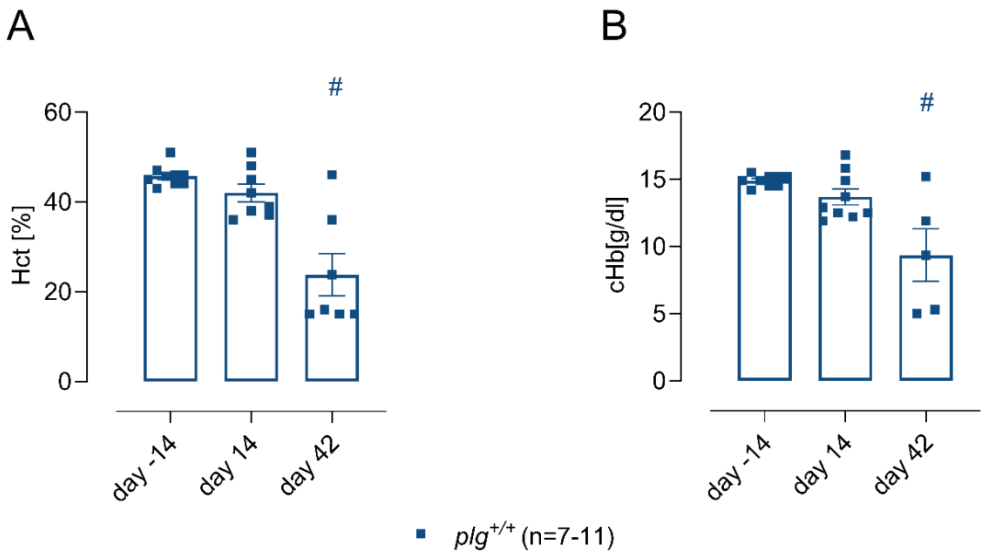

Figure 56 Long term investigation of Hct and cHb values in *nphs2*$^{\Delta ipod}$**plg*$^{+/+}$ mice

(A-B) Both Hct and cHb values showed a reduced tendency in nephrotic *nphs2*$^{\Delta ipod}$**plg*$^{+/+}$ mice on day 14, however, the difference was not significant from baseline values. Along with the development of NS, Hct and cHb values significantly decreased in *nphs2*$^{\Delta ipod}$**plg*$^{+/+}$ mice on day 42.
Arithmetic means ± SEM. $^{\#}$ significant difference between uninduced and nephrotic mice.

As previously mentioned in Table 4[74], there was a tendency towards decreased Hct and cHb values measured by a BGA analyzer, suggesting anemia in nephrotic mice of both genotypes. However, the difference did not reach a statistical significance. We further investigate the Hct and cHb values in *nphs2*$^{\Delta ipod}$**plg*$^{+/+}$ mice on day 42. We could not measure the values in *nphs2*$^{\Delta ipod}$**plg*$^{-/-}$ mice on day 42 because of reduced survival and the fear that they were more likely intolerant to a 175µl of blood sampling than their wild type littermates and would die. Results showed both Hct and cHb values were significantly reduced in *nphs2*$^{\Delta ipod}$**plg*$^{+/+}$ mice on day 42 compared to baseline (Hct value was 44 ± 1 % on day -14, and was 24 ± 5 % on day 42, $p<0.0001$; cHb was 14.6 ± 0.3 g/dl on day -14, and was 9.4 ± 2 g/dl on day 42, $p=0.0005$, Figure 56 A-B[74]). These results suggest the development of renal anemia in these mice.

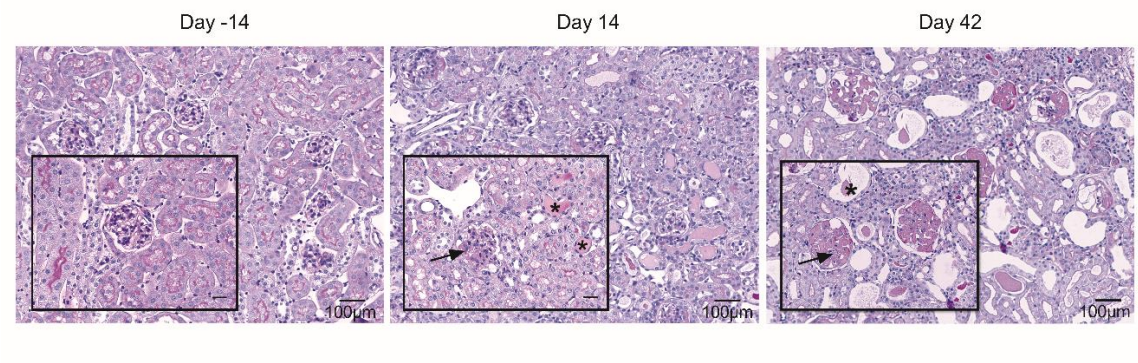

Figure 57 The histology of kidney from long-term study in *nphs2*$^{\Delta ipod}$**plg*$^{+/+}$ mcie

Proteinuria (arrow), and protein droplets in tubule (star).

PAS staining showed a progressive damage of glomerular in nephrotic mice (Figure 57). FSGS was able to be observed on day 14. Glomerulosclerosis, and damage of tubular were observed from the kidney harvested on day 42 of nephrotic mice. Immunohistochemistry showed that both α and γ-ENaC expression were significantly upregulated in distal tubule 10 days after induction in *nphs2*$^{\Delta ipod}$ mice, however this upregulation was reduced on day 42 (Figure 58). Fusion of foot processes of podocyte were already visible by electron microscopy on day 10, and there was a significant progression in loss of podocyte foot processes on day 40 in both genotypes (Figure 59).

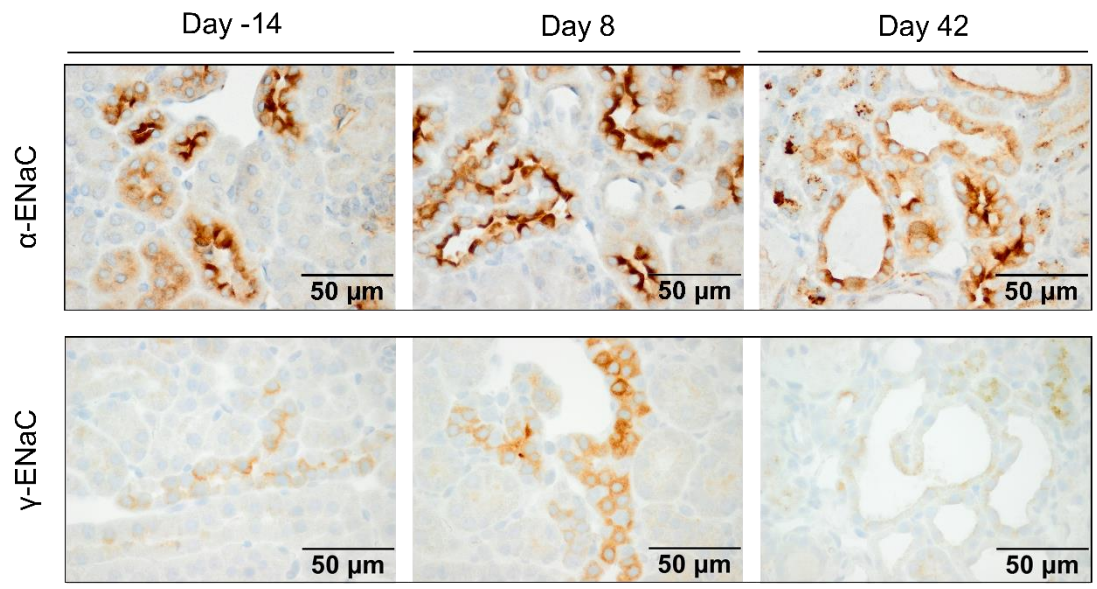

Figure 58 Long term study of the expression of α-ENaC and γ-ENaC by immunohistochemistry in kidney tissues from *nphs2*$^{\Delta ipod}$**plg*$^{+/+}$ mice

The expression of α-ENaC and γ-ENaC was slightly upregulated on day 8 and was downregulated on day 42, compared to the baseline.

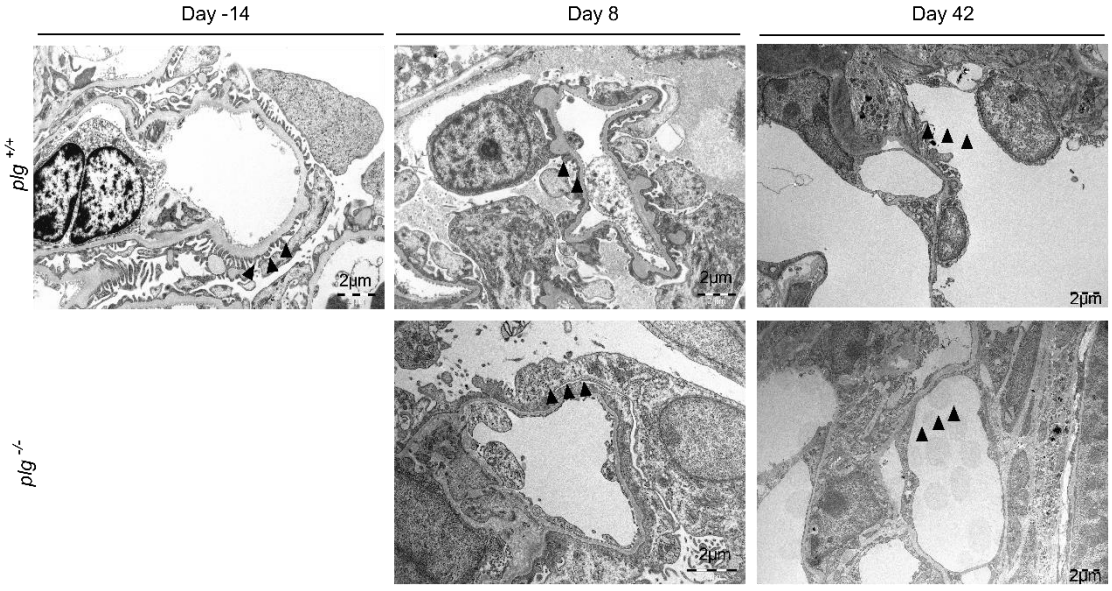

Figure 59 Long term study of Electron microscopy of kidneys from *nphs2*$^{\Delta ipod}$**plg*$^{+/+}$ and *nphs2*$^{\Delta ipod}$**plg*$^{-/-}$ mice before induction, on day 8 and day 40 after induction of NS respectively

In uninduced kidney from *plg*$^{+/+}$ mice, a normal structure of GFB, and normal podocyte with fine foot-process were observed. The ultrastructure result of podocyte on day 8 showed foot-process fusion, as well as a collapsed structure of fenestrated endothelial cells in both genotypes. Electron microscopy result of podocyte on day 40 showed incomplete GFB. Foot process was barely observed in both genotypes. arrowheads: the change of foot process. Scale bar: 2 µm.

4 Discussion

4.1 A new mouse model with an inducible podocin deficient develops experimental nephrotic syndrome and develops chronic kidney disease

Nphs2 is the gene encoding for the protein podocin that is the structurally and functionally critical for the podocyte and the glomerular filtration barrier. Our study firstly characterized an experimental NS mouse-model that, with conditional and podocyte-specific Podocin deletion (*nphs2*$^{\Delta ipod}$ mice), fully developed the symptoms of NS in patients, including massive proteinuria, hypoalbuminemia, sodium retention and hyperlipidemia. This basis of NS is the high proteinuria which reached values > 100 – 140 mg protein mg/creatinine (corresponding to > 50 – 70 mg protein mg/ 24 h) in this model[74]. Notably, the downregulation of podocin was accompanied by a diminished nephrin expression, another protein expressed in podocytes. Both podocin and nephrin are key molecules for maintaining the glomerular filtration barrier. Several studies have reported that there might be some cross-talk and interactions among these molecules[96-98]. In both human patients with mutation of *nphs2* gene[21] and animal models[99], distribution of nephrin was altered, indicating that the normal distribution of nephrin may relate to a podocin expression[23].

All the features of the experimental nephrotic syndrome in *nphs2*$^{\Delta ipod}$ mice were comparable with those observed in the doxorubicin-induced nephropathy model (DIN), which is a commonly used model of experimental nephrotic syndrome established by our group[32]. Published data indicated that features of experimental NS in *nphs2*$^{\Delta ipod}$ mice are comparable to those observed in the DIN[31,74]. Proteinuria as the most important indicator for NS reached 205 ± 30 mg/mg crea[35,36,100] in DIN model and 161 ± 18 mg/mg crea in *nphs2*$^{\Delta ipod}$ mice. This was accompanied by a decrease of plasma albumin concentration by 4-5 fold in both models. These differences in proteinuria and hypoalbuminemia between the two models were not significant (p=0.4641 in proteinuria, p=0.99 in hypoalbuminemia). In addition to proteinuria and hypoalbuminemia, both models experienced the same chronology of sodium retention and edema formation. Urinary sodium retention occurred from day 6 to day 8 after induction. As a consequence, body weight increase and edema developed from day 6 on and reached the maximum on day 10. However, unexpectedly in both models, Na^+ excretion in spot urine increased spontaneously 9-10 days after the induction of NS, followed by complete remission of

edema[32,74]. This finding had also previously been reported in the PAN nephrosis model in rats[95].

Histologically, the DIN and *nphs2*$^{\Delta ipod}$ mice presented as podocytopathy and focal segmental glomerulosclerosis (FSGS) without involvement of an immunological insult. Compared to the DIN model, induction of NS in *nphs2*$^{\Delta ipod}$ mice is easier, and unlike doxorubicin, doxycycline is not tissue-toxic to mice at all as demonstrated in control mice (Figure 22 A-B, and Figure 52). However, the dose of doxycycline intake cannot be accurately monitored. To account for this induction treatment was given over 14 days and was obtained highly efficient, reliable and highly reproducible results. However, breeding is much more time consuming than for the DIN model relying in wild-type BALB/c mice or 129S1/SvImJ mice due to the three allelic character of the *nphs2*$^{\Delta ipod}$ model.

Except for studying of the mechanisms of proteinuria and edema during the first 10 days, *nphs2*$^{\Delta ipod}$ mice are also a suitable model for studying chronic kidney disease because of the progression of renal failure, development of complications of CKD and eventually death after a median survival of six weeks. For example hyperkalemia was observed on day 14, and anemia occurred on day 42, which may contribute to mortality in these mice as in patients with CKD[101,102]. The cause of hyperkalemia in *nphs2*$^{\Delta ipod}$ mice is most likely related to the decrease of the glomerular filtration rate along and the reduced potassium secretion by the distal tubule. Regarding anemia, the lack of erythropoietin (EPO) could be one of the mechanisms in *nphs2*$^{\Delta ipod}$ mice. In addition, reduced erythrocyte survival (or so-called eryptosis) could also contribute to the development of anemia[103].

4.2 The impact of plasminogen deficiency in *nphs2*$^{\Delta ipod}$ mice

In a study using antibodies against the glomerular basement membrane showed that in an experimental glomerulonephritis model, mice with plasminogen deficiency tended to develop more severe glomerular damage[104]. This suggested that plasminogen might play a critical role in protecting glomeruli in acute inflammatory kidney injury in mice. Plasminogen also had an influence on the development of the DIN model. It was found that *plg*$^{-/-}$ mice on a 129S1/SvImJ background were completely protected from the induction of nephrotic proteinuria[105]. Histological studies revealed that plasminogen binding to endothelium within hours after doxorubicin injection was a prerequisite for the toxic effect of doxorubicin to induce experimental NS[106]. Therefore, plasminogen had

detrimental effects in the DIN model and was an essential contributor to podocyte damage. The exact mechanisms for this remain unclear.

The failure to induce NS in *plg*$^{-/-}$ mice on a 129S1/SvImJ background prevented to study the role of plasminogen in sodium retention. Thus, *nphs2*$^{\Delta ipod}$ mice were imported as an alternative model of NS. By intercrossing these *plg*$^{-/-}$ mice with triallelic *nphs2*$^{\Delta ipod}$ mice to generate the *nphs2*$^{\Delta ipod}$**plg*$^{-/-}$ mice that allowed to investigate the role of plasminogen in sodium retention and ENaC activation in experimental NS in vivo.

As plasminogen deficient mice suffer from fibrin deposition into internal organs such as lungs, liver or the gastrointestinal tract[107], we first looked at the kidney function and histology in *nphs2*$^{\Delta ipod}$**plg*$^{-/-}$ mice to rule out structural and functional changes that would have had an impact on the results of the NS model. To this end, we investigated the growth curve and the appearance of uninduced *nphs2*$^{\Delta ipod}$**plg*$^{-/-}$ mice, kidney structure, kidney function and sodium handling compared to *nphs2*$^{\Delta ipod}$**plg*$^{+/+}$ mice. Our results showed that, on the one hand, uninduced plasminogen deficient mice (*nphs2*$^{\Delta ipod}$**plg*$^{-/-}$) were smaller than the wild types (Figure 28 A-B), and experienced rectal prolapse. These findings were in accordance with the result showed for plasminogen deficient mice previously[73]. The diseased state was associated with higher food intake than in wild type mice (Table 3, Figure 54), indicating there might be a higher energy demand/expenditure in *nphs2*$^{\Delta ipod}$**plg*$^{-/-}$ mice. On the other hand, uninduced *nphs2*$^{\Delta ipod}$**plg*$^{-/-}$ mice had a normal glomerular structure, kidney function, as well as a normal sodium handling (Figure 29 A-D, Figure 30, and Figure 31 A-B). Therefore, there was no obstacle to use *nphs2*$^{\Delta ipod}$**plg*$^{-/-}$ mice as a model for investigating the role of plasminogen on sodium retention in experimental NS.

In the long-term observation, there was a significantly reduced survival time in *nphs2*$^{\Delta ipod}$**plg*$^{-/-}$ mice (Figure 55 A), indicating that the lack of plasminogen might increase the risk of death in nephrotic mice. The results of plasma urea, plasma cystatin C, and urinary cystatin C showed that the earlier death in nephrotic *nphs2*$^{\Delta ipod}$**plg*$^{-/-}$ mice were not related to a different declined kidney function than the wildtypes (Figure 55 B-D). The ultrastructure of *nphs2*$^{\Delta ipod}$**plg*$^{-/-}$ mice also did not show a worse glomerular damage than those in *nphs2*$^{\Delta ipod}$**plg*$^{+/+}$ mice (Figure 59). The possible causes of a reduced survival of *nphs2*$^{\Delta ipod}$**plg*$^{-/-}$ mice could be due to plasminogen deficiency increases the chances of fibrin deposition, and known hypercoagulability in NS. This could have,

caused more severe damage to other tissues[76,94]. Besides, as shown in Figure 53 B, *nphs2*$^{\Delta ipod}$***plg*$^{-/-}$ mice showed a significantly faster body weight loss or wasting than the *nphs2*$^{\Delta ipod}$***plg*$^{+/+}$ mice. This finding might be caused by a higher negative protein and energy balance due to the liver damage induced by plasminogen deficiency.

The evidence of ENaC inactivation are the decreased amiloride natriuresis in both *nphs2*$^{\Delta ipod}$***plg*$^{+/+}$ mice and *nphs2*$^{\Delta ipod}$***plg*$^{-/-}$ mice after 14 days of developing NS (Figure 39 A-B), and the down-regulated expression of both α-ENaC and γ-ENaC on day 42 (Figure 58). The increased urinary Na^+ excretion may cause hyponatremia and hyperkalemia (Table 4) indicating a significant change in the internal environment or even lethal to the nephrotic mice especially with the absence of plasminogen. However, the exact causes for difference in survival between two genotypes were not clear.

4.3 The role of proteasuria and the uPA-plasminogen-plasmin axis in ENaC activation and sodium retention in experimental nephrotic syndrome

Nphs2$^{\Delta ipod}$ mouse is a good model for investigating the underlying mechanisms of sodium retention and edema formation. As the same with DIN model, the genetic model combines elements of both the overfill and underfill theories to explain the mechanisms of sodium retention. As a matter of fact, both theories are not mutually exclusive and coexist[52,108].

The renin-angiotensin-aldosterone system (RAAS) can be provoked by arterial underfill, and elevated aldosterone level leads to sodium retention by the up-regulation of ENaC[74]. In nephrotic mice, plasma aldosterone concentration was not significantly changed on day 7 which coincided with the minimum urinary sodium excretion (Figure 36 A) in both genotypes, indicating that the activation of ENaC may be independent from plasma aldosterone in this experimental NS model. This evidence supports the independent aldosterone activation of ENaC in experimental NS which has been also encountered in aldosterone-resistant nephrotic mice with the serum and glucocorticoid kinase 1 (SGK1) deficiency[32]. Moreover, blockade of the mineralocorticoid receptor by canorenoat did not prevent sodium retention in DIN[35]. The concentration of plasma aldosterone reached a statistical significance in *nphs2*$^{\Delta ipod}$***plg*$^{-/-}$ mice (Figure 36) on day 14[74]. The variance in plasma aldosterone concentration of nephrotic mice could be explained by diversity in aldosterone secretion according to the severity of the albumin loss and artery-underfill. It is known that nephrotic mice increase hepatic albumin synthesis to counteract urinary

loss[109]. This could be impaired in nephrotic *nphs2$^{\Delta ipod}$*plg$^{-/-}$* mice which have liver disease and therefore would suffer from more severe protein loss inducing a state of underfill with increased plasma aldosterone secretion. The idea of ENaC activation causes sodium retention was brought up for more than twenty years[57,58]. However, the mechanism of ENaC activation was still debating. The up-regulated expression of ENaC was observed in PAN-induced nephrotic rats, with or without the presence of aldosterone[61]. The similar finding was also observed by our study, as the increased expression of ENaC on day 8 was detected by the immunohistochemistry in Figure 52, and Figure 58, while the plasma aldosterone concentration did not significantly increase on day 7 (Figure 36) in nephrotic *nphs2$^{\Delta ipod}$*plg$^{+/+}$* and *nphs2$^{\Delta ipod}$*plg$^{-/-}$* mice. These findings might indicate the ENaC regulation in this model was aldosterone independent, and some other mechanisms might involve in the activation of ENaC.

More than one decade ago, plasmin was found to be the most abundant serine protease in nephrotic urine and was suggested to be responsible for ENaC activation in NS[62]. This hypothesis was drawn by the findings of the ability of plasmin to stimulate ENaC currents *in vitro* by cleavage of human γ-ENaC, which may take place at two distinct sites (K189 and RKRK178)[74,110,111]. Yet, this hypothesis has never been proven in an *in-vivo* study before. In the current study, we confirmed the presence of large amounts of plasminogen and active plasmin in nephrotic urine from *nphs2$^{\Delta ipod}$* mice (Figure 37-38), as previously described to be the case in DIN model[35].

In a previous study using nephrotic mice lacking the uPA (*uPA$^{-/-}$*), nephrotic urine expressed almost no active plasmin[36]. The similar findings were presented in another uPA deficient mouse model, which used an antibody against tubular uPA activity in conditional podocin knockout NS mouse model[112]. However, the residual plasmin could not be ruled out by these two studies (Figure 60). In contrast, plasminogen and plasmin were absolutely absent in *nphs2$^{\Delta ipod}$*plg$^{-/-}$* mice, as shown in Figure 60, making it an ideal model to investigate the role of plasminogen in mediating ENaC in NS *in vivo*.

Our study, for the first time, investigated ENaC activation and sodium retention in an experimental nephrotic mouse model with plasminogen absence. And the results clearly demonstrated that nephrotic mice were not protected from ENaC activation and sodium retention even though without plasminogen[74]. This result was in agreement with data from nephrotic *uPA$^{-/-}$* mice[36] which were also not protected from sodium retention (Figure 61).

Taken together, the two consecutive studies strongly argued against the current concept of proteolytic ENaC activation mediated by the uPA-plasminogen-plasmin axis in NS[74,94].

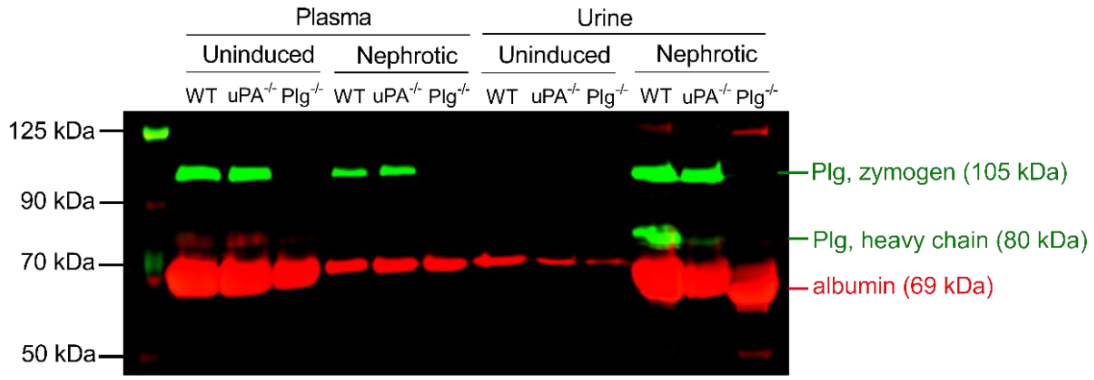

Figure 60 Expression of albumin and plasmin(ogen) in wild type mice (wt), and mice with uPA (*uPA*$^{-/-}$) and plg (*plg*$^{-/-}$) deficiency.

Albumin was strongly expressed in plasma samples which was reduced in nephrotic mice. In healthy urine, albumin expression was minimal and increased massively under nephrotic conditions. Plasminogen expression at 105 kDa, and its heavy chain at 80 kDa was not present in uninduced urine samples from each genotype. Plasminogen-plasmin expression was upregulated in nephrotic wt mice. In nephrotic *uPA*$^{-/-}$ mice plasminogen activation was almost completely absent except for a faint band at the height of the heavy chain. The expression of either plasminogen or plasmin was not detectable in plasma and urine samples from uninduced and nephrotic *nphs2*$^{\Delta ipod}$**plg*$^{-/-}$ mice (This Figure was provided by Mr. Matthias Wörn).

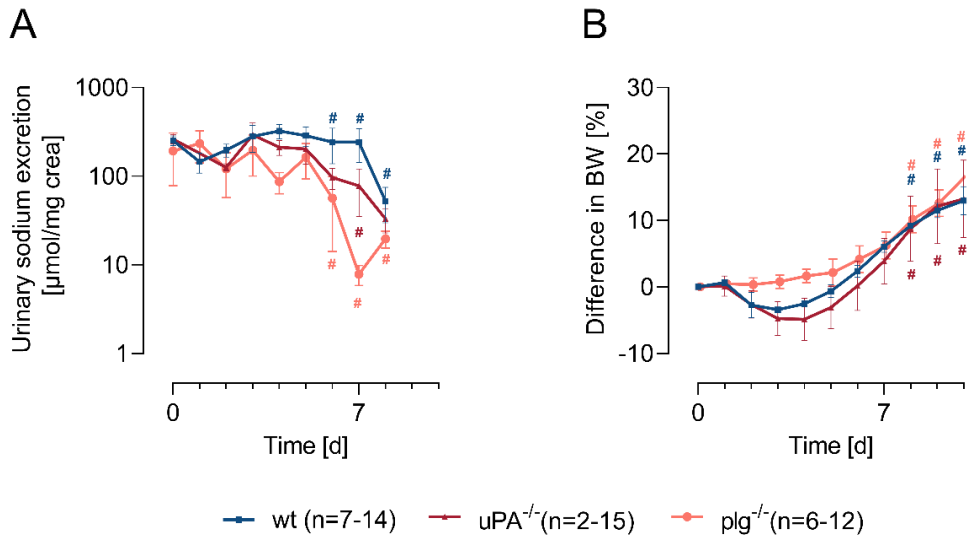

Figure 61 Summary of urinary sodium excretion and body weight increase in wt mice, *uPA*$^{-/-}$ mice, and *nphs2*$^{\Delta ipod}$**plg*$^{-/-}$ mice

After induction of NS, wt mice, *uPA*$^{-/-}$ mice, and *nphs2*$^{\Delta ipod}$**plg*$^{-/-}$ mice all underwent the decrease in urinary sodium excretion and body weight increase, and reached to a similar extent.

4.4 The potential treatment of sodium retention and edema by inhibiting ENaC activation in nephrotic syndrome

The treatment of severe edema in NS is always a challenge. According to the underfill theory, plasma oncotic pressure is reduced, and the RAAS is activated consequently. However, the treatment of volume correction by albumin substitution seems neither reducing edema nor increasing natriuresis[113,114]. On the other hand, blocking of RAAS by using angiotensin-converting enzyme inhibitors (ACEI) or angiotensin II receptor blockers (ARBs) in nephrotic patients[115], or adrenalectomy in animals cannot resolve edema alone[61].

The traditional and primary therapeutic choice for edema is a diuretic strategy, which is commonly pointed to use loop-diuretics[116,117]. However, the treatment effect of loop diuretics to edema is variable depending on glomerular filtration rate (GFR)[118], and the degree of edema. Because of the resistant tendency to the loop diuretics, patients with nephrotic edema usually need an incremental dose or intravenous administration, while for the extreme severe cases an additional treatment of human-albumin, or even dialysis. Increasing evidences have suggested that ENaC is the site of sodium retention occurred, and the blockade of ENaC showed significantly increased natriuresis and reduced body weight in both patients and animals[36,72,116,117,119]. Amiloride, which is a well-known blocker of ENaC, has been proven that inhibits ENaC activation in experimental NS[36,58,74]. The amiloride-sensitive natriuresis was increased, and sodium retention was prevented in daily amiloride-treated nephrotic mice[58]. Besides, the activity of both uPA and plasmin were inhibited in the first 4 hours after amiloride injection. These findings indicated the mechanisms of amiloride in prevention edema by directly blocking ENaC, and the possible inhibition of ENaC activation by preventing plasmin[36,72]. In our study[74], we observed increasing natriuresis to amiloride in nephrotic *nphs2*$^{\Delta ipod}$***plg*$^{+/+}$ and *nphs2*$^{\Delta ipod}$***plg*$^{-/-}$ mice (Figure 39), which clearly showed ENaC activation in NS, even with the absence of plasmin. Small intervention trials with amiloride treatment were applied to patients with proteinuric diseases as well. Results showed attenuated edema, reduced blood pressure, and reduced total and active plasmin in urine[117,120-122]. It seems rational to use amiloride as an alternative treatment for edema especially to the patients who are resistant to loop diuretics. Yet, the application of amiloride for edema treatment

is still limited due to the low oral bioavailability (~50b)[123], and the risk of hyperkalemia[117,122].

Since the abnormally filtered serine proteases were claimed significantly involved in ENaC activation, sodium retention, and edema, it makes targeting the inhibition of serine proteases a promising treatment for edema. Aprotinin is an antifibrinolytic molecular that has a wide spectrum inhibition to serine protease, including plasmin, trypsin, kallikrein, tissue plasminogen activator (tPA) and urokinase-type plasminogen activator (uPA)[124,125]. Aprotinin was once used as the treatment for prophylactic patients with a risk of blood loss and blood transfusion. However, aprotinin was suspended because of the increase in all-cause mortality, which was studied by a large, double-blind, randomized clinical trial (Blood Conservation Using Antifibrinolytics in a Randomized Trial, BART)[126]. Aprotinin was proved efficiency in inhibiting ENaC activity in *Xenopus* kidney epithelial cells[65].

In 2018, a study observed that subcutaneously implanted of sustained release-pellets aprotinin prevented sodium retention, and edema completely[35] in nephrotic mice. The same finding was proved in our study[74]. In nephrotic *nphs2*$^{\Delta ipod}$ mice, aprotinin treatment from day 7 on reversed, and from day 3 on prevented sodium retention and ascites development (Figure 25 E-F, Figure 48 A-B). These findings would prove the hypothesis of ENaC activation by proteasuria and would be in agreement with the overfill theory postulating a defect in tubular sodium handling with increased sodium avidity. The inhibitory effect of aprotinin on aldosterone secretion (Figure 49) has been reported in this and previous study, however, the mechanisms remain unclear[35,74]. This beneficial effect of aprotinin on sodium retention and edema suggests that targeting proteasuria might be a promising treatment for nephrotic edema. Unlike the mechanism of blockade ENaC by amiloride completely, aprotinin prevented over-activation of ENaC by inhibiting the serine proteases-mediated cleavage of ENaC subunits[35].

However, aprotinin seems not to be the ideal inhibitor that can be used in humans as it is related to severe side effects such as kidney injury, myocardial infarction, heart failure and stroke[125]. It would also be a promising alternative therapy by using the specific serine protease(s) inhibitor, which is (are) responsible for ENaC activation in nephrotic patients with diuretic resistance[116]. Therefore, the responsible serine protease(s) for activating ENaC have to be identified to enable a targeted inhibition in the urinary space. A novel finding in our study was, aprotinin treatment was still effective in nephrotic

nphs2$^{\Delta ipod}$**plg*$^{-/-}$ mice[74] underscoring other serine proteases than plasmin are indispensable in ENaC activation in experimental NS (Figure 47 and Figure 48). The activity of these protease(s) was (were) suggested by the residual amidolytic activity in *nphs2*$^{\Delta ipod}$**plg*$^{-/-}$ mice that treated by placebo pellets[74], as shown in Figure 47.

We believe that this perception will promote recognizing those serine proteases abnormally increased in nephrotic urine, which should be aprotinin-sensitive (Figure 62). It should keep in mind that any promising serine protease should be testified accordingly by a knockout mouse that is subjected to experimental nephrotic syndrome. The gold standard for diagnosing sodium retention should be an abrupt body weight gain. However, the single knockout models might not elucidate the possibility of a cascade reaction among the excess serine proteases in nephrotic animals that regulates the ENaC in a proteolytic manner. With this regard, the prevention of sodium retention by aprotinin in nephrotic mice could result from the inhibition of multiple serine proteases in ENaC activation[74].

In an experimental NS with inducible mutation of *nphs2*, inducing by tamoxifen injection, researchers identified several proteases in nephrotic mouse urine[64], such as Hepatocyte growth factor activator, Napsin-A, Lactotransferrin, Cathepsin B, Kallikrein-1, Cathepsin D, Prostasin, etc. Notably, some of the identified serine proteases are aprotinin-sensitive. For example, urinary active plasma kallikrein, which has been shown that was closely correlated with albuminuria in about in 30% of patients with CKD[111]. However, this candidate was reported not essential in the activation of ENaC in a DIN model previously[100]. For a better understanding of the pathophysiologic relevance of the exact serine protease or the interactions among serine proteases involved in the activation of ENaC in NS, more *in vivo* studies are required.

The expression of ENaC subunits by immunohistochemical analysis highlighted the increased expression of α- and γ-ENaC at the apical membrane on day 8[74], which is the so-called apical targeting. This is related to the increased cleavage of α- and γ-ENaC by furin, which are the dominant forms of ENaC found in the plasma membrane[127]. This phenomenon was also observed by Western blot which detected mild up-regulation of the furin-cleaved α- and γ-ENaC, most likely by increased aldosterone level. However, it was difficult to detect the fully cleaved γ-ENaC in either nephrotic *nphs2*$^{\Delta ipod}$ mice (C57Bl6 background)[74] or in doxorubicin induced experimental nephrotic mice (129/SvImJ

background)[35,36,100], at least by our group, and is still needed to be improved. The amount of fully cleaved ENaC protein, which locally lies in the apical membrane, might not be sufficiently identified by the antibody applied in Western blot in this study[74]. Thus, we cannot provide direct evidence of the increased ratio of fully cleaved γ-ENaC at the cell surface of renal tubular by filtered urinary serine proteases in NS[74]. In general, the complex of ENaC regulation should always be taken into account[128,129]. Except for proteases, there are several other extracellular and intracellular factors that may involve in ENaC regulation in NS as well, such as diet habits (intake of Na^+), regulatory proteins, phosphorylation status, acidic phospholipids or palmitoylation[74].

In conclusion, our study proved for the first time that plasminogen is not required in ENaC activation in experimental nephrotic syndrome. In contrast, we emphasized that the treatment with serine proteases inhibitor aprotinin effectively prevented sodium retention and edema in nephrotic animals with plasminogen deficiency[74]. These findings contribute to searching for the essential role of other serine proteases in regulating sodium retention in NS. The present study strongly argues against the current concept of plasmin-mediated proteolytic ENaC activation in NS[74].

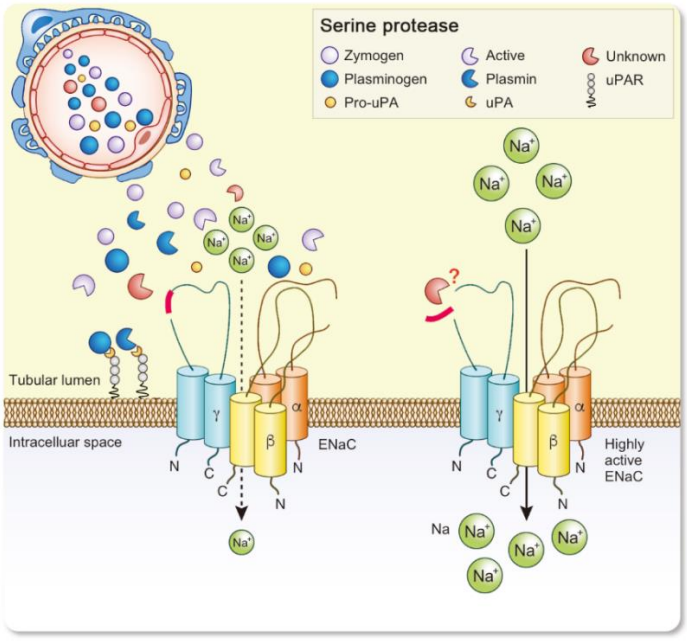

Figure 62 The current model of the role of proteasuria in activation EnaC in experimental NS

In experimental NS, due to the damaged podocyte, proteasuria reaches to distal tubular and activates ENaC in a proteolytic manner. Plasmin(ogen) is one of highly acquainted serine proteases in nephrotic urine, which was proved not essential for ENaC activation by this study. However aprotinin inhibited the activation of ENaC in nephrotic plasminogen-null mice. These findings indicate that one or more over-filtered serine protease(s) in experimental NS may be responsible for ENaC activation and edema. The

specific urinary serine protease(s) is (are) still unknown[74] (This artwork was supported by Ms. Marina Corral Spence and Mr. Hao Tian).

Summary

Sodium retention is the hallmark of nephrotic syndrome (NS) and is considered as a consequence of epithelial sodium channel (ENaC) activation by proteasuria in a proteolytic way. Plasmin is the most adequate serine proteases in urine from nephrotic patients and experimental animal models, and has been proposed indispensable for ENaC activation. However, evidence of the crucial role of plasmin in ENaC activation lacks *in vivo*. Thus a reliable mouse model developing experimental NS with plasminogen deficiency was needed. In this study, mice with conditional *nphs2* deficiency were used for modeling experimental NS (*nphs2*$^{\Delta ipod}$ mice), based on a podocyte specific deletion of podocin. These mice were crossed with mice lacking plasminogen (Bl6-Plg^{tm1Jld} or plg$^{-/-}$) to generate a double knockout mouse-model (*nphs2*$^{\Delta ipod}$**plg*$^{-/-}$). After a 14-day oral doxycycline treatment, both *nphs2*$^{\Delta ipod}$**plg*$^{+/+}$ and *nphs2*$^{\Delta ipod}$**plg*$^{-/-}$ mice developed NS. Nephrotic mice were investigated for the ENaC activation and sodium retention during follow-up. *Nphs2*$^{\Delta ipod}$**plg*$^{+/+}$ and *nphs2*$^{\Delta ipod}$**plg*$^{-/-}$ mice received the implantation of sustained release pellets containing aprotinin to determine if the serine protease inhibitor prevented sodium retention. Podocin was completely deleted from podocytes in *nphs2*$^{\Delta ipod}$ mice after doxycycline treatment and recapitulated all the features of NS in patients including massive proteinuria, hypoalbuminemia, severe edema, and hyperlipidemia. Function of kidney and ENaC were not different in uninduced *nphs2*$^{\Delta ipod}$**plg*$^{-/-}$ mice compared to the wild type mice. Quantitative of proteinuria was similar in both nephrotic *nphs2*$^{\Delta ipod}$**plg*$^{+/+}$ and *nphs2*$^{\Delta ipod}$**plg*$^{-/-}$ mice. Western blot detected plasmin (ogen) in urine from nephrotic *nphs2*$^{\Delta ipod}$**plg*$^{+/+}$ mice which was absent in *nphs2*$^{\Delta ipod}$**plg*$^{-/-}$ mice. The natriuresis response to amiloride was increased similarly in both genotypes after induction of NS compared to the uninduced state, which indicated ENaC activation. The decline of sodium excretion in both genotypes led to body weight increase and edema. Sodium retention and edema were then lost in nephrotic mice 10 days after the end of induction in both genotypes. Treatment with the serine protease inhibitor aprotinin prevented sodium retention in not only *nphs2*$^{\Delta ipod}$**plg* mice but also in *nphs2*$^{\Delta ipod}$**plg*$^{-/-}$ mice. In the long-term, and *nphs2*$^{\Delta ipod}$**plg*$^{-/-}$ mice lost more body weight than *nphs2*$^{\Delta ipod}$**plg*$^{+/+}$ mice and had a shorter survival time. In conclusion, a new mouse model with inducible podocin deficiency was characterized featuring all aspects of nephrotic syndrome including sodium retention by ENaC activation. This model is ideal

for studying postnatal *nphs2* mutation and ENaC activation by proteasuria. Beside, this model is also sufficient for studying chronic kidney disease, and its complications, such as anemia. For the first time, this study indicated that mice lacking plasminogen were not protected from ENaC-mediated sodium retention, even though plasminogen-plasmin was highly abundant in the urine from experimental nephrotic syndrome. In contrast, treatment with serine protease inhibitor aprotinin abolished sodium retention in both genotypes. These findings highlighted that plasmin is not essential for ENaC activation in experimental NS *in vivo*. The essential aprotinin-sensitive serine protease(s) in NS remains to be identified.

Zusammenfassung

Die Natriumretention ist das Kennzeichen des nephrotischen Syndroms (NS) und wird wahrscheinlich durch die proteolytische Aktivierung des epithelialen Natriumkanals (ENaC) durch aberrant gefilterte Serinproteasen vermittelt. Plasmin ist die am häufigsten vorkommende Serinprotease im nephrotischen Urin von Patienten und Tierversuchsmodellen und wurde als verantwortlich für die ENaC-Aktivierung vorgeschlagen. In vivo fehlt jedoch ein Beweis für die wesentliche Rolle der ENaC-Aktivierung durch Plasmin im experimentellen NS. Daher wurde ein zuverlässiges Mausmodell benötigt, das experimentelle NS mit Plasminogenmangel entwickelt.

In dieser Studie wurden Mäuse mit induzierbarem *nphs2*-Mangel in Kombination mit einem podozytenspezifischen TetO-Cre-Lox-P-System zur Modellierung von experimentellem NS verwendet (im folgenden $nphs2^{\Delta ipod}$-Mäuse genannt). Diese Mäuse wurden mit Mäusen mit Plasminogenmangel (Bl6-Plgtm1Jld oder $plg^{-/-}$) gekreuzt, um Double-Knockout-Mäuse ($nphs2^{\Delta ipod}$*$plg^{-/-}$) zu erzeugen. NS wurde nach einer oralen Doxycyclin-Behandlung für 14 Tage sowohl in $nphs2^{\Delta ipod}$*$plg^{+/+}$ als auch in $nphs2^{\Delta ipod}$*$plg^{-/-}$ Mäusen induziert und die Mäuse sodann auf die Entwicklung einer Natriumretention und ENaC-Aktivierung untersucht. Zur Prüfung des Effekts des Serinproteaseinhibitors Aprotinin wurden Mäusen von jedem Genotyp subkutane Pellets mit verzögerter Freisetzung von Aprotinin implantiert.

Podocin wurde in $nphs2^{\Delta ipod}$-Mäusen nach Doxycyclin-Behandlung vollständig aus Podozyten entfernt. Dies führte zur Ausprägung aller Merkmale eines NS bei Patienten, einschließlich massiver Proteinurie, Hypoalbuminämie, ausgeprägten Ödem und Hyperlipidämie. Nicht induzierte $nphs2^{\Delta ipod}$*$plg^{-/-}$ Mäuse hatten im Vergleich zu Wildtyp-Mäusen eine normale Nierenfunktion und Natriumhandhabung. Nach der Induktion nahm die Proteinurie sowohl bei $nphs2^{\Delta ipod}$*$plg^{-/-}$ Mäusen ähnlich zu. Western Blot zeigte eine Ausscheidung von Plasminogen-Plasmin im Urin bei $nphs2^{\Delta ipod}$*$plg^{+/+}$ Mäusen, die bei $nphs2^{\Delta ipod}$*$plg^{-/-}$ Mäusen fehlte. Nach dem Einsetzen der Proteinurie war die Amilorid-sensitive Natriurese in beiden Genotypen im Vergleich zum nicht induzierten Zustand erhöht, was auf eine ENaC-Aktivierung in beiden Genotypen von ähnlichem Ausmaß hinweist. Anschließend sank die Natriumausscheidung im Urin bei beiden Genotypen, was zu einer Zunahme des Körpergewichts und der Entwicklung von Aszites führte. Natriumretention und Ödem waren bei nephrotischen Mäusen 10 Tage nach dem Ende

der Induktion in beiden Genotypen reversibel. Im weiteren verloren nephrotische *nphs2*$^{\Delta ipod}$**plg*$^{-/-}$ Mäuse verloren mehr Körpergewicht als *nphs2*$^{\Delta ipod}$**plg*$^{+/+}$ Mäuse und wiesen eine kürzere Überlebenszeit auf. Die Behandlung mit dem Serinproteaseinhibitor Aprotinin verhinderte die Natriumretention nicht nur bei *nphs2*$^{\Delta ipod}$**plg*$^{+/+}$ Mäusen, sondern auch bei *nphs2*$^{\Delta ipod}$**plg*$^{-/-}$ Mäusen.

In dieser Arbeit wurde ein neues Mausmodell mit induzierbarem Podocin-Mangel charakterisiert, das zur Untersuchung der postnatalen *nphs2*-Mutation und der ENaC-Aktivierung durch Proteasurie ideal ist. Daneben ist dieses Modell auch geeignet, um chronische Nierenerkrankungen und deren Komplikationen wie Anämie zu untersuchen. Obwohl Plasminogen-Plasmin reichlich im Urin nachzuweisen war, waren nephrotischen *nphs2*$^{\Delta ipod}$**plg*$^{-/-}$-Mäusen nicht vor einer ENaC-bedingten Natriumretention geschützt. Im Gegensatz dazu waren beide Genotypen durch die Behandlung mit dem Serinproteaseinhibitor Aprotinin geschützt. Diese Befunde weisen darauf hin, dass Plasmin für die ENaC-Aktivierung in experimentellen NS in vivo nicht erforderlich ist. Die Identität der essenziellen aprotinin-sensitiven Serinprotease(n) beim NS bleibt noch verborgen.

References:

1. Tapia C, Bashir K. Nephrotic Syndrome. StatPearls. Treasure Island (FL)2020.
2. Eddy AA, Symons JM. Nephrotic syndrome in childhood. Lancet 2003;362:629-39.
3. Tapia C BK. Nephrotic Syndrome. Medline 2019.
4. Haas M, Spargo BH, Coventry S. Increasing Incidence of Focal-Segmental Glomerulosclerosis among Adult Nephropathies - a 20-Year Renal Biopsy Study. American Journal of Kidney Diseases 1995;26:740-50.
5. Briganti EM, Dowling J, Finlay M, et al. The incidence of biopsy-proven glomerulonephritis in Australia. Nephrol Dial Transplant 2001;16:1364-7.
6. Kitiyakara C, Eggers P, Kopp JB. Twenty-one-year trend in ESRD due to focal segmental glomerulosclerosis in the United States. American Journal of Kidney Diseases 2004;44:815-25.
7. McGrogan A, Franssen CF, de Vries CS. The incidence of primary glomerulonephritis worldwide: a systematic review of the literature. Nephrol Dial Transplant 2011;26:414-30.
8. Asinobi AO, Ademola AD, Okolo CA, Yaria JO. Trends in the histopathology of childhood nephrotic syndrome in Ibadan Nigeria: preponderance of idiopathic focal segmental glomerulosclerosis. Bmc Nephrology 2015;16.
9. Sim JJ, Batech M, Hever A, et al. Distribution of Biopsy-Proven Presumed Primary Glomerulonephropathies in 2000-2011 Among a Racially and Ethnically Diverse US Population. American Journal of Kidney Diseases 2016;68:533-44.
10. Rosenberg AZ, Kopp JB. Focal Segmental Glomerulosclerosis. Clin J Am Soc Nephrol 2017;12:502-17.
11. Sako M, Nakanishi K, Obana M, et al. Analysis of NPHS1, NPHS2, ACTN4, and WT1 in Japanese patients with congenital nephrotic syndrome. Kidney Int 2005;67:1248-55.
12. Koeppen BM, Stanton BA. 3 - Glomerular Filtration and Renal Blood Flow. In: Koeppen BM, Stanton BA, eds. Renal Physiology (Fifth Edition). Philadelphia: Mosby; 2013:27-43.
13. Ng JK, Ma TK, Lai FM, et al. Causes of nephrotic syndrome and nephrotic-range proteinuria are different in adult Chinese patients: A single centre study over 33 years. Nephrology (Carlton) 2018;23:565-72.
14. Kodner C. Diagnosis and Management of Nephrotic Syndrome in Adults. Am Fam Physician 2016;93:479-85.
15. Simic I, Tabatabaeifar M, Schaefer F. Animal models of nephrotic syndrome. Pediatr Nephrol 2013;28:2079-88.
16. Boute N, Gribouval O, Roselli S, et al. NPHS2, encoding the glomerular protein podocin, is mutated in autosomal recessive steroid-resistant nephrotic syndrome. Nature Genetics 2000;24:349-54.
17. Liu G, Kaw B, Kurfis J, Rahmanuddin S, Kanwar YS, Chugh SS. Neph1 and nephrin interaction in the slit diaphragm is an important determinant of glomerular permeability.

J Clin Invest 2003;112:209-21.
18. Kang HG, Lee M, Lee KB, et al. Loss of podocalyxin causes a novel syndromic type of congenital nephrotic syndrome. Exp Mol Med 2017;49:e414.
19. Putaala H, Soininen R, Kilpelainen P, Wartiovaara J, Tryggvason K. The murine nephrin gene is specifically expressed in kidney, brain and pancreas: inactivation of the gene leads to massive proteinuria and neonatal death. Hum Mol Genet 2001;10:1-8.
20. Jalanko H. Congenital nephrotic syndrome. Pediatr Nephrol 2009;24:2121-8.
21. Roselli S, Heidet L, Sich M, et al. Early glomerular filtration defect and severe renal disease in podocin-deficient mice. Molecular and Cellular Biology 2004;24:550-60.
22. Weber S, Gribouval O, Esquivel EL, et al. NPHS2 mutation analysis shows genetic heterogeneity of steroid-resistant nephrotic syndrome and low post-transplant recurrence. Kidney International 2004;66:571-9.
23. Fan Q, Xing Y, Ding J, Guan N, Zhang J. The relationship among nephrin, podocin, CD2AP, and alpha-actinin might not be a true 'interaction' in podocyte. Kidney Int 2006;69:1207-15.
24. Caridi G, Gigante M, Ravani P, et al. Clinical features and long-term outcome of nephrotic syndrome associated with heterozygous NPHS1 and NPHS2 mutations. Clin J Am Soc Nephrol 2009;4:1065-72.
25. Bierzynska A, Soderquest K, Koziell A. Genes and podocytes - new insights into mechanisms of podocytopathy. Front Endocrinol (Lausanne) 2014;5:226.
26. Gao F, Maiti S, Sun G, et al. The Wt1+/R394W mouse displays glomerulosclerosis and early-onset renal failure characteristic of human Denys-Drash syndrome. Mol Cell Biol 2004;24:9899-910.
27. Shigehara T, Zaragoza C, Kitiyakara C, et al. Inducible podocyte-specific gene expression in transgenic mice. J Am Soc Nephrol 2003;14:1998-2003.
28. Juhila J, Roozendaal R, Lassila M, Verbeek SJ, Holthofer H. Podocyte cell-specific expression of doxycycline inducible Cre recombinase in mice. J Am Soc Nephrol 2006;17:648-54.
29. Hinkes B, Vlangos C, Heeringa S, et al. Specific podocin mutations correlate with age of onset in steroid-resistant nephrotic syndrome. Journal of the American Society of Nephrology 2008;19:365-71.
30. Orth P, Schnappinger D, Hillen W, Saenger W, Hinrichs W. Structural basis of gene regulation by the tetracycline inducible Tet repressor-operator system. Nat Struct Biol 2000;7:215-9.
31. Mollet G, Ratelade J, Boyer O, et al. Podocin inactivation in mature kidneys causes focal segmental glomerulosclerosis and nephrotic syndrome. J Am Soc Nephrol 2009;20:2181-9.
32. Artunc F, Nasir O, Amann K, et al. Serum- and glucocorticoid-inducible kinase 1 in doxorubicin-induced nephrotic syndrome. Am J Physiol Renal Physiol 2008;295:F1624-34.

33. Bohnert BN, Daniel C, Amann K, et al. Impact of phosphorus restriction and vitamin D-substitution on secondary hyperparathyroidism in a proteinuric mouse model. Kidney & blood pressure research 2015;40:153-65.
34. Bohnert BN, Artunc F. Induction of Nephrotic Syndrome in Mice by Retrobulbar Injection of Doxorubicin and Prevention of Volume Retention by Sustained Release Aprotinin. J Vis Exp 2018.
35. Bohnert BN, Menacher M, Janessa A, et al. Aprotinin prevents proteolytic epithelial sodium channel (ENaC) activation and volume retention in nephrotic syndrome. Kidney international 2018;93:159-72.
36. Bohnert BN, Daiminger S, Worn M, et al. Urokinase-type plasminogen activator (uPA) is not essential for epithelial sodium channel (ENaC)-mediated sodium retention in experimental nephrotic syndrome. Acta physiologica (Oxford, England) 2019;227:e13286.
37. Kim YH, Goyal M, Kurnit D, et al. Podocyte depletion and glomerulosclerosis have a direct relationship in the PAN-treated rat. Kidney International 2001;60:957-68.
38. Ydegaard R, Svenningsen P, Bistrup C, et al. Nephrotic syndrome is associated with increased plasma K(+) concentration, intestinal K(+) losses and attenuated urinary K(+) excretion - studies in rats and humans. Am J Physiol Renal Physiol 2019.
39. Hulkko J, Patrakka J, Lal M, Tryggvason K, Hultenby K, Wernerson A. Neph1 is reduced in primary focal segmental glomerulosclerosis, minimal change nephrotic syndrome, and corresponding experimental animal models of adriamycin-induced nephropathy and puromycin aminonucleoside nephrosis. Nephron Extra 2014;4:146-54.
40. Wang Y, Wang YP, Tay YC, Harris DCH. Progressive adriamycin nephropathy in mice: Sequence of histologic and immunohistochemical events. Kidney International 2000;58:1797-804.
41. Bohnert BN, Dorffel T, Daiminger S, et al. Retrobulbar Sinus Injection of Doxorubicin is More Efficient Than Lateral Tail Vein Injection at Inducing Experimental Nephrotic Syndrome in Mice: A Pilot Study. Lab Anim 2019;53:564-76.
42. Jeansson M, Bjorck K, Tenstad O, Haraldsson B. Adriamycin alters glomerular endothelium to induce proteinuria. J Am Soc Nephrol 2009;20:114-22.
43. Wang Y, Lei T, Yuan J, et al. GCN2 deficiency ameliorates doxorubicin-induced cardiotoxicity by decreasing cardiomyocyte apoptosis and myocardial oxidative stress. Redox Biol 2018;17:25-34.
44. Moruno-Manchon JF, Uzor NE, Kesler SR, et al. Peroxisomes contribute to oxidative stress in neurons during doxorubicin-based chemotherapy. Mol Cell Neurosci 2018;86:65-71.
45. Chen JS, Chen A, Chang LC, et al. Mouse model of membranous nephropathy induced by cationic bovine serum albumin: antigen dose-response relations and strain differences. Nephrol Dial Transplant 2004;19:2721-8.
46. Wu CC, Chen JS, Lin SH, Chen A, Sytwu HK, Lin YF. Experimental model of

membranous nephropathy in mice: sequence of histological and biochemical events. Lab Anim 2008;42:350-9.
47. Ophascharoensuk V, Pippin JW, Gordon KL, Shankland SJ, Couser WG, Johnson RJ. Role of intrinsic renal cells versus infiltrating cells in glomerular crescent formation. Kidney International 1998;54:416-25.
48. Ohse T, Vaughan MR, Kopp JB, et al. De novo expression of podocyte proteins in parietal epithelial cells during experimental glomerular disease. Am J Physiol-Renal 2010;298:F702-F11.
49. Lichtnekert J, Kaverina NV, Eng DG, et al. Renin-Angiotensin-Aldosterone System Inhibition Increases Podocyte Derivation from Cells of Renin Lineage. Journal of the American Society of Nephrology 2016;27:3611-27.
50. Roeder SS, Barnes TJ, Lee JS, et al. Activated ERK1/2 increases CD44 in glomerular parietal epithelial cells leading to matrix expansion. Kidney International 2017;91:896-913.
51. Epstein AA. Concerning the causation of edema in chronic parenchymatous nephritis; method for its alleviation. Am J Med 1952;13:556-61.
52. Artunc F, Worn M, Schork A, Bohnert BN. Proteasuria-The impact of active urinary proteases on sodium retention in nephrotic syndrome. Acta physiologica (Oxford, England) 2019;225:e13249.
53. Nagase M. Recent topics on podocytes and aldosterone. J Ren Nutr 2015;25:201-4.
54. Meltzer JI, Keim HJ, Laragh JH, Sealey JE, Jan KM, Chien S. Nephrotic syndrome: vasoconstriction and hypervolemic types indicated by renin-sodium profiling. Annals of internal medicine 1979;91:688-96.
55. Canessa CM, Schild L, Buell G, et al. Amiloride-sensitive epithelial Na+ channel is made of three homologous subunits. Nature 1994;367:463-7.
56. Rossier BC, Stutts MJ. Activation of the epithelial sodium channel (ENaC) by serine proteases. Annu Rev Physiol 2009;71:361-79.
57. Ichikawa I, Rennke HG, Hoyer JR, et al. Role for Intrarenal Mechanisms in the Impaired Salt Excretion of Experimental Nephrotic Syndrome. J Clin Invest 1983;71:91-103.
58. Deschenes G, Wittner M, Di Stefano A, Jounier S, Doucet A. Collecting duct is a site of sodium retention in PAN nephrosis: A rationale for amiloride therapy. Journal of the American Society of Nephrology 2001;12:598-601.
59. Marieb ENH, Katja. "Chapter 16". Human anatomy & physiology (9th ed.). . Boston: Pearson 2013;pp. 629, Question 14.
60. Masilamani S, Kim GH, Mitchell C, Wade JB, Knepper MA. Aldosterone-mediated regulation of ENaC alpha, beta, and gamma subunit proteins in rat kidney. J Clin Invest 1999;104:R19-23.
61. de Seigneux S, Kim SW, Hemmingsen SC, Frøkiaer J, Nielsen S. Increased expression but not targeting of ENaC in adrenalectomized rats with PAN-induced nephrotic syndrome. Am J Physiol Renal Physiol 2006;291:F208-17.

62. Svenningsen P, Bistrup C, Friis UG, et al. Plasmin in nephrotic urine activates the epithelial sodium channel. J Am Soc Nephrol 2009;20:299-310.
63. Chen JL, Wang L, Yao XM, et al. Association of Urinary Plasminogen-Plasmin with Edema and Epithelial Sodium Channel Activation in Patients with Nephrotic Syndrome. Am J Nephrol 2019;50:92-104.
64. Larionov A, Dahlke E, Kunke M, et al. Cathepsin B increases ENaC activity leading to hypertension early in nephrotic syndrome. J Cell Mol Med 2019;23:6543-53.
65. Vallet V, Chraibi A, Gaeggeler H-P, Horisberger J-D, Rossier BC. An epithelial serine protease activates the amiloride-sensitive sodium channel. Nature 1997;389:607-10.
66. Hughey RP, Bruns JB, Kinlough CL, et al. Epithelial sodium channels are activated by furin-dependent proteolysis. J Biol Chem 2004;279:18111-4.
67. Hughey RP, Mueller GM, Bruns JB, et al. Maturation of the epithelial Na+ channel involves proteolytic processing of the alpha- and gamma-subunits. J Biol Chem 2003;278:37073-82.
68. Carattino MD, Sheng S, Bruns JB, Pilewski JM, Hughey RP, Kleyman TR. The epithelial Na+ channel is inhibited by a peptide derived from proteolytic processing of its alpha subunit. J Biol Chem 2006;281:18901-7.
69. Harris M, Garcia-Caballero A, Stutts MJ, Firsov D, Rossier BC. Preferential assembly of epithelial sodium channel (ENaC) subunits in Xenopus oocytes: role of furin-mediated endogenous proteolysis. J Biol Chem 2008;283:7455-63.
70. Bruns JB, Carattino MD, Sheng S, et al. Epithelial Na+ channels are fully activated by furin- and prostasin-dependent release of an inhibitory peptide from the gamma-subunit. J Biol Chem 2007;282:6153-60.
71. Carattino MD, Hughey RP, Kleyman TR. Proteolytic processing of the epithelial sodium channel gamma subunit has a dominant role in channel activation. J Biol Chem 2008;283:25290-5.
72. Hinrichs GR, Weyer K, Friis UG, et al. Urokinase-type plasminogen activator contributes to amiloride-sensitive sodium retention in nephrotic range glomerular proteinuria in mice. Acta Physiol (Oxf) 2019;227:e13362.
73. Bugge TH, Flick MJ, Daugherty CC, Degen JL. Plasminogen deficiency causes severe thrombosis but is compatible with development and reproduction. Genes & Development 1995;9:794-807.
74. Xiao M, Bohnert BN, Aypek H, et al. Plasminogen deficiency does not prevent sodium retention in a genetic mouse model of experimental nephrotic syndrome. Acta Physiol (Oxf) 2020:e13512.
75. Lin X, Suh JH, Go G, Miner JH. Feasibility of Repairing Glomerular Basement Membrane Defects in Alport Syndrome. Journal of the American Society of Nephrology 2014;25:687.
76. Ploplis VA, Carmeliet P, Vazirzadeh S, et al. Effects of disruption of the plasminogen

gene on thrombosis, growth, and health in mice. Circulation 1995;92:2585-93.
77. Wex T, Kuester D, Mönkemüller K, et al. Assessment of desmosomal components (desmoglein 1-3, plakoglobin) in cardia mucosa in relation to gastroesophageal reflux disease and Helicobacter pylori infection. Human Pathology 2012;43:1745-54.
78. Suelves M, Lopez-Alemany R, Lluis F, et al. Plasmin activity is required for myogenesis in vitro and skeletal muscle regeneration in vivo. Blood 2002;99:2835-44.
79. Lin X, Suh JH, Go G, Miner JH. Feasibility of repairing glomerular basement membrane defects in Alport syndrome. J Am Soc Nephrol 2014;25:687-92.
80. Perl AK, Wert SE, Nagy A, Lobe CG, Whitsett JA. Early restriction of peripheral and proximal cell lineages during formation of the lung. Proceedings of the National Academy of Sciences of the United States of America 2002;99:10482-7.
81. Parasuraman S, Raveendran R, Kesavan R. Blood sample collection in small laboratory animals. J Pharmacol Pharmacother 2010;1:87-93.
82. Bradford MM. A rapid and sensitive method for the quantitation of microgram quantities of protein utilizing the principle of protein-dye binding. Analytical Biochemistry 1976;72:248-54.
83. Rexhepaj R, Artunc F, Grahammer F, et al. SGK1 is not required for regulation of colonic ENaC activity. Pflugers Arch 2006;453:97-105.
84. Baum ML, Wilton DK, Muthukumar A, et al. CUB and Sushi Multiple Domains 1 (CSMD1) opposes the complement cascade in neural tissues. bioRxiv 2020:2020.09.11.291427.
85. Onopiuk A, Tokarzewicz A, Gorodkiewicz E. Cystatin C: a kidney function biomarker. Adv Clin Chem 2015;68:57-69.
86. Herget-Rosenthal S, Poppen D, Hüsing J, et al. Prognostic value of tubular proteinuria and enzymuria in nonoliguric acute tubular necrosis. Clin Chem 2004;50:552-8.
87. Herget-Rosenthal S, Feldkamp T, Volbracht L, Kribben A. Measurement of urinary cystatin C by particle-enhanced nephelometric immunoassay: precision, interferences, stability and reference range. Ann Clin Biochem 2004;41:111-8.
88. Uchida K, Gotoh A. Measurement of cystatin-C and creatinine in urine. Clin Chim Acta 2002;323:121-8.
89. Kim SS, Song SH, Kim IJ, et al. Urinary cystatin C and tubular proteinuria predict progression of diabetic nephropathy. Diabetes care 2013;36:656-61.
90. Boerries M, Grahammer F, Eiselein S, et al. Molecular fingerprinting of the podocyte reveals novel gene and protein regulatory networks. Kidney international 2013;83:1052-64.
91. Nesterov V, Krueger B, Bertog M, Dahlmann A, Palmisano R, Korbmacher C. In Liddle Syndrome, Epithelial Sodium Channel Is Hyperactive Mainly in the Early Part of the Aldosterone-Sensitive Distal Nephron. Hypertension 2016;67:1256-62.
92. Krueger B, Haerteis S, Yang L, et al. Cholesterol depletion of the plasma membrane

prevents activation of the epithelial sodium channel (ENaC) by SGK1. Cell Physiol Biochem 2009;24:605-18.
93. Xiao M, Bohnert BN, Woern M, et al. MO061PLASMINOGEN DEFIENCY DOES NOT PROTECT MICE FROM SODIUM RETENTION IN EXPERIMENTAL NEPHROTIC SYNDROME. Nephrol Dial Transpl 2020;35.
94. Bugge TH, Flick MJ, Daugherty CC, Degen JL. Plasminogen deficiency causes severe thrombosis but is compatible with development and reproduction. Genes Dev 1995;9:794-807.
95. Deschenes G, Doucet A. Collecting duct (Na+/K+)-ATPase activity is correlated with urinary sodium excretion in rat nephrotic syndromes. J Am Soc Nephrol 2000;11.
96. Huber TB, Kottgen M, Schilling B, Walz G, Benzing T. Interaction with podocin facilitates nephrin signaling. J Biol Chem 2001;276:41543-6.
97. Schwarz K, Simons M, Reiser J, et al. Podocin, a raft-associated component of the glomerular slit diaphragm, interacts with CD2AP and nephrin. J Clin Invest 2001;108:1621-9.
98. Saleem MA, Ni L, Witherden I, et al. Co-localization of nephrin, podocin, and the actin cytoskeleton: evidence for a role in podocyte foot process formation. Am J Pathol 2002;161:1459-66.
99. Zhang SY, Marlier A, Gribouval O, et al. In vivo expression of podocyte slit diaphragm-associated proteins in nephrotic patients with NPHS2 mutation. Kidney Int 2004;66:945-54.
100. Haerteis S, Schork A, Dorffel T, et al. Plasma kallikrein activates the epithelial sodium channel in vitro but is not essential for volume retention in nephrotic mice. Acta Physiol (Oxf) 2018;224:e13060.
101. Zachée P, Vermylen J, Boogaerts MA. Hematologic aspects of end-stage renal failure. Ann Hematol 1994;69:33-40.
102. Watanabe R. Hyperkalemia in chronic kidney disease. Revista da Associação Médica Brasileira 2020;66:s31-s6.
103. Lang F, Bissinger R, Abed M, Artunc F. Eryptosis - the Neglected Cause of Anemia in End Stage Renal Disease. Kidney and Blood Pressure Research 2017;42:749-60.
104. Kitching AR, Holdsworth SR, Ploplis VA, et al. Plasminogen and Plasminogen Activators Protect against Renal Injury in Crescentic Glomerulonephritis. Journal of Experimental Medicine 1997;185:963-8.
105. Dörffel T, Bohnert B, Grahammer F, Das R, Plow EF, Artunc F. Mice lacking plasminogen are protected from doxorubicin-induced nephrotic syndrome. 9th Annual Meeting of the German Society for Nephrology, Mannheim 2017;http://www.abstractserver.com/publication/nephro2017/nephro2017Abstracts.PDF.
106. Bohnert BN MI, Dörffel T, Plow E.F, Grahammer F, Quintanilla-Martinez L, Artunc F. . Glomerular binding of plasminogen is essential for podocyte toxicity of doxorubicin in

129S1 mice. 10th Annual Meeting of the German Society of Nephrology 2018;https://www.abstractserver.com/publication/nephro2018/.
107. Lijnen HR. Pathophysiology of the plasminogen/plasmin system. Int J Clin Lab Res 1996;26:1-6.
108. Bohnert BN, Artunc F. Induction of nephrotic syndrome in mice by retrobulbar injection of doxorubicin and prevention of volume retention by sustained release aprotinin. Journal of Visualized Experiments 2018;135:e57642.
109. Weyer K, Andersen PK, Schmidt K, et al. Abolishment of proximal tubule albumin endocytosis does not affect plasma albumin during nephrotic syndrome in mice. Kidney Int 2018;93:335-42.
110. Haerteis S, Krappitz M, Diakov A, Krappitz A, Rauh R, Korbmacher C. Plasmin and chymotrypsin have distinct preferences for channel activating cleavage sites in the gamma subunit of the human epithelial sodium channel. The Journal of general physiology 2012;140:375–89.
111. Schork A, Woern M, Kalbacher H, et al. Association of Plasminuria with Overhydration in Patients with CKD. Clinical journal of the American Society of Nephrology : CJASN 2016;11:761-9.
112. Hinrichs GR, Weyer K, Friis UG, et al. Urokinase-type plasminogen activator contributes to amiloride-sensitive sodium retention in nephrotic range glomerular proteinuria in mice. Acta physiologica (Oxford, England) 2019:e13362.
113. Geers AB, Koomans HA, Boer P, Dorhout Mees EJ. Plasma and blood volumes in patients with the nephrotic syndrome. Nephron 1984;38:170-3.
114. Koomans HA, Geers AB, v.d. Meiracker AH, Roos JC, Boer P, Mees EJD. Effects of Plasma Volume Expansion on Renal Salt Handling in Patients with the Nephrotic Syndrome. American Journal of Nephrology 1984;4:227-34.
115. Brown EA, Markandu ND, Sagnella GA, Jones BE, MacGregor GA. Lack of Effect of Captopril on the Sodium Retention of the Nephrotic Syndrome. Nephron 1984;37:43-8.
116. Gupta S, Pepper RJ, Ashman N, Walsh SB. Nephrotic Syndrome: Oedema Formation and Its Treatment With Diuretics. Front Physiol 2018;9:1868.
117. Hinrichs GR, Mortensen LA, Jensen BL, Bistrup C. Amiloride resolves resistant edema and hypertension in a patient with nephrotic syndrome; a case report. Physiol Rep 2018;6:e13743.
118. Oh SW, Han SY. Loop Diuretics in Clinical Practice. Electrolyte & blood pressure : E & BP 2015;13:17-21.
119. Hoorn EJ, Ellison DH. Diuretic Resistance. Am J Kidney Dis 2017;69:136-42.
120. Oxlund CS, Buhl KB, Jacobsen IA, et al. Amiloride lowers blood pressure and attenuates urine plasminogen activation in patients with treatment-resistant hypertension. J Am Soc Hypertens 2014;8:872-81.
121. Andersen H, Hansen PB, Bistrup C, Nielsen F, Henriksen JE, Jensen BL. Significant

natriuretic and antihypertensive action of the epithelial sodium channel blocker amiloride in diabetic patients with and without nephropathy. J Hypertens 2016;34:1621-9.
122. Unruh ML, Pankratz VS, Demko JE, Ray EC, Hughey RP, Kleyman TR. Trial of Amiloride in Type 2 Diabetes with Proteinuria. Kidney international reports 2017;2:893-904.
123. Ellison DH. Clinical Pharmacology in Diuretic Use. Clinical Journal of the American Society of Nephrology 2019;14:1248.
124. Kim S, Chen J, Cheng T, et al. PubChem 2019 update: improved access to chemical data. Nucleic Acids Res 2018;47:D1102-D9.
125. Aprotinin. In: Aronson JK, ed. Meyler's Side Effects of Drugs (Sixteenth Edition). Oxford: Elsevier; 2016:660-7.
126. Fergusson DA, Hébert PC, Mazer CD, et al. A Comparison of Aprotinin and Lysine Analogues in High-Risk Cardiac Surgery. New England Journal of Medicine 2008;358:2319-31.
127. Frindt G, Gravotta D, Palmer LG. Regulation of ENaC trafficking in rat kidney. J Gen Physiol 2016;147:217-27.
128. Kleyman TR, Kashlan OB, Hughey RP. Epithelial Na(+) Channel Regulation by Extracellular and Intracellular Factors. Annu Rev Physiol 2018;80:263-81.
129. Kleyman TR, Eaton DC. Regulating ENaC's gate. American journal of physiology Cell physiology 2019.

Publication:

Mengyun Xiao, Bernhard N. Bohnert, Hande Aypek, Oliver Kretz, Florian Grahammer, Ute Aukschun, Matthias Wörn, Andrea Janessa, Daniel Essigke, Christoph Daniel, Kerstin Amann, Tobias B. Huber, Edward F. Plow, Andreas L. Birkenfeld, Ferruh Artunc. Plasminogen deficiency does not prevent sodium retention in a genetic mouse model of experimental nephrotic syndrome. Acta Physiol (Oxf). 2020 May 26;e13512. doi: 10.1111/apha.13512.

Explanation of the personal contribution to this dissertation

The conception of this study was brought up by my doctoral supervisor Professor Artunc and the co-supervisor, Dr. Bernhard N. Bohnert. My supervisors regulated the quality of the experiments and data.

After training, all animal experiments, PCRs, and laboratory measurements, were conducted by myself except for subcutaneously pellet implantation. The data analysis, statistical evaluation were carried out by myself and checked by my supervisors.

Dr. Bernhard N. Bohnert helped me with the aprotinin/ placebo pellets implantation to mice. Mr. Matthias Wörn performed the Western blot showing plasminogen and albumin in plasma and urine samples. Ms. Andrea Janessa performed the Western blot showing the expression of ENaC subunits in the kidney cortex from mice. Western blot of kidneys for podocin detection before and after induction were provided by Mr. Ute Aukschun at Faculty and University Medical Center Freiburg. Histology study of kidneys, including immunohistochemistry and immunofluorescence, were performed by Ms. Hande Aypek; PAS staining and electron microscopy were contributed by Dr. Oliver Kretz at the University Medical Center Hamburg-Eppendorf, respectively.

I assure you that this dissertation is my original work, except where indicated through the proper use of citations and references. I used no sources or aids other than those explicitly mentioned. Support provided by other persons is marked and acknowledged as such in this dissertation.

Acknowledgment

Looking back on the last three years, I spent on my research and my life in Tuebingen, only great memories left. Of course, I have been through a lot of difficulties, especially in the first few months in a different country. It is my first time abroad, thousands of miles away from my family. Luckily, I have met some good friends and outstanding colleagues here, and they helped me a lot. I would love to thank all those kind people at the time of my leaving.

Thank you, Professor Artunc, you are my role model in my career life of research. You passionate about science and always optimistic about the results that inspire me a lot, especially when I felt frustrated about the failure of the experiments or the time I got the first rejection from the journal. Besides, you also work so hard with a high efficiency. I was always surprised by the way you managed your time because you have patients, meetings, paperwork, research, writing, tons of things to handle every day. Thanks to you, I can finish my project on time.

Thank you, Dr. Bohnert. I bet I asked you a lot of stupid questions at the beginning of my study, and I hope you were not annoyed. You are a lifesaver in our lab because of the professional for the flame photometer. You helped me a lot with my dissertation, my presentation, and so on. I do not think I can finish the project successfully without your help. I also would like to dedicate my sincere appreciation to Dr. Montero, and other colleagues from the lab, Adrea, Matthias, Daniel, Nuray, Jonas, Firas, Dr. Omage, as well as my friends Bo, Dr. Ping Li, Jingtao, Yujia and Lingjun who supported me in any way during my stay in Tuebingen.

At last and most important, I would like to express my sincerest thanks to my family, especially my husband Hao Tian. Without your understanding and support, I wouldn't make it so far. I know how difficult it is for us apart from distant oceans for three years, and we only meet each other twice a year. I can't count how many times my friends asked me that how we survived from the illness of missing each other during the rest of the days that we were not together. Thanks to the internet, it makes online chatting much more easier than decades ago. A beautiful sentence from an ancient Chinese poem says, "even though the mountains and the oceans separate lovers, love can make them flat." I guess love is what we need for life to overcome any difficulties.